

Copyright

by

Ryan David Kalina

2009

**Comparative Study of the Corrosion Resistance of Different
Prestressing Strand Types for use in Post-Tensioning of Bridges**

by

Ryan David Kalina, B.S.C.E.

Thesis

Presented to the Faculty of the Graduate School of
The University of Texas at Austin
in Partial Fulfillment
of the Requirements
for the Degree of

Master of Science in Engineering

The University of Texas at Austin

May 2009

**Comparative Study of the Corrosion Resistance of Different
Prestressing Strand Types for use in Post-Tensioning of Bridges**

**Approved by
Supervising Committee:**

John E. Breen

Harovel Wheat

Acknowledgments

During my time at the University of Texas the most influential person in my life outside of my family has been Dr. Breen. Ever since we met in reinforced concrete design Dr. Breen has been a mentor to me not only in my academic career but also in life. He has helped me so much through the years in advancing my education and knowledge. His stories and experiences shared will be remembered greatly and I can not thank him enough. I will always cherish the relationship we have.

I would also like to thank Dr. Wheat for taking the time to be on my committee and helping me throughout the research process and giving me insight into the wonderful world of corrosion.

The most thanks goes to my wonderful family who were instrumental in the completion of this work. They have always been there to give me the support and motivation to get me through school and life; especially my father. He has always been someone I admired and whom I aspired to be like and I would not be where I am today without him. I have to thank my mother for taking the time and effort to proofread this work; I know my grammar can be poor at times. Thank you Rachel for agreeing to stir salt when I needed to finish a test quickly and thank you Nikki for helping me create a great figure.

Special thanks to Sean Mac Lean for being patient with my questions and guiding me through the research process. This would not have been possible without your help.

Finally, I want to thank the entire staff at Ferguson Laboratory including Barbara, Jessica, Cari, Ella, Eric, Blake, Dennis, Mike, and Andrew. Your hard work and dedication are appreciated and it was a pleasure working with you all. I especially would like to thank Andrew for his great conversation; it definitely made the time spent at the lab enjoyable.

Comparative Study of the Corrosion Resistance of Different Prestressing Strand Types for use in Post-Tensioning of Bridges

Ryan David Kalina, M.S.E.

The University of Texas at Austin, 2009

SUPERVISOR: John E. Breen

Project 4562 was launched with support from the Texas Department of Transportation and the Federal Highway Administration. The project was designed to test the relative corrosion resistance of various post-tensioned systems. These systems have utilized new and innovative strand types not commonly used in current post-tensioning projects. The project consists of various parts including large beam exposures. These large beam specimens are currently being exposed to a salt solution cycle at the Phil M. Ferguson Structural Engineering Laboratory at the University of Texas at Austin. From a previous project that was similar in scale, it was noticed that there was a need to know the corrosive properties before the autopsy of the large specimens. The grouts and grouting techniques had previously been tested by various researchers. Therefore, it was important to establish the corrosive properties of the strands used in the post-tensioning of the large beam specimens. The goal of this research was to establish the corrosive properties of the different strand and grout interactions. This included establishing appropriate testing techniques to compare times to corrosion and relative corrosion resistance.

These objectives were achieved in two stages. The corrosive properties of the different strand and grout interactions were established through active and passive corrosion tests. Different electrochemical testing techniques were employed to attain the corrosive properties which consist of the active corrosion tests. Most importantly was the use of the linear polarization resistance testing technique to compare the times to corrosion for each strand specimen. The passive corrosion tests utilized exposing the bare strands to a salt water solution and determining relative corrosion properties by final weight loss and visual inspection. Another passive test has the strands encased in grout and exposed to a salt water solution full time causing the strands to

undergo electrochemical processes. The specimens are monitored for potential and current created during these processes.

Table of Contents

Chapter 1: Introduction	1
1.1 Background	1
1.2 Research Objectives.....	2
1.3 Corrosion on Prestressing Materials.....	3
1.3.1 Corrosion of Metal.....	3
1.3.2 Passivity.....	3
1.3.3 Types of Corrosion.....	4
1.4 Durability of Post-tensioned Systems.....	5
1.5 Materials.....	7
1.5.1 Strand Tests.....	7
1.5.2 Long Term Beam Setup.....	8
1.6 Thesis Overview: Chapter Outline.....	9
Chapter 2: Ongoing Research on Post-Tensioned Concrete Exposure Beams Systems	11
2.1 Project Background.....	11
2.2 Project Maintenance.....	12
2.3 Project Data.....	15
2.4 Observations.....	17
Chapter 3: Passive Corrosion Exposure Testing	23
3.1 Overview.....	23
3.2 Exposed Strand Test.....	23
3.2.1 Test Description.....	23
3.2.2 Test Setup.....	24

3.3 Grouted Strand Test.....	28
3.3.1 Test Description.....	28
3.3.2 Test Setup.....	28
3.3.2.1 Specimen Preparation.....	28
3.3.2.2 Equipment Preparation.....	36
Chapter 4: Results of Passive Corrosion Exposure Testing	40
4.1 Overview.....	40
4.2 Results of Exposed Strand Test.....	41
4.2.1 Flow-Filled Epoxy Coated (EC).....	42
4.2.2 Stainless Clad (SC).....	44
4.2.3 Stainless Steel (SS).....	46
4.2.4 Hot Dip Galvanized (GV).....	48
4.2.5 Copper Clad (CC).....	50
4.2.6 Conventional (CN).....	52
4.2.7 Summary of Exposed Strand Test.....	55
4.3 Results of Grouted Strand Test.....	58
4.3.1 Conventional (CN).....	59
4.3.2 Copper Clad (CC).....	60
4.3.3 Hot Dip Galvanized (GV).....	61
4.3.4 Stainless Clad (SC).....	62
4.3.5 Stainless Steel (SS).....	63
4.3 Summary of Grouted Strand Test.....	64
Chapter 5: Accelerated Active Corrosion Testing	67
5.1 Overview.....	67
5.2 Description of System.....	67

5.2.1 Half-Cell Reactions.....	67
5.2.2 Mixed Potential Theory.....	70
5.3 Linear Polarization Resistance Accelerated Corrosion Testing.....	72
5.4 Potentiodynamic Accelerated Corrosion Testing.....	74
5.5 Testing Setup and Procedure.....	75
5.6 Specimen Design and Construction.....	79
Chapter 6: Results of Accelerated Active Corrosion Testing	84
6.1 Overview.....	84
6.2 Conventional.....	86
6.2.1 Potentiodynamic Tests.....	86
6.2.2 Linear Polarization Resistance Tests.....	87
6.3 Copper Clad.....	88
6.3.1 Potentiodynamic Tests.....	88
6.3.2 Linear Polarization Resistance Tests.....	89
6.4 Flow-Filled Epoxy Coated.....	90
6.4.1 Potentiodynamic Tests.....	91
6.4.2 Linear Polarization Resistance Tests.....	92
6.5 Hot Dip Galvanized.....	93
6.5.1 Potentiodynamic Tests.....	93
6.5.2 Linear Polarization Resistance Tests.....	94
6.6 Stainless Clad.....	96
6.6.1 Potentiodynamic Tests.....	96
6.6.2 Linear Polarization Resistance Tests.....	97
6.7 Stainless Steel.....	98
6.7.1 Potentiodynamic Tests.....	98
6.7.2 Linear Polarization Resistance Tests.....	98

6.8 Summary.....	101
Chapter 7: Indications of Tests	106
7.1 Major Trends.....	106
7.1.1 Large Scale Exposure Beams Half-Cell Data.....	106
7.1.2 Exposed Strand Test.....	107
7.1.3 Grouted Strand Test.....	109
7.1.4 Accelerated Active Corrosion Test.....	111
7.2 Strand Type Recommendations.....	113
Chapter 8: Conclusions	116
8.1 Conclusions.....	116
8.2 Recommendations.....	117
Bibliography	118
VITA	121

List of Tables

Table 2.1: Probability of Corrosion Occurring (ASTM C 876 1999) ^{3,14}	16
Table 2.2: Least Corroded Specimens	18
Table 2.3: Most Corroded Specimens	18
Table 2.4: Beams with Rust Spots	21
Table 3.1: Corrosion Rating System ¹⁸	24
Table 4.1: Corrosion Rating for Exposed Strand Test ¹⁸	41
Table 4.2: Results of Flow-Filled Epoxy Coated Strands at Six Months	43
Table 4.3: Results of Stainless Clad Strands at Six Months	45
Table 4.4: Results of Stainless Steel Strands at Six Months	47
Table 4.5: Results of Hot Dip Galvanized Strands at Six Months	49
Table 4.6: Results of Copper Clad Strands at Six Months	51
Table 4.7: Results of Conventional Strands at Six Months	53
Table 4.8: Results of All Strands Relative to Epoxy Coated	55
Table 4.9: Corrosion Potentials of Representative Specimens	66
Table 5.1: Standard Electromotive Force Potentials ¹²	68
Table 5.2: Common Secondary Reference Electrodes ¹²	69
Table 5.3: Testing Variables	79
Table 6.1: Linear Polarization Resistance Results for Conventional Strand Tests	88
Table 6.2: Linear Polarization Resistance Results for Copper Clad Strand Tests	90
Table 6.3: Linear Polarization Resistance Results for Flow-Filled Epoxy Coated Strand Tests	93
Table 6.4: Linear Polarization Resistance Results for Hot Dip Galvanized Strand Tests	95
Table 6.5: Linear Polarization Resistance Results for Stainless Clad Strand Tests	98
Table 6.6: Linear Polarization Resistance Results for Stainless Steel Strand Tests	100
Table 6.7: Summary of the Linear Polarization Resistance Results for All Tests	101
Table 6.8: Comparative Results of Linear Polarization Resistance Tests	104
Table 6.9: Percent Differences Between Normal and Pre-cracked Specimens	105
Table 7.1: Least Corroded Specimens	106
Table 7.2: Most Corroded Specimens	107
Table 7.3: Corrosion Potential of Representative Specimens	110
Table 7.4: Comparative Results of Linear Polarization Resistance Tests	111
Table 7.5: Ultimate Strengths ¹⁴	114
Table 7.6: Strand Rankings Based on Corrosion Resistance	115
Table 8.1: Autopsy Layout of the Large-Scale Beam Specimens	117

List of Figures

Figure 1.1: Passive Polarization Behavior ¹⁹	4
Figure 1.2: Examples of Uniform and Pitting Corrosion ¹²	5
Figure 1.3: Corroded Hot Dip Galvanized Duct ²²	6
Figure 1.4: Post-Tensioning Anchorage System ¹⁹	7
Figure 1.5: Duct Types.....	9
Figure 1.6: Bearing Plate Types.....	9
Figure 2.1: Layout of Large Scale Exposure Specimens.....	11
Figure 2.2: Specimen Embedment and Equipment Used to Apply Solution.....	12
Figure 2.3: System Spraying Chloride Solution onto the Bearing Plates Beneath the Grout.....	13
Figure 2.4: Equipment Used to Measure Half-Cell Potentials.....	13
Figure 2.5: Caulked Region on Beam Specimens and Type of Caulk Used.....	14
Figure 2.6: Plot of Half-Cell Potential versus Time.....	15
Figure 2.7: Impedance Measurement Device.....	17
Figure 2.8: Rust Spots on Beam 1.2 and 2.2.....	20
Figure 2.9: Rust Spots on Beams 4.1 ad 1.4.....	20
Figure 2.10: Rust Spots on Beam 3.1.....	22
Figure 3.1: Chop Saw and Table Grinder	25
Figure 3.2: Specimens Used in Exposed Strand Test.....	25
Figure 3.3: Strands with Epoxy Ends and the Epoxy Used.....	26
Figure 3.4: Pipe Configuration with Capped Ends and Holes Drilled.....	26
Figure 3.5: Strand Centered Inside Pipe Using Foam Cell.....	27
Figure 3.6: Wood Rack and Final Specimen Setup.....	27
Figure 3.7: Design of Different Types of Specimens.....	29
Figure 3.8: Lathe Used For Machining.....	30
Figure 3.9: Diagram of Bored Elements ¹⁴	31
Figure 3.10: Milling Machine Used During Machining.....	31
Figure 3.11: Section of Pipe Grooved and Bored Out ¹⁴	32
Figure 3.12: Grid of Acrylic Rods.....	32
Figure 3.13: Quick Set Epoxy Used to Fill Acrylic Holes.....	33
Figure 3.14: Applying Epoxy to the Bottom of the Strand.....	34
Figure 3.15: Silicone Used to Assemble Pipe Components.....	34
Figure 3.16: Grout Type and Variable Speed Mixer.....	35
Figure 3.17: Final Configuration Before Curing.....	36
Figure 3.18: Saturated Calomel Electrode.....	37
Figure 3.19: Grouted Strand Test Cell Setup.....	38
Figure 3.20: Grouted Strand Test Complete Setup.....	39
Figure 4.1: Flow Filled Epoxy Coated Strands at Six Months.....	43
Figure 4.2: Corrosion Rating Over Time for Flow-Filled Epoxy Coated Strands.....	44
Figure 4.3: Stainless Clad Strands at Six Months.....	45
Figure 4.4: Corrosion Rating Over Time for Stainless Clad Strands.....	46
Figure 4.5: Stainless Steel Strands at Six Months.....	47
Figure 4.6: Corrosion Rating Over Time for Stainless Steel Strands.....	48

Figure 4.7: Hot Dip Galvanized Strands at Six Months.....	49
Figure 4.8: Corrosion Rating Over Time for Hot Dip Galvanized Strands.....	50
Figure 4.9: Copper Clad Strands at Six Months.....	51
Figure: 4.10: Corrosion Rating Over Time for Copper Clad Strands.....	52
Figure 4.11: Conventional Strands at Six Months.....	53
Figure 4.12: Corrosion Rating Over Time for Conventional Strands.....	54
Figure 4.13: Corrosion Rating Over Time for All Strands.....	56
Figure 4.14: Average Six Month Rating vs Epoxy Coated Strand.....	56
Figure 4.15: Average Weight Loss vs Epoxy Coated.....	57
Figure 4.16: All the Strands After Six Months.....	57
Figure 4.17: Potential vs Time for Conventional Strand.....	60
Figure 4.18: Potential vs Time for Copper Clad Strand.....	61
Figure 4.19: Potential vs Time for Hot Dip Galvanized Strand.....	62
Figure 4.20: Potential vs Time for Stainless Clad Strand.....	63
Figure 4.21: Potential vs Time for Stainless Steel Strand.....	64
Figure 4.22: Potential vs Time for the Representative Specimens.....	65
Figure 5.1: Basic Test Setup ¹⁴	69
Figure 5.2: Plot of Applied Potential vs log of Current Density ¹⁴	71
Figure 5.3: Mixed Potential Plot ¹⁴	72
Figure 5.4: Plot of Linear Polarization Resistance ¹⁴	73
Figure 5.5: Plot of Applied Voltage vs Log of Current from Potentiodynamic Test ¹⁴	74
Figure 5.6: Potentiodynamic Plots of All Strand Types.....	75
Figure 5.7: Pre-Cracking Device.....	76
Figure 5.8: Potentiostat Built into Computer.....	77
Figure 5.9: Test Setup with Different Electrodes ¹⁴	78
Figure 5.10: Design of Different Types of Specimens ¹⁴	80
Figure 5.11: Boring Diagram for 0.6 in. Specimens ¹⁴	81
Figure 5.12: Grid Pattern and Location of Acrylic Rods ¹⁴	82
Figure 5.13: Specimen After Removal of Pipe Over Exposed Region.....	83
Figure 6.1: Corrosion Potential of Potentiodynamic Plot.....	85
Figure 6.2: Potentiodynamic Plot of Conventional Strand Tests.....	86
Figure 6.3: Linear Polarization Resistance Plot of Conventional Strand Tests.....	87
Figure 6.4: Potentiodynamic Plot of Copper Clad Strand Tests.....	89
Figure 6.5: Linear Polarization Resistance Plot of Copper Clad Strand Tests.....	90
Figure 6.6: Potentiodynamic Plot of Flow Filled Epoxy Coated Strand Tests.....	91
Figure 6.7: Linear Polarization Resistance Plot of Flow-Filled Epoxy Coated Strand Tests.....	92
Figure 6.8: Potentiodynamic Plot of Hot Dip Galvanized Strand Tests.....	94
Figure 6.9: Linear Polarization Resistance Plot of Hot Dip Galvanized Strand Tests.....	95
Figure 6.10: Potentiodynamic Plot of Stainless Clad Strand Tests.....	96
Figure 6.11: Linear Polarization Resistance Plot of Stainless Clad Strand Tests.....	97
Figure 6.12: Potentiodynamic Plot of Stainless Steel Strand Tests.....	99
Figure 6.13: Linear Polarization Resistance Plot of Stainless Steel Strand Tests.....	100
Figure 6.14: Comparison of Times to Corrosion For Pre-Cracked Specimens.....	102
Figure 6.15: Comparison of Times to Corrosion For Normal Specimens.....	103
Figure 7.1: Average Six Month Rating vs Epoxy Coated Strand.....	108

Figure 7.2: Average Weight Loss vs Epoxy Coated.....	108
Figure 7.3: Potential vs Time for the Representative Specimens.....	110
Figure 7.4: Comparison of Times to Corrosion for Normal Specimens ¹⁴	112
Figure 7.5: Comparison of Times to Corrosion for Pre-Cracked Specimens.....	112

Chapter 1

Introduction

1.1 Background

With the popularity of post-tensioned bridge construction in the United States and the world, the need for corrosion protection is great. The steel materials used in the prestressing elements of post-tensioned systems are very high strength and are vulnerable to corrosion attacks. Techniques are used during construction which try to prevent such corrosive action. Some of these techniques include coating the prestressing strands with oil and grouting the ducts after placement. Due to the corrosive nature of steel, the post-tensioned strands are highly vulnerable even with these precautions. A different possible solution could be the use of materials other than the conventional steels used today. There is ongoing research to discover new materials that can match the durability of steel while preventing corrosion and be economically reasonable^{1,11,14,19, & 21}. In an effort to explore these options further, The Texas Department of Transportation and the Federal Highway Administration began funding of research on the topic of creating better systems for post-tensioned bridge construction. This research has already found new construction methods and has broadened the scope of research to develop more test methods^{1,11,14,19,&21}.

The cost of corrosion of reinforced concrete structures is of concern in the United States with an estimated cost of \$8.3 billion annually²². A major problem with post-tensioned systems is that it is very difficult to detect corrosion in the tendon even when regular maintenance checks are made. These regular checks lead to high costs in the lifetime of a structure. Also, in order to be inspected, the ducts must be left ungrouted. This leaves the tendon exposed and vulnerable to atmospheric conditions which can be harsh, especially in a marine environment. Even with the ducts grouted, there is still no guarantee to the protection of the tendon from corrosive agents. The grout placed after the tendon is tensioned is only bonded to the tendon through curing. Since grout has similar properties to concrete and is weak in tension, the grout is susceptible to

cracking and with any penetration of the outer duct allows the corrosive agents to reach the tendon.

Apart from the corrosion of the tendons, the durability of the ducts in the post-tensioning system is also in question. The material, placement, and function failures of the system are all potential problems possibly leading to the corrosion of the tendon stored inside. The main issue is one where there is a need to find a material for the strands which reflects the strength of conventional steel but is capable of resisting corrosion. The secondary issue, which relates to the corrosion of the tendon, is finding a duct system durable enough to outlast the wear of normal use.

1.2 Research Objectives

The current project being conducted at Ferguson Structural Engineering Laboratory is 0-4562 and was begun in 2003. The project, funded by The Texas Department of Transportation and the Federal Highway Administration, focuses on developing new methods and materials for the construction of post-tensioned bridges. The research includes new materials for the strands as well as for the ducts. Large scale cracked post-tensioned concrete specimens are being tested through a cycle of chloride exposure. Companion small scale tests of strand or grout and strand are being conducted on the proposed materials for the strands. These small scale tests on the tendons are active accelerated corrosion tests and passive corrosion tests used to gather enough information on the proposed materials to have a better understanding and predictability of the large specimens when autopsied. These autopsies will be conducted on the large specimens at the end of the cycle which is between four to eight years¹. During the autopsies, the corrosion of the tendon will be studied as well as the durability of the ducts.

1.3 Corrosion on Prestressing Materials

In order to understand the development of this research, a general knowledge of the corrosion of the prestressing materials must be explored. The main corrosive action is the one with metals. Different types of corrosion occur and vary in severity and the way it affects the material.

1.3.1 Corrosion of Metal

The basic corrosion of metal is an electrochemical process made up of half-cell reactions. These half-cell reactions consist of an anodic and a cathodic reaction. Oxidation occurs on the anodic reaction while reduction occurs on the cathodic reaction. The regions where the anodic and cathodic processes are located have different electrochemical potential leading to the type of corrosion that will be present¹². The electrochemical potential present from the reactions also allows the monitoring of the corrosion by the use of a voltmeter and a reference electrode when the material is covered such as in the case of prestressing tendons. This monitoring can be used to determine the severity and rate of corrosion.

1.3.2 Passivity

Steel and all the different forms of steel, such as stainless, exhibit passivity in some degree among active, passive, and transpassive states¹². See Figure 1.1 below for the different ranges. The state at which a metal is acting depends on the potential of the metal which governs the corrosion rate¹². Conventional steel in concrete exhibits a passive state, and a passive protective layer is formed. Therefore, grouting the ducts of a post-tensioning system helps create this passive layer¹⁹. Chlorides have been found to enter the concrete through cracking which then break down this protective layer causing the metal to enter a transpassive state and begin to corrode. This has been the motivation for the research in finding a material that can withstand chloride exposure and keep the passive protective layer longer. Some materials tested, such as the stainless steel, are developed with a natural passive protective layer which makes it appealing to use for corrosion resistance.

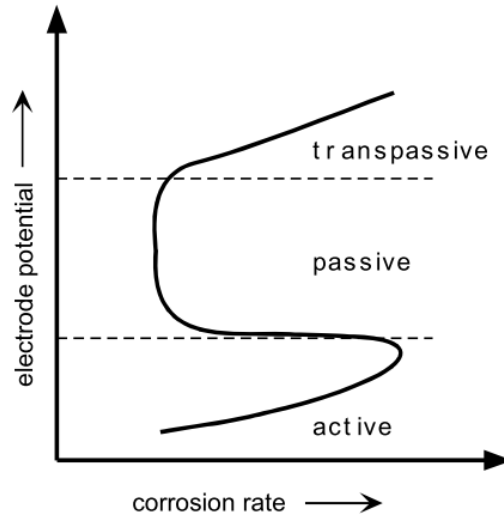


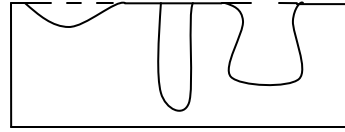
Figure 1.1: Passive Polarization Behavior¹⁹

1.3.3 Types of Corrosion

When a metal corrodes, it can undergo many types of corrosion depending on the type of metal and its passivity capabilities, chemical exposure, exposure duration, exposure cycle, temperature, and concentration of corrosive. Some of the most common types of corrosion are uniform, galvanic, crevice, pitting, and blistering¹². See Figure 1.2 below for examples of uniform and pitting corrosion. Many times, the corrosion will start out as uniform and build up to create blisters, while in some instances the corrosion is local and will result in pitting or crevices.



Uniform Corrosion



Pitting Corrosion¹²

Figure 1.2: Examples of Uniform and Pitting Corrosion¹²

1.4 Durability of Post-tensioned Systems

The durability of the post-tensioning systems is a major part of the success in fighting corrosion. The problem is that the current methods are full of areas which are susceptible to damage and corrosion. If the duct surrounding a post-tensioned tendon fails, then corrosives such as chlorides may enter the duct and reach the tendon. The main component on the duct system for resisting corrosion is the material of the duct. The most common materials used for ducts are hot dip galvanized steel and plastic. The problem with hot dip galvanized is that the zinc coating is a sacrificial element which means once the entire zinc coating has fully reacted, the steel will begin to corrode. This is an obvious long-term problem. Figure 1.3 shows the remains of a galvanized duct after eight years of chloride solution exposure inside a post-tensioned concrete beam.



Figure 1.3: Corroded Hot Dip Galvanized Duct²²

From the above Figure, the major corrosion problem with the hot dip galvanized duct system can be seen. The remains of the duct provide no tendon protection.

The alternative is plastic, but the problem with this material is often the tendons rub against the ducts during stressing due to harping of the tendons¹⁰. This causes the material to break down and eventually fail, allowing chlorides to enter. Apart from the material aspects, another issue of durability is splice details. Poor technology of splice designs allows failure at these points, and once again, the system is susceptible to chloride exposure.

Another concern of durability is the anchorage of the system. The strands are tensioned and held using a hydraulic jack. When they are cut, the strands are resisted by a system of wedges. Figure 1.4 shows a layout of a post-tensioned anchorage system.

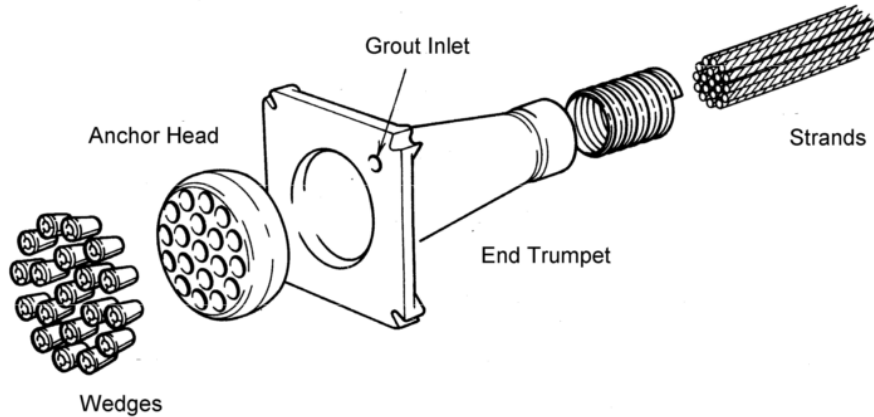


Figure 1.4: Post-Tensioning Anchorage System¹⁹

The force pulling on the strands creates interstitial defects in the strand as they bear against the wedges creating higher stresses at these locations¹⁹. The ends are grouted, but if chlorides are able to penetrate, they are able to enter the ducts and reach the entire tendon through these defects. Also, the corrosion at these affected cross-sections increases the stress, and ultimately, failure will occur at these points.

1.5 Materials

1.5.1 Strand Tests

The materials used for the different strand tests were chosen for optimal corrosion resistance. Sean Mac Lean outlined the materials in his Introduction¹⁴. The materials to be tested in this current program are seven-wire strands consisting of the following:

1. Conventional Strand (CN) (0.6 in)
2. Hot Dip Galvanized Strand (GV) (0.5 in)
3. Stainless Steel Strand (SS) (0.6 in)
4. Copper Clad Strand (CC) (0.5 in)
5. Stainless Clad Strand (SC) (0.6 in)
6. Flow-Filled Epoxy Coated Strand (EC) (0.5 in)

The copper and steel clad strands are smaller diameter steel strands with the appropriate cladding to make the final diameter. Tension tests were done on the strands by Mac Lean to determine if the alternate materials could compare in mechanical properties with the conventional strand. The results of his research conclude that the stainless steel, copper clad, stainless clad, and hot dip galvanized did not meet the requirements for Grade 270¹⁴. However, the stainless clad and the hot dip galvanized did meet the requirements of Grade 250¹⁴. These results determined that to be able to utilize these materials, advances in the mechanical properties must be developed.

1.5.2 Long-Term Beam Set-up

The long-term beam research is the large scale post-tensioned specimens undergoing chloride exposure cycles. There are a total of 24 specimens having variables in material of the tendons, ducts, and bearing plates. The tendons consist varyingly of the six materials presented above which are used in the strand tests. The ducts consist varyingly of hot dip galvanized, one-way ribbed plastic, and two-way ribbed plastic. See Figure 1.5 for the different types of ducts. As can be seen, the one-way ribbed plastic duct is similar to the hot dip galvanized duct with the ribs acting as structural components. The two-way ribbed plastic ducts have a rib running along the length of the duct in addition to the transverse rib. This rib along the length acts as an extra structural component and also allows the grout to flow easier along the length. The bearing plates consist of galvanized and non-galvanized material. Figure 1.6 shows the two types of bearing plates. The specimens are arranged in order to have a variety of combinations between tendon and duct type.

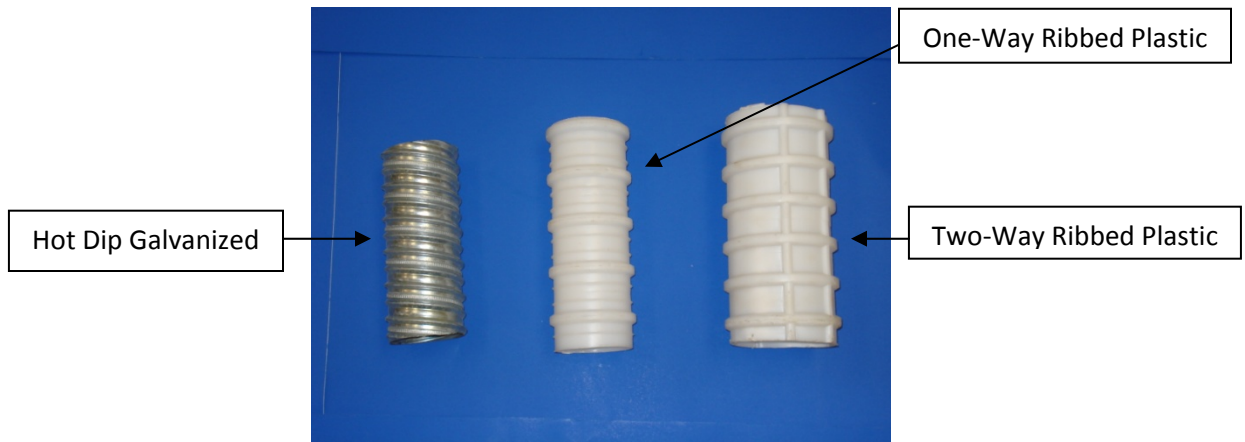


Figure 1.5: Duct Types



Figure 1.6: Bearing Plate Types

1.6 Thesis Overview: Chapter Outline

Chapter 2 explains the ongoing research of Project 0-4562 dealing with the large scale post-tensioned concrete exposure beams. A background of the project and its conception is explained along with the daily maintenance and testing done on the beam. Data from these tests and the observations are presented.

Chapter 3 gives a description of the passive corrosion exposure tests done on individual strand types. The tests consist of an exposed strand test and a grouted strand test. It shows the two different tests conducted and how they were set up.

The results of Chapter 3 are discussed in Chapter 4 with a monthly observation of each test and plots of corrosion over time.

Chapter 5 examines the accelerated active corrosion testing which is similar to Mac Lean's with the addition of pre-cracking the elements. An overview of the set-up and test methods will be discussed.

Chapter 6 gives the results of the testing of Chapter 5 with linear polarization resistance and potentiodynamic plots of each strand type.

Chapter 7 will discuss the trends of all the tests conducted and sum up the materials and their corrosion resistance properties. Recommendations in the field of corrosion resistance will be made based on the results.

Chapter 8 will have conclusions of the testing sequences along with recommendations for future research.

Chapter 2

Ongoing Research on Post-Tensioned Concrete Exposure Beams Systems

2.1 Project Background

Project 0-4562 is a large scale assessment of post-tensioned concrete exposure beams currently being conducted at the Phil M. Ferguson Laboratory at the University of Texas at Austin. The project is being supported by the Texas Department of Transportation and the Federal Highway Administration and is a continuation of Project 0-1405 started by West²³ and Schokker¹⁹. The beam specimens consist of a variety of combinations of such aspects as tendon type, duct type, and bearing plate¹. There are a total of twenty-four beam specimens that all undergo a biweekly wet and dry cycle which consists of keeping the specimens wet with a chloride solution for two weeks and completely dry for the remaining two weeks. Ten of the specimens undergo a chloride solution spray exposure on the ends once a month to attack the grouted bearing plates. At the end of four to six years, the specimens will be autopsied to determine the level of corrosion to the ducts, tendons, and bearing plates. Figure 2.1 shows a layout of the specimens at Ferguson Laboratory.



Figure 2.1: Layout of Large Scale Exposure Specimens

2.2 Project Maintenance

The beam specimens must undergo daily and weekly maintenance and monitoring. The specimens undergo a biweekly wet and dry cycle where for the first two weeks of the month, they are exposed to a 3.5% by weight chloride solution which is placed in an embedment on top of the specimens. Figure 2.2 shows the embedment and the equipment used to apply the solution; this consists of a five-gallon bucket and a bag of salt.



Figure 2.2: Specimen Embedment and Equipment Used to Apply Solution

Throughout the last two weeks of the month, the specimens are cleared of the solution and are kept completely dry. During the wet cycle, a 3.5% by weight chloride spray is applied to the grouted ends of ten of the beams to determine the exposure properties of the grout. Figure 2.3 shows the system used to apply the spray. As can be seen, a pump is used to take water from a holding tank and send it through a pipe system that then sprays the ends. The water is collected by plastic troughs that take the water back to the holding tank. During the dry cycle, half-cell potentials are taken to help determine the corrosive state of the tendons. The process is carried out by following ASTM C 876 – 99: *Standard Test Method for Half-Cell Potentials of Uncoated Reinforcing Steel in Concrete*³. This is done by hooking one side of a voltmeter to exposed copper wires attached to the tendons inside the specimen.



Figure 2.3: System Spraying Chloride Solution onto the Bearing Plates Beneath the Grout

The other side of the voltmeter is attached to a calomel reference electrode. See Figure 2.4 for the configuration. The electrode is placed on certain points along the embedment of the specimen, and a potential reading is obtained.



Figure 2.4: Equipment Used to Measure Half-Cell Potentials

To help get a uniform reading, an electrical contact solution is used which consists of liquid household detergent mixed with water and applied with a sponge against which the electrode is placed. The potential readings are taken on a grid along the specimen embedment. The maximum value of potential of each specimen is used to plot potential versus time to follow the corrosive activity. Also, the grid of potential readings can be used to show contour schemes along the length of the embedment.

Other miscellaneous maintenance is done to the beam specimens. Initially, the specimen was cracked on top under service loads to allow the chloride solution to enter more easily. These cracks propagated along the sides of the specimen, therefore needing to be plugged. Caulk is used to plug these cracks, so water will not be able to leak out of the sides. Over time, the caulk deteriorates and must be scraped off and reapplied. The caulk used is a 100% Silicone Sealant by GE. Figure 2.5 shows the caulked areas along with the type of caulk used.



Figure 2.5: Caulked Region on Beam Specimens and Type of Caulk Used

2.3 Project Data

The data gathered from the collection of half-cell potentials is plotted in Figure 2.6 with potential versus time.

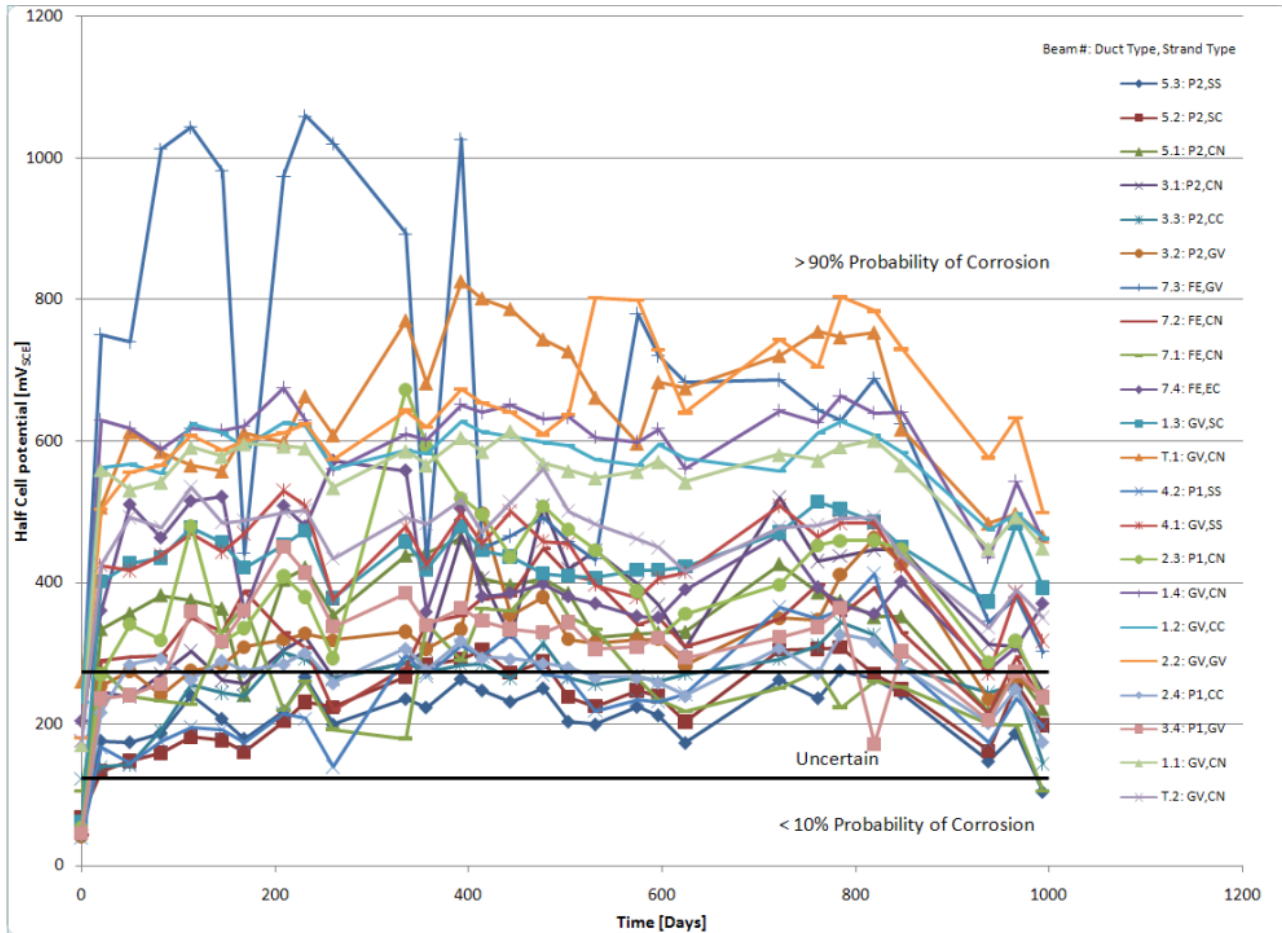


Figure 2.6: Plot of Half-Cell Potential versus Time

The initial readings began in March 2006 and continue with present data. The legend of the plot consists of the beam number, the duct type, and the tendon type. The tendon types are abbreviated using those of Section 1.5.1. The duct types are abbreviated using the following:

- 1) P1 – One-way plastic ribbed
- 2) P2 – Two-way plastic ribbed
- 3) GV – Hot dip galvanized
- 4) FE – Fully encapsulated

On the plot in Figure 2.6, two black lines appear. These represent boundaries of predicted corrosion activity. Any potential below the bottom black line which corresponds to 123 mV_{SCE} represents a value that is predicted to have a less than 10% probability of corrosion activity. Any potential above the top black line which corresponds to 273 mV_{SCE} represents a value predicted to have a greater than 90% probability of corrosion activity. Any value falling in between the two black lines represents a value that is uncertain of corrosion activity. Table 2.1 summarizes the values according to ASTM C 876 1999³.

Table 2.1: Probability of Corrosion Occurring (ASTM C 876 1999)^{3,14}

E_{corr} (mV _{CSE} ¹)	E_{corr} (mV _{SCE} ²)	Probability of Corrosion
More positive than -200	More positive than -123	Higher than 90% that no corrosion is occurring
Between -200 and -350	Between -123 and -273	Corrosion is uncertain
More negative than -350	More negative than -273	Higher than 90% that corrosion is occurring

¹ Potential is given in terms of the Copper-copper sulfate reference electrode

² Potential is given in terms of the Saturated Calomel reference electrode

The data gathered from the ten beams sprayed with chloride solution on the grouted ends described in Section 2.2 will be gathered during the autopsy of the beam specimens. The data expected to be gathered is on the durability of the end bearing plates and the grouted cover.

The four beam specimens with fully encapsulated ducts have data gathered on the AC Impedance during the dry cycle. The data collected consists of a resistance, a parallel capacitance, and a quality factor. All of these measurements are taken at a frequency of one kHz and are used to calculate the impedance. The impedance is a way of predicting corrosion

because it changes as a function of corrosion. The equipment used to gather the data is a LCR/ESR meter made by BK Precision and provided by VSL. The equipment can be seen in Figure 2.7. The equipment attaches to a coil tendon wire and a copper reinforcing bar wire of the specimen.



Figure 2.7: Impedance Measurement Device

2.4 Observations

The plot of the half-cell potentials versus time found in Figure 2.6 yields information on the corrosive nature of the materials present. None of the beam specimens ever have a less than 10% chance of having corrosion except from the first reading. Some of the beam specimens follow the less than 10% probability line closely while others exceed the greater than 90% probability line. Tables 2.2 and 2.3 below summarize the findings.

Table 2.2: Least Corroded Specimens

	Beam #	Duct Type	Tendon Type
1)	5.3	P2	SS
2)	5.2	P2	SC
3)	7.1	FE	CN
4)	4.2	P1	SS
5)	2.4	P1	CC
6)	3.3	P2	CC
7)	3.2	P2	GV
8)	3.4	P1	GV
9)	3.1	P2	CN

Table 2.3: Most Corroded Specimens

	Beam #	Duct Type	Tendon Type
1)	7.3	FE	GV
2)	2.2	GV	GV
3)	T.1	GV	CN
4)	1.4	GV	CN
5)	1.2	GV	CC
6)	1.1	GV	CN

The numbering sequence for the least corroded start with 1) being the least corroded and the numbering sequence for the worst corroded start with 1) being the most corroded. The order of the least and worst corroded specimens was chosen by following the specimen half-cell readings

over time and determining which values represent the status of the specimen best instead of looking at just the final half-cell values. There is a definite trend in the data that follows expected results. Looking at the least corroded specimens, the duct types that yield the best results are all plastic with the exception of one fully encapsulated. This strengthens the notion that plastic ducts, especially two-way ribbed, perform better in protecting the tendon while galvanized ducts perform poorly, deteriorating over time. Also on the least corroded specimens, there is no one strand type that stands out as the best. There is an even distribution of all the strand types used. The observation made of this distribution is that the two least corroded tendons are some form of stainless steel, the least being stainless steel and the second least being stainless clad. The last two on the least corroded list consist of hot dip galvanized and conventional strand sequentially. This observation leads into the worst corroded of the specimens found in Table 2.3.

When comparing the worst corroded specimens, the common duct type is hot dip galvanized with the exception of one which is fully encapsulated. This fully encapsulated duct also happens to be the highest half-cell reading specimen which could have stemmed from a flaw in construction. Another reason why the fully encapsulated specimen has the highest half-cell reading could be the corrosion of a stirrup or other component of reinforcement near the area where the half-cell readings are taken. Looking at the remaining hot dip galvanized ducts confirms the notion that this material is worse and corrodes faster than plastic duct. When comparing strand types found in the worst corroded specimens, the most common is conventional, followed by hot dip galvanized. One specimen of copper cladding was found which does not fit the trend.

Overall, the trend of the specimens tends to show that the worst systems on a durability standpoint tend to have ducts made of hot dip galvanized and strands made of conventional steel. These trends match the hypotheses made and are also reinforced with visual observations. On the specimens containing hot dip galvanized ducts, rust spots appear on the top of the specimen in the embedment along the cracks. These spots do not appear on the specimens containing plastic ducts. See the Figures below which show the rust spots on the designated specimens.

Duct Type: Galvanized

Strand Type: Copper Clad



Duct Type: Galvanized

Strand Type: Hot Dip Galvanized



Figure 2.8: Rust Spots on Beam 1.2 and 2.2

Duct Type: Galvanized

Strand Type: Stainless Steel



Duct Type: Galvanized

Strand Type: Conventional



Figure 2.9: Rust Spots on Beams 4.1 and 1.4

As can be seen, rust has formed on the top of the beam specimens probably due to the corrosion of the hot dip galvanized duct. A compilation of the beams with the type of duct and strands is found below. One observation is the two beams with the worst appearance of rust contained strands made of hot dip galvanized and conventional steel (Beams 2.2 and 1.4 respectively). The beams with lesser amounts of rust appearance are beams containing strands of copper clad and stainless steel (Beams 1.2 and 4.1 respectively). These lead to the conclusion

that beyond the corrosion of the galvanized duct, some of the strands may be corroded as well which follow the hypotheses made. This hypotheses is that the stainless steel and copper clad strands perform better in resisting corrosion than hot dip galvanized and certainly conventional steel. Further testing of the strands will show the same trends in strand resistance to corrosion.

Table 2.4: Beams with Rust Spots

	Beam #	Duct Type	Strand Type
1)	1.2	GV	CC
2)	2.2	GV	GV
3)	4.1	GV	SS
4)	1.4	GV	CN

One outlier was present among the beam specimens in which corrosion spots were present on the embedment of a specimen containing a two-way ribbed plastic duct and conventional strand. This was the only specimen with a plastic duct to exhibit any type of corrosion on the surface. The specimen is Beam 3.1 and can be seen in Figure 2.10. There are many possibilities as to the origin of these rust spots. The spots are positioned over each of the ducts and one of the cracks. A reasonable possibility for the spots could be the corrosion of the stirrups or wire ties located near this region.

Duct Type: Two-Way Ribbed Plastic

Strand Type: Conventional

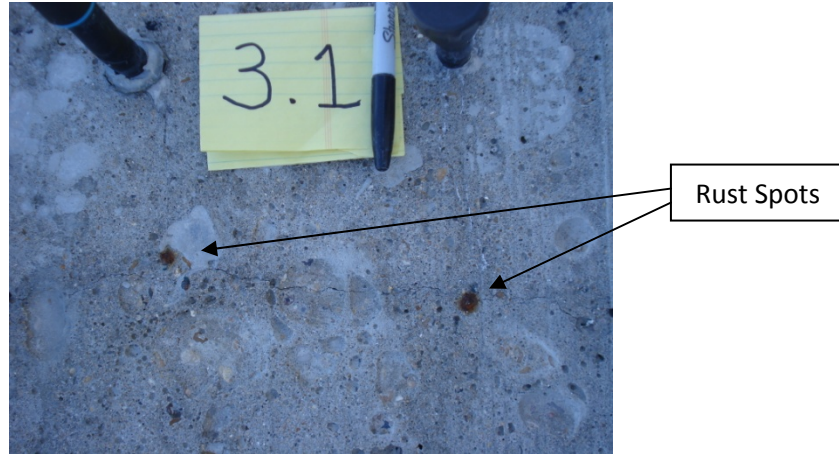


Figure 2.10: Rust Spots on Beam 3.1

Chapter 3

Passive Corrosion Exposure Testing

3.1 Overview

Along with the development of the large scale beam specimens to test for corrosion, a need to know the corrosive properties of the strand types used is necessary. There are several tests that can be performed to determine these properties, and this chapter explains the tests known as passive corrosion exposure testing. The term passive, when referring to electrochemical testing, refers to the type of test in which electrical impulses are recorded instead of applied. There are two types of passive tests conducted. The first test involves the bare strands undergoing a wet and dry cycle while they are exposed to a chloride solution. The strands are not encased in anything but left fully exposed to the solution. The second test involves the casting of the strands in a grouted encasement with a lead wire attached and then immersed in a chloride solution. The goal of this test is to take potential and current readings through a series between the lead wire and a reference electrode. The data will then be compared over time to track the corrosion rate of each strand type.

3.2 Exposed Strand Test

The exposed strand test will allow the tracking of corrosion over several months. At the end, a weight loss will be calculated for each strand which will correlate to a relative corrosion rate among the different strand types.

3.2.1 Test Description

The exposed strand test involves taking each of the six types of tendons described in Section 1.5.1 and exposing them to a wet and dry cycle of a 5% chloride solution by weight. Three strands of each type are being tested making a total of eighteen specimens. The strands are placed in a plastic pipe that is sealed except for holes which allow the atmosphere to enter.

Also, the holes are used to fill and drain the solution. The ends of the strands are ground down and smoothed using a table grinder, and then the strand is initially weighed. Then the ends are covered with epoxy to shield the defects from solution. The strands are weighed a second time. At the end of testing, a final weight with the epoxy will be recorded. A weight loss will be calculated and correlated to produce a relative corrosion rate among the strand types.

The beginning of the cycles is the wet cycle which lasts for a week at which time the solution is drained, and the strands begin the dry cycle. This dry cycle lasts for three weeks, and at the end, the strands are removed from the pipe for inspection. Each strand is designated by a numerical value which follows a corrosive rating system. Table 3.1 is the rating system used. Note that half integers may be used if the corrosion level falls between two descriptions. Testing should last approximately six months.

Table 3.1: Corrosion Rating System¹⁸

Rating	Description
1	As received from manufacturer and completely clean from any corrosion products
2	No signs of corrosion at any level, or there might be small spots of rust material present
3	Small blisters, superficial but widely spread corrosion, pitting is unusual
4	Small blisters, uniform corrosion or initial signs of wide pitting in centralized areas
5	Large blisters, trail of blisters does not exceed 2-in. (51-mm.), deep and wide pitting is visible, corrosion products and pitting does not affect more than 50% of steel area
6	Large blisters, trail of blisters along the strand exceeds 2-in. (51-mm.), deep and wide pitting cover most of the strand surface, corrosion products and pitting affect over 50% of the steel surface, and several forms of corrosion are present simultaneously
7	High levels of corrosion with visible large areas of steel lost

3.2.2 Test Setup

The test setup began with the strands being cut to length using a chop saw, then grinding the ends using a table grinder. The strands were cleaned of debris and defects, had the ends

covered with epoxy, and placed in a pipe that was closed off. The equipment used to cut and grind the strands is shown in Figure 3.1.



Figure 3.1: Chop Saw and Table Grinder

Figure 3.2 shows all the strand types along with the ground ends. The specimens in Figure 3.2 are identified from left to right as stainless steel, hot dip galvanized, copper clad, stainless clad, flow-filled epoxy, and conventional steel. Notice the ends are ground down to round the cut edge.



Figure 3.2: Specimens Used in Exposed Strand Test

The epoxy used was a one-to-one ratio by volume mix provided by Shepler's and was of the type SHEP-POXY Tx V. Figure 3.3 below shows each type of strand with epoxy applied to the ends along with the type of epoxy used.



Figure 3.3: Strands with Epoxy Ends and the Epoxy Used

The length of each strand and corresponding pipe is 18 in. The pipe used is PVC pipe with a 1.25 in. inside diameter. The pipe is then closed off, but not sealed, with an end-cap on each end. To allow the exposure of the atmosphere, three holes are drilled on one side of the pipe using a 1/8 in. drill bit. A fourth hole is drilled using a 1/2 in. drill bit to allow a funnel to be placed inside when filling the pipe with solution. Figure 3.4 shows the configuration.



Figure 3.4: Pipe Configuration with Capped Ends and Holes Drilled

When the strands are placed in the sealed pipe, they must be kept centered in the pipe to allow even distribution of solution along the length of the pipe. To do this, an Armacell foam cell used to insulate ½ in. conduit is cut into strips that are placed around the strand at each end of the pipe. Figure 3.5 shows the final configuration of the strand centered inside the pipe.

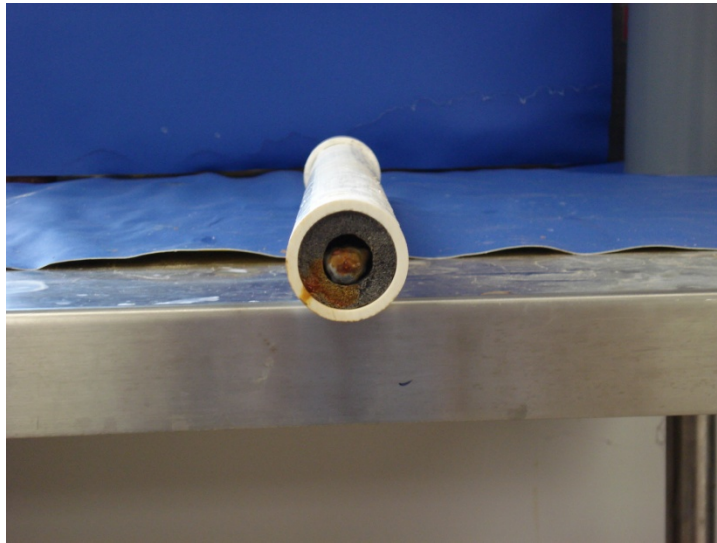


Figure 3.5: Strand Centered Inside Pipe Using Foam Cell

The final task was to build a rack to keep the sealed pipes horizontal in order to have even distribution of solution. A rack was constructed of 2x4 lumber and can be seen in Figure 3.6 along with the final setup of the specimens.



Figure 3.6: Wood Rack and Final Specimen Setup

3.3 Grouted Strand Tests

The accelerated corrosion tests done by Mac Lean¹⁴ helped gather information on the corrosive behavior of the different tendon types in a relatively small amount of time. In order to get a feeling for how the corrosive activity builds over time, a test was developed that is similar to the accelerated tests in setup, but instead of applying a potential, it is recorded.

3.3.1 Test Description

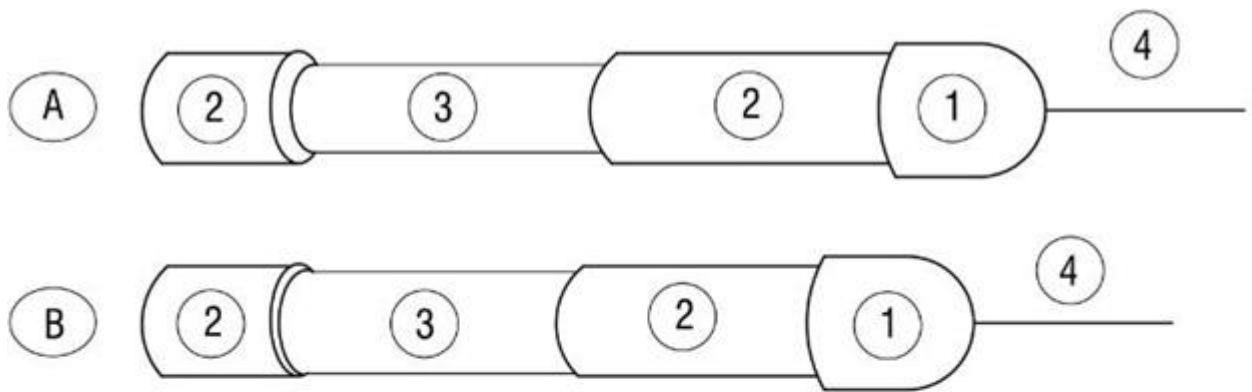
The passive corrosion testing of grouted strands has very similar specimens as those of Mac Lean's¹⁴ accelerated corrosion testing. The strands are placed in a clear pipe and grouted to imitate actual conditions where a tendon is grouted in a duct. Instead of having part of the strand exposed to allow a connection to apply potential, the strand is fully encapsulated within the pipe with the ends epoxied. Before the ends of the system are epoxied, a copper wire is attached to the strand to allow a connection for reading a current. This is similar to the copper wires attached to the tendons of the large-scale specimens. The grouted system is placed in a beaker containing a 5% chloride solution by weight. Over time, the strands undergo some corrosive activity, and an electrochemical process will occur. The system acts like a battery where a potential builds within the system. The test is set up to where a recording of potential and current is taken twice a day. The data is stored and can be used to compare the corrosive activity of the strands over a chosen period of time. The length of the test will be approximately four months.

3.3.2 Test Setup

3.3.2.1 Specimen Preparation

The grouted strand test utilizes all the strand types summarized in Section 1.5.1 except for the flow-filled epoxy coated. It was omitted from the test because the results of Mac Lean's¹⁴ work showed that the epoxy coated strand performed well, and the data from this test would not

prove to be useful. Also, the short time frame of the test would not yield good enough results to analyze. Three specimens of each of the types are used making a total of fifteen specimens. The strands are cut to length using the chop saw as in Section 3.3.1. Since the strands vary in diameter, the overall length of the pipe is different. This is a result of the length of the exposed grout region of the strand. The 0.6 in. diameter strands require the pipe to be bored out to have the same amount of grout cover as the 0.5 in. strands. Figure 3.7 shows the configuration of the two different systems.



A: Specimen for 0.5 in. strands

1. 25.4 mm (1 in.) PVC end cap
2. Clear PVC tubing: 50.8 mm (2 in.) & 101.6 mm (4 in.) in end cap
3. Exposed Grout: 25.4 mm (1 in.) dia., length 90 mm (3.5 in.)
4. 6 AWG gauge copper wire

B: Specimen for 0.6 in. strands

1. 25.4 mm (1 in.) PVC end cap
2. Clear PVC tubing: 50.8 mm (2 in.) & 101.6 mm (4 in.) in end cap
3. Exposed Grout: 28 mm (1.1 in.) dia., length 81.3 mm (3.2 in.)
4. 6 AWG gauge copper wire

Figure 3.7: Design of Different Types of Specimens

As can be seen, the exposed grout region for the 0.5 in. specimens is 3.5 in. as opposed to 3.2 in. for the 0.6 in. specimens. The strands were cut to length so they would have a 0.25 in.

cover of epoxy over each end. After the strands were cut, they were cleaned of debris, and the ends were ground using the same table grinder as the previous section.

The next phase of the setup involved preparing the PVC pipes. As mentioned above, since the strand diameters are of different size, machining of the pipes is necessary to keep the variables the same. A lathe was used to bore the inside of the PVC pipes (See Figure 3.8).



Figure 3.8: Lathe Used For Machining

The initial inside diameter of the pipes is one inch and the final diameter of the pipes used for 0.6 in. strand is 1.1 in. Therefore a total of 0.1 in. in diameter must be bored out. The boring action caused the clear pipe to become slightly distorted due to the passing of the lathe tool but not enough to keep the grout from being seen. To prevent unnecessary stresses in the specimen due to an abrupt change in diameter, the outer components of the 0.6 in. specimen pipes were bored out one inch. This allows a more gradual transition in the exposed grout region which can be seen in Figure 3.9.

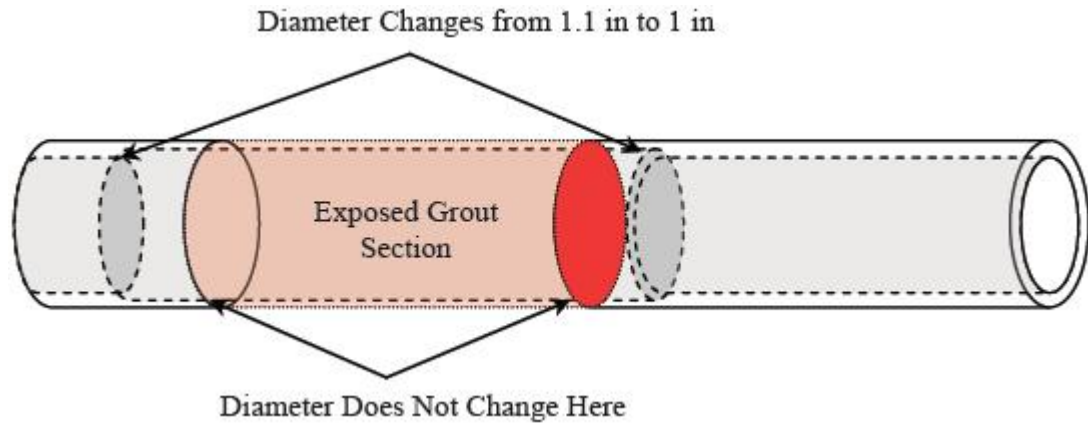


Figure 3.9: Diagram of Bored Elements¹⁴

The next step in preparing the PVC pipes was to mill grooves in the section over the exposed grout region. The grooves were milled using a Lagun Republic milling machine shown in Figure 3.10.

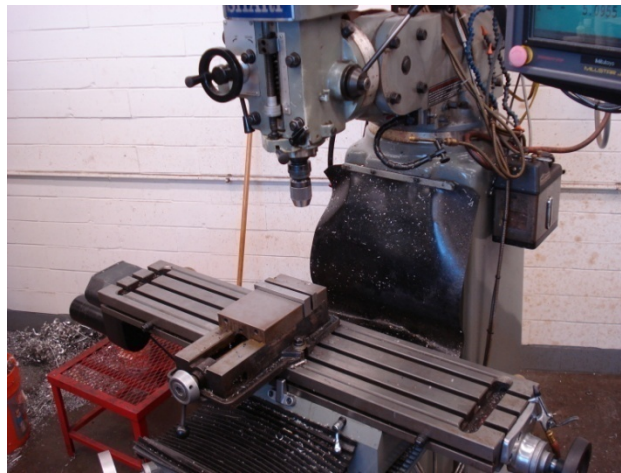


Figure 3.10: Milling Machine Used During Machining

These grooves would allow easier removal of this section after curing. The grooves were made as deep as possible, so there would be just enough material left as seen in Figure 3.11. Note in Figure 3.11, the inside diameter is bored out for the 0.6 in. strand.



Figure 3.11: Section of Pipe Grooved and Bored Out¹⁴

In order to keep the strands centered in the pipes, a grid of 1/16 in. acrylic rods was placed in the outer sections. Holes were drilled using the Lagun Republic milling machine, and the grid can be seen in Figure 3.12. Notice the difference in wall thickness of the two different specimens - the left being for the 0.6 in. and the right for the 0.5 in.

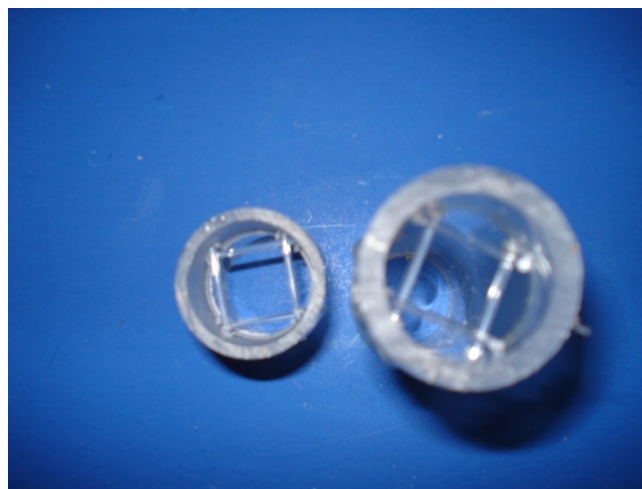


Figure 3.12: Grid of Acrylic Rods

The acrylic rods were placed through the holes and sealed with Loctite Quick Set epoxy shown in Figure 3.13. The epoxy is fast drying and water tight, keeping any grout from escaping.



Figure 3.13: Quick Set Epoxy Used to Fill Acrylic Holes

The next phase of the setup was to set one end of the strand in high-strength epoxy. The high-strength epoxy used is the same as in the previous section. This was done by setting the two-inch outer end on plastic, placing the strand through the acrylic grid, and holding it 0.25 in. from the bottom. The strands were held using grips from the accelerated test setup. The epoxy was then poured into the pipe filling the bottom to where the end of the strand was covered in epoxy. Figure 3.14 shows this process.



Figure 3.14: Applying Epoxy to the Bottom of the Strand

After the epoxy cured, the rest of the pipe was placed around the strand. The middle section of the pipe was first attached to the outer two-inch section using an adhesive silicone seen in Figure 3.15. The adhesive silicone allowed fast drying and a water tight connection among the parts of the pipe.



Figure 3.15: Silicone Used to Assemble Pipe Components

Finally, the four-inch outer section was placed over the strand and attached to the middle section using the same adhesive silicone. Before the four-inch outer section was placed, a 6 AWG gauge copper wire was attached to the top of each strand using duct tape. The diameter was chosen, so that the copper wire would fit in between two of the individual wires of the strands for easier attachment. The wire can be seen in Figure 3.17.

After the preparation of the specimens, the grout was mixed and poured into the pipe. The grout used was SikaGrout 300 PT because it is a pre-mixed, non-bleed, high-flow grout. The water to cement ratio was chosen to be 0.3 to allow easy flowing into the pipes. The grout was mixed using a variable speed mixer attached with a high shear blade. The grout and mixer can be seen in Figure 3.16.



Figure 3.16: Grout Type and Variable Speed Mixer

The grout was poured into each specimen using a funnel and then agitated to remove any air bubbles created. The tops of each specimen were left ungrouted a distance of 0.25 in. Immediately after pouring the grout, epoxy was poured to form a cap. To keep the epoxy covered during curing, a plastic cap was placed over the top. Figure 3.17 shows the final stage of specimen preparation before curing.



Figure 3.17: Final Configuration Before Curing

The specimens were left in a fog room and allowed to cure for twenty-eight days. After curing, the plastic caps were removed and replaced with PVC end caps. A hole had to be drilled in the end cap to allow the copper wire to pass through, and finally, the cap was placed on the specimen and attached with PVC cement. Before the specimens were put into the setup, the middle section of the pipe was removed, exposing the grout.

3.3.2.2 Equipment Preparation

The specimens were first immersed in a 5% chloride solution by weight in a 3000 mL beaker. In the system, the specimen acts as the working electrode accompanied by a counter electrode and a reference electrode. The counter electrode is a 0.05 in. platinum clad wire provided by Anomet products. The reference electrode is a saturated calomel electrode (SCE) manufactured by Fisher Scientific (See Figure 3.18).



Figure 3.18: Saturated Calomel Electrode

All the electrodes are held in place by the cell cover which fits over the beaker. The cell cover is made from 0.25 in. acrylic and was manufactured at the lab. First, the acrylic was cut into squares, followed by lathing the squares into the required diameter, and finally lathing the inside diameter for the specimen to fit through. The same lathe was used as in Section 3.3.1. The holes needed in the cell cover for the other electrodes were drilled using a hand drill. The platinum clad counter electrode was attached using the quick-dry epoxy. Figure 3.19 shows the complete setup of electrodes and wire attachments.

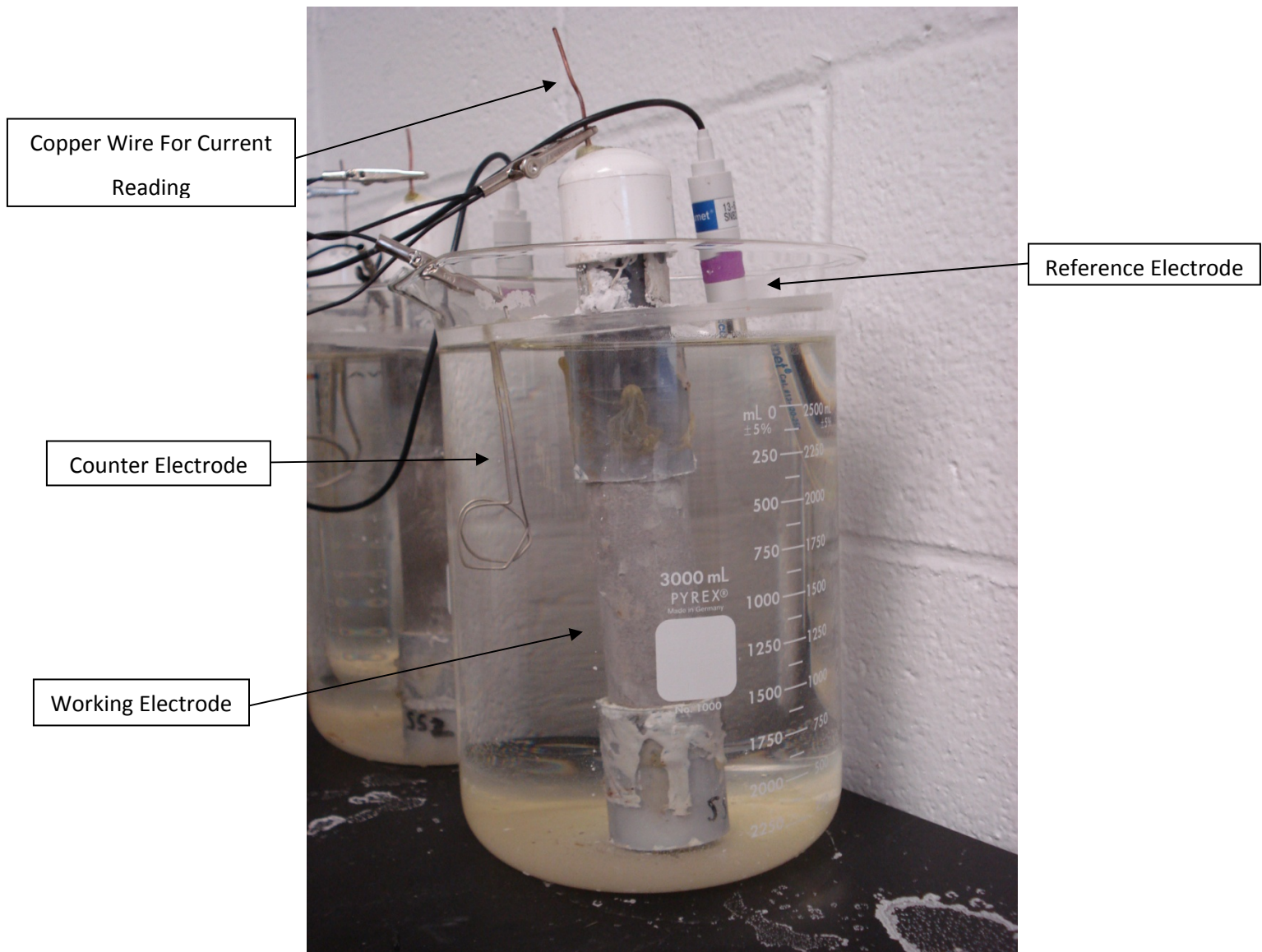


Figure 3.19: Grouted Strand Test Cell Setup

In order to gather the data from the electrochemical processes, basic electrical equipment was needed. Two multiplexers were used, one for gathering potential and the second for current. In the multiplexer for potential, one cell of the individual port is connected to the reference electrode and the other to the copper wire attached to the strand. In the multiplexer for current, one cell is used to connect to the copper wire and the other to the counter electrode. The wires used consist of 22 AWG gauge wire and had to have alligator clips soldered to the ends. The multiplexer for current then has one common port shared by all the specimens that has a twenty $k\Omega$ resistor connected in series. Both multiplexers are then connected to a data logger which is

programmed to take data readings twice a day. The readings will then be used to plot potential and current versus time to get an idea as to how the specimens corrode relative to each other. Figure 3.20 shows the final test setup with the wires attached from the specimens to the multiplexer and data logger.



Figure 3.20: Grouted Strand Test Complete Setup

Chapter 4

Results of Passive Corrosion Exposure Testing

4.1 Overview

Two types of passive tests were performed to gather corrosion resistance properties of the strands. The tests were both run over a period of several months. The first of these tests is the exposed strand test outlined in Chapter 3. This test involves the bare strands exposed to a 5 % chloride solution cycle followed by a corrosion rating at the end of each cycle. The weight loss of each strand type will be correlated to a relative corrosion rate. The final state of each strand type based on a corrosion rating is documented below. A plot of the average corrosion rating of the strands versus time is also shown to compare an effective time to corrosion and corrosion rate of the different strands.

The second passive corrosion test is the grouted strand test also outlined in Chapter 3. In test the strands are encased in grout inside PVC with the ends covered with epoxy to prevent corrosion of the bare cut strand. A copper wire is attached to the strand to allow the collection of data. The specimens are immersed in a 5% chloride solution, and a series of electrodes are placed within the system to create a cell. When corrosion takes place on the specimen, electrochemical activity will occur creating a half-cell potential. This potential along with the current created are stored in a data logger for review. The results of this test include plots of the potential (E_{corr}) versus time. The plots will help determine which strands have the best resistive properties.

4.2 Results of Exposed Strand Test

The exposed strand test was conducted for a period of six months. A weight loss and a corrosion rating of each strand will indicate the corrosion resistance properties of the strands relative to each other. The corrosion rating system found in Table 4.1 was used each month to rate how corroded the strands were. Note that if a strand's corrosion rating was in between two integers, a half number could be designated.

Table 4.1: Corrosion Ratings for Exposed Strand Test¹⁸

Rating	Description
1	As received from manufacturer and completely clean from any corrosion products
2	No signs of corrosion at any level, or there might be small spots of rust material present
3	Small blisters, superficial but widely spread corrosion, pitting is unusual
4	Small blisters, uniform corrosion or initial signs of wide pitting in centralized areas
5	Large blisters, trail of blisters does not exceed 2-in. (51-mm.), deep and wide pitting is visible, corrosion products and pitting does not affect more than 50% of steel area
6	Large blisters, trail of blisters along the strand exceeds 2-in. (51-mm.), deep and wide pitting cover most of the strand surface, corrosion products and pitting affect over 50% of the steel surface, and several forms of corrosion are present simultaneously
7	High levels of corrosion with visible large areas of steel lost

The results of each strand are presented below with first a table showing both the weight loss and corrosion rating at six months. The initial weights of each strand at the conclusion of exposure showed a weight gain due to excess water saturated within the strands and the weight of the corrosion products. In order to calculate a weight loss, the strands had to be dried in order to dissipate the excess water. First, the strands were dried in ambient air, but the weight readings

were still erroneous. Therefore, the strands were placed in an oven at 250°F for seven days followed by a light uniform brushing with a wire brush to remove any excess corrosion products.

A plot of corrosion rating versus time will be given to show how each strand corroded over time. A figure of each strand at six months will be shown with the first specimen of each strand being on top and the third specimen on the bottom. Note that the ends of the strands were epoxyed to prevent corrosion of the bare cut ends. Even though the epoxy was applied to the ends, it could not cover the interstices of the strands. This allowed the chloride solution to reach the bare cut ends of some of the strands. This also allowed some of the strands to show signs of corrosion at the ends. The properties of the strands are still valid in that their resistive properties would show how well they stopped the spread of corrosion. This was also taken into account in the rating system. If a strand showed signs of corrosion only near the ends, then the rating would not be as high as if corrosion was found on the rest of the strand.

4.2.1 Flow-Filled Epoxy Coated (EC)

The flow-filled epoxy coated strand was used in this test as a basis to compare the other strands. Since the ends of the strand were epoxyed, there was no chance for corrosion to begin. Therefore, the epoxy coated strand should have no change in corrosion rating and weight change. This was not totally true in the test, since the outer layer of epoxy coating had very small tears in them in some locations. Corrosion began at these areas but was confined there. The epoxy coated strands at six months can be seen in Figure 4.1. Note the small region of corrosion in strand number two (middle strand).



Figure 4.1: Flow Filled Epoxy Coated Strands at Six Months

Due to the small areas of corrosion, the strands could not receive a true value of one from the rating system, so they were given a final value of 1.5. See Table 4.2 for a summary of the strand at six months and Figure 4.2 for the corrosion ratings over time.

Table 4.2: Results of Flow-Filled Epoxy Coated Strands at Six Months

	EC1	EC2	EC3
Corrosion Rating	1.5	1.5	1.5
Weight Loss (grams)	0.7	0.5	0.6

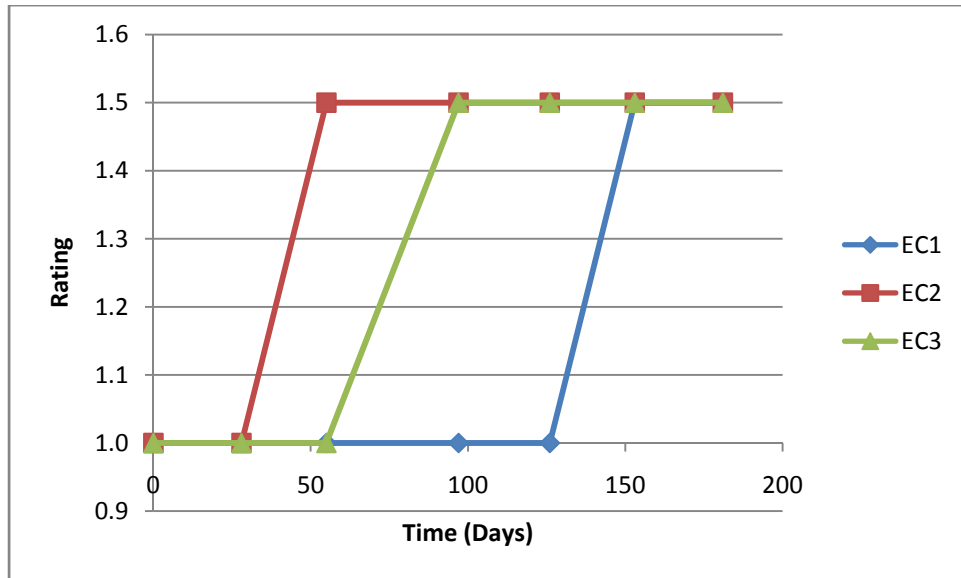


Figure 4.2: Corrosion Rating Over Time for Flow-Filled Epoxy Coated Strands

Note that all the strands ended with a corrosion rating of 1.5 due to the small defects in the epoxy coating, and that even one strand (EC1) took about five months to reach this rating value. From Figure 4.2, it can be seen that the second specimen (EC2) reached the corrosion rating of 1.5 the soonest (two months) which can be explained by the larger defect in the epoxy coating seen in Figure 4.1. Since the strands are coated with epoxy, the chloride solution was unable to reach the bare cut ends which kept the strands from corroding in these regions.

4.2.2 Stainless Clad (SC)

The stainless clad strands were expected to perform very well in this test considering that the cut ends were protected by epoxy, and there were no defects on the strands before the test began. The strands at six months are shown in Figure 4.3.



Figure 4.3: Stainless Clad Strands at Six Months

Notice that the only corrosion present is near the ends of the strands where the chloride solution was able to reach the bare cut ends but is perfectly clean everywhere else. The corrosion rating and weight loss for each strand at six months is given in Table 4.3. The corrosion rating versus time for each strand is shown in Figure 4.4.

Table 4.3: Results of Stainless Clad Strands at Six Months

	SC1	SC2	SC3
Corrosion Rating	1.5	1.5	1.5
Weight Loss (grams)	1.3	1.0	0.9

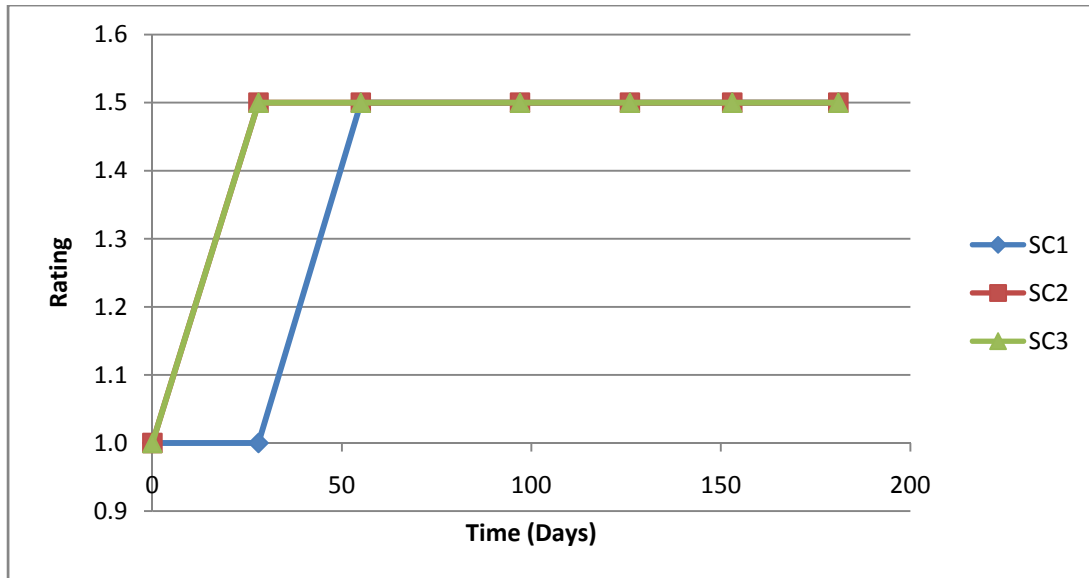


Figure 4.4: Corrosion Rating Over Time for Stainless Clad Strands

When comparing the stainless clad strands to that of the flow-filled epoxy coated strands, it can be seen that the final corrosion ratings are the same, but that the stainless clad strands achieved this rating sooner. This can be explained by the fact that the stainless clad strands were able to corrode near the ends which caused the strands to show some corrosion sooner but did a great job in containing this corrosion. These strands compare very well against that of the flow filled epoxy coated strands. The weight loss of the stainless clad strands was slightly higher than the epoxy coated strands.

4.2.3 Stainless Steel (SS)

The stainless steel strands were expected to do very similar to the stainless clad strands during this testing. The strands at six months are shown in Figure 4.5. Note that the behavior is similar to the stainless clad in that there is small corrosion in the middle of the strands. The stainless steel strands did not show as much corrosion near the ends as the stainless clad strands because the material is fully stainless steel.



Figure 4.5: Stainless Steel Strands at Six Months

Although it appears that the stainless strands performed closely to the stainless clad, the results at six months were worse. Table 4.4 outlines these results. One of the strands performed very well showing no signs of corrosion at all (SS2), while the other two strands showed worse signs. These worse results could be explained by the higher amount of corrosion near the ends. The corrosion ratings over time are shown in Figure 4.6.

Table 4.4: Results of Stainless Steel Strands at Six Months

	SS1	SS2	SS3
Corrosion Rating	2.0	1.0	2.0
Weight Loss (grams)	1.0	1.2	1.1

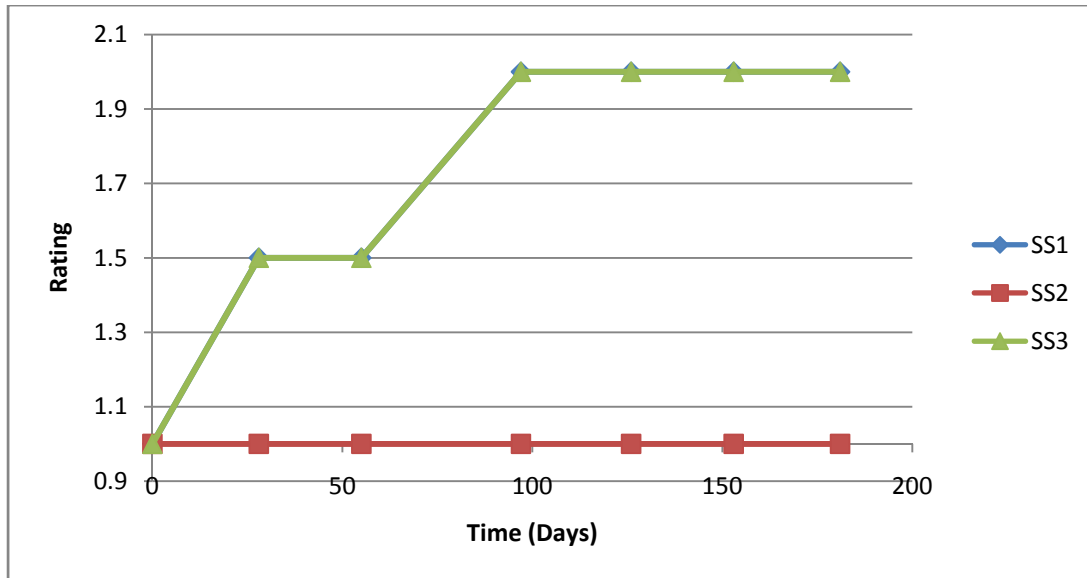


Figure 4.6: Corrosion Rating over Time for Stainless Steel Strands

Note from Figure 4.6 that two of the strands (SS1 and SS3) increased to a rating of 1.5 after one month of exposure and then to a rating of 2.0 after another month of exposure where they then stayed constant. This behavior helps confirm that the ends were exposed to the chloride solution and corrosion attacked these areas quickly. When comparing the stainless steel strands to the stainless clad, they both exhibited corrosion near the ends of the strands while the stainless clad showed signs of corrosion later and performed better in resisting this corrosion. The weight loss of the stainless steel strands is similar to the stainless clad.

4.2.4 Hot Dip Galvanized (GV)

The hot dip galvanizing is known for being a sacrificial anode to the steel it encounters due to its more active position in the emf table. This means that any corrosion present will occur on the zinc coating first. The hot dip galvanized strands of this test performed well showing only signs of corrosion on the zinc coating in the form of a white film. The strands can be seen at six months in Figure 4.7. Notice that there is no rust present, even at the ends, but that the outer layer is covered with a white film. This is what caused the strands to have slightly higher

corrosion ratings even though no rust is present. The corrosion ratings and weight losses of the strands at six months can be found in Table 4.5.



Figure 4.7: Hot Dip Galvanized Strands at Six Months

From Table 4.5, it can be seen that all the strands performed similar at six months ending with an overall corrosion rating of 2.0. The corrosion ratings over time can be seen in Figure 4.8.

Table 4.5: Results of Hot Dip Galvanized Strands at Six Months

	GV1	GV2	GV3
Corrosion Rating	2.0	2.0	2.0
Weight Loss (grams)	2.1	1.9	2.1

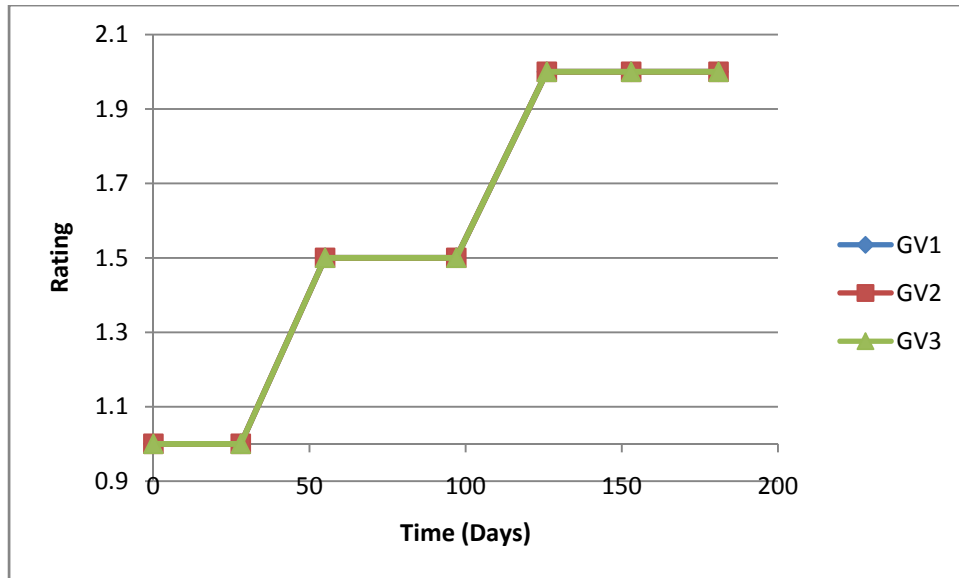


Figure 4.8: Corrosion Rating Over Time for Hot Dip Galvanized Strands

Notice from Figure 4.8 that all the strands performed the same over time, receiving the same corrosion rating at each month. When comparing the hot dip galvanized strands to stainless steel and stainless clad strands, they are very similar in that it took about two months to reach a rating of 1.5, but the overall rating of 2.0 after another two months is what makes the corrosion resistance slightly worse. The weight loss of each of the strands are very close and are higher than the stainless clad and stainless steel strands because of the formation of the white passive film.

4.2.5 Copper Clad (CC)

Copper is known for its corrosion resistance by forming a green oxide film that helps protect the metal. This green oxide film was present on the strands after the testing was complete. Once the strands reach the transpassive region, the green film begins to break down, and corrosion of the metal begins. This is also shown on the strands at six months in Figure 4.9. Notice that the green oxide film is present in the middle of the specimens, while the breakdown and corrosion is present near the ends which is consistent with the other strand types due to the

penetration of the chloride solution within the interstices of the strand. The corrosion rating and weight loss for each strand at six months is found in Table 4.6.



Figure 4.9: Copper Clad Strands at Six Months

Notice from Table 4.6 that the strands all performed the same in terms of corrosion rating at six months with a rating of 3.0. The corrosion rating over time for the strands can be seen in Figure 4.10.

Table 4.6: Results of Copper Clad Strands at Six Months

	CC1	CC2	CC3
Corrosion Rating	3.0	3.0	3.0
Weight Loss (grams)	1.1	1.2	0.8

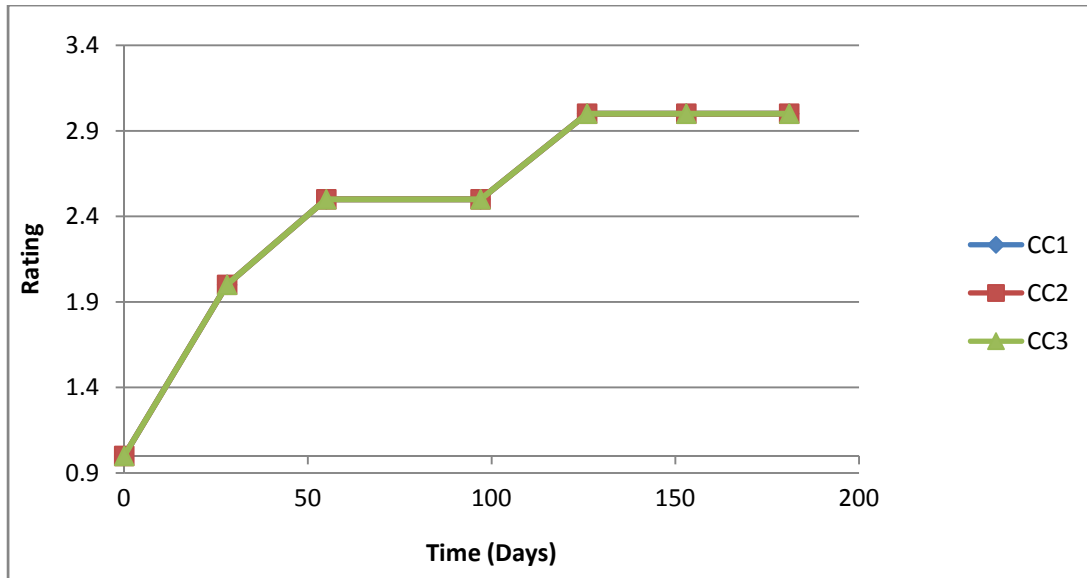


Figure: 4.10: Corrosion Rating Over Time for Copper Clad Strands

Notice from Figure 4.10 that all the strands performed exactly the same at each month. Also notice the steady increase in corrosion rating starting after only one month. This is due to the presence of the green oxide film which formed on the strands. When comparing the copper clad strands to the other strand types, the behavior is similar with steel corrosion present on the ends while the oxide film protected the rest of the strand. The weight loss of the strands is very similar to the stainless clad and stainless steel strands showing that the corrosion resistance of the copper clad is good.

4.2.6 Conventional (CN)

The conventional strands were expected to severely corrode, and they all did exactly that. The strands at six months can be seen in Figure 4.11. Notice the blisters and pitting that have formed on each of the strands which are both signs of extreme corrosion.



Figure 4.11: Conventional Strands at Six Months

The corrosion rates and weight loss at six months are given in Table 4.7. The strands all had corrosion ratings of 7.0+ at six months which means that the corrosion rating table did not go any higher. Although the strands ended with the same corrosion rating, they did not follow the exact same path each month but followed similar trends. The corrosion rating over time for the strands is seen in Figure 4.12.

Table 4.7: Results of Conventional Strands at Six Months

	CN1	CN2	CN3
Corrosion Rating	7.0+	7.0+	7.0+
Weight Loss (grams)	8.3	9.5	12.6

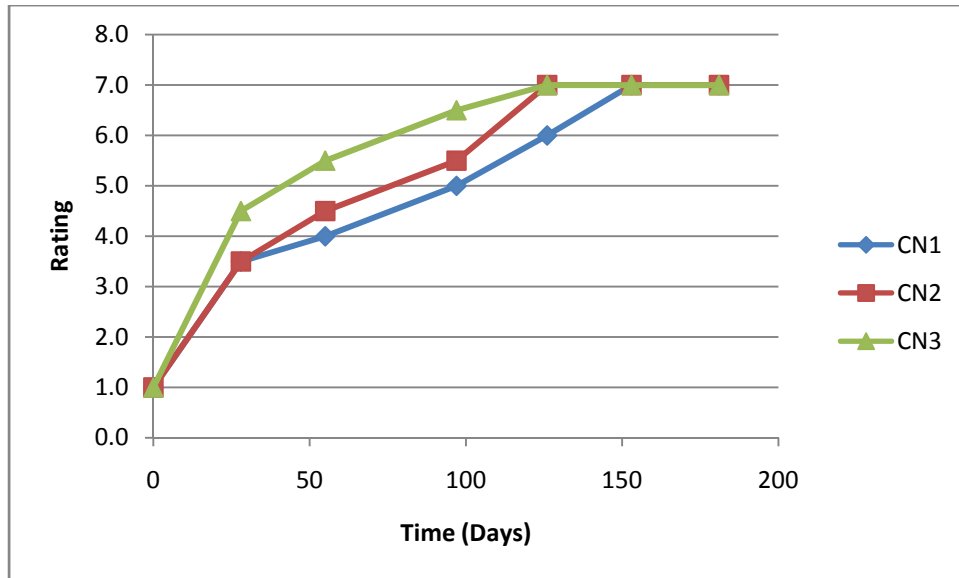


Figure 4.12: Corrosion Rating Over Time for Conventional Strands

Notice from Figure 4.12 that the specimens all followed similar trends over time ending with the highest corrosion rating available. This shows that if the bare strands are exposed to any form of chloride solution, there is no protection at all from corrosion. Also from Figure 4.12, notice the sudden increase in corrosion rating after one month and then the steady increase in corrosion rating each month. This kind of behavior was only seen in the conventional strand as all the others had some form of protection and had final corrosion ratings much less than 7.0+. The weight loss of the conventional strands is much higher than any of the other strands. This is due to the high level of corrosion products removed from the strands. Also, notice the higher scatter in weight loss among the conventional strands when compared to the other strands. This is caused by the high level of corrosion and the variability in the corrosion rating over time. The highest weight loss is in strand CN3 which followed the fastest path to corrosion as shown in Figure 4.12, while the lowest weight loss is in strand CN1 which followed the slowest path to corrosion as shown in Figure 4.12.

4.2.7 Summary of Exposed Strand Test

The exposed strand test gave a great insight into the corrosion resistance of the different types of strands. The results showed trends that were expected such as the epoxy coated strand performing the best and the conventional strand the worst. The other strands followed similar trends between the corrosion ratings and the weight loss. The stainless clad performed slightly better than the stainless steel based on the corrosion ratings and the weight loss. The copper clad showed some variability between the two criteria with a slightly higher average six month rating and a slightly lower average weight loss when compared to the stainless clad and stainless steel. Also, the copper clad had a higher average six month rating than the hot dip galvanized which can be explained by the small corrosion present at the ends due to the chloride penetration. Table 4.8 summarizes the results of average six month rating and average weight loss compared relatively to the epoxy coated base strand.

Table 4.8: Results of All Strands Relative to Epoxy Coated

	EC	SC	SS	GV	CC	CN
AVG 6 Month Rating	1.5	1.5	1.7	2.0	3.0	7.0
vs EC	1.00	1.00	1.13	1.33	2.00	4.67
AVG Weight Loss	0.60	1.07	1.10	2.03	1.03	10.13
vs EC	1.00	1.78	1.83	3.39	1.72	16.89

Notice the similarities in trends of the strands between the average six month rating and average weight loss. The only difference is the slightly lower average weight loss of the copper clad than the other strands. Figure 4.13 shows the corrosion rating over time among all the strands while Figure 4.14 shows the average six month rating relative to the epoxy coated strands. Figure 4.15 shows the average weight loss relative to the epoxy coated strands. Note that the conventional strand has a rating of 16.89, and the plots of the ratings were stopped at 5 to

better show the other strands. Finally, all the strands compared to each other at six months can be seen in Figure 4.16.

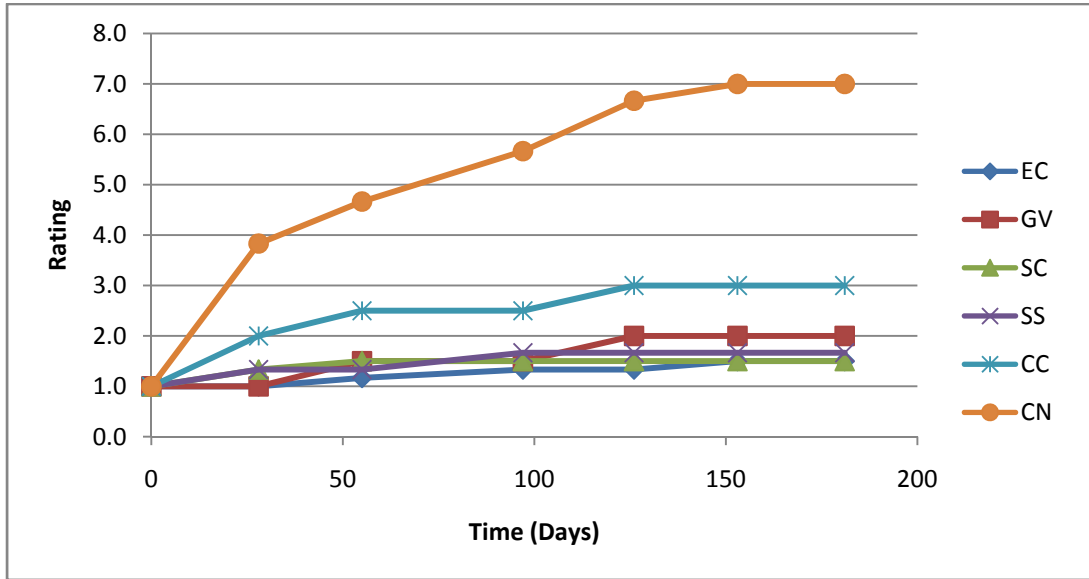


Figure 4.13: Corrosion Rating Over Time for All Strands

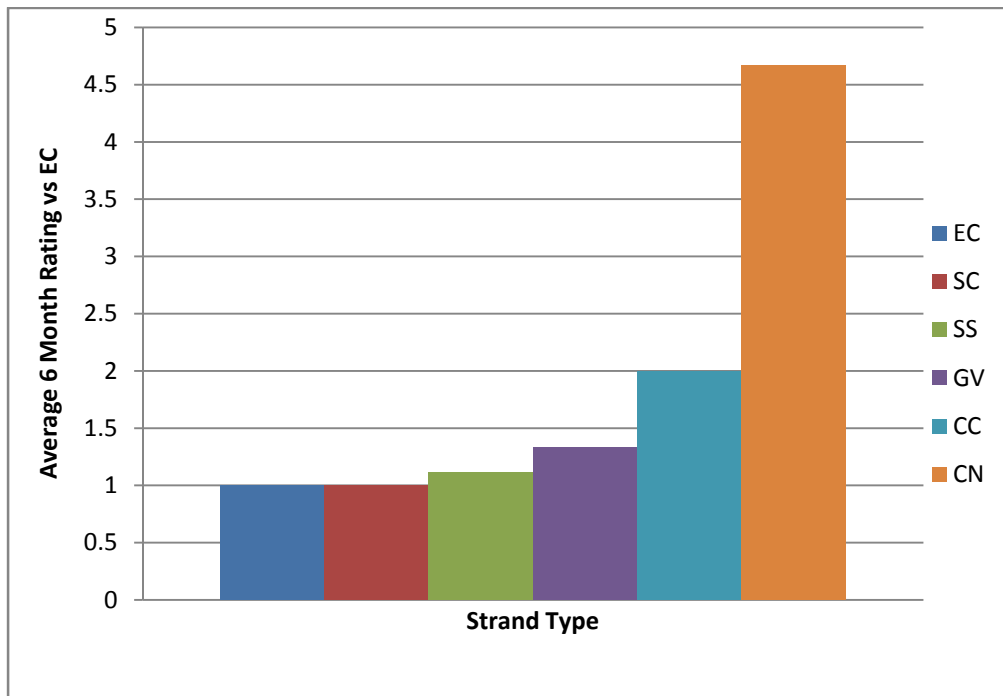


Figure 4.14: Average Six Month Rating vs Epoxy Coated Strand

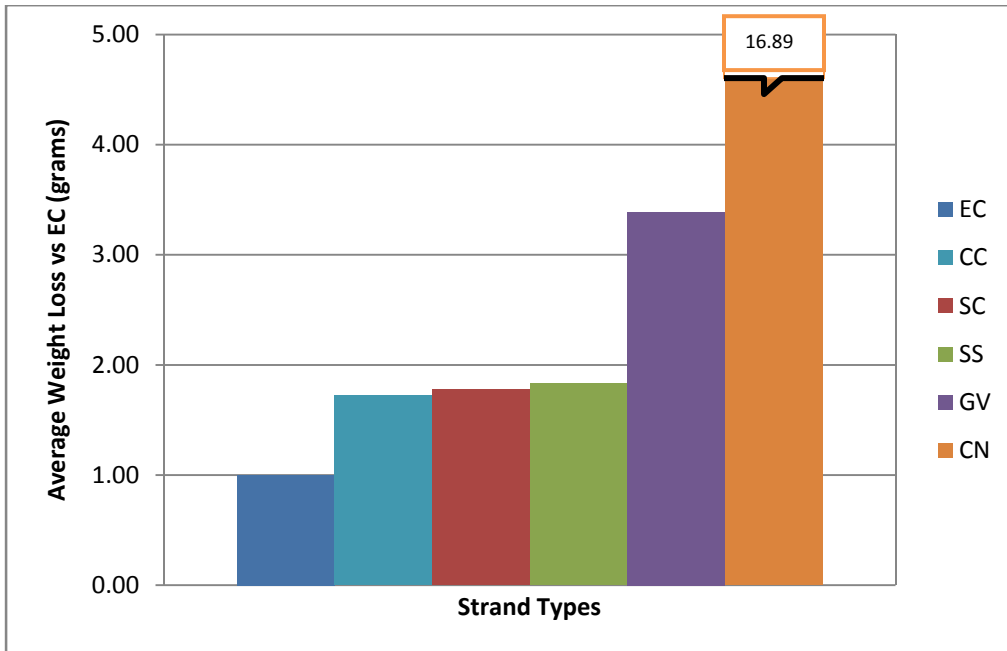


Figure 4.15: Average Weight Loss vs Epoxy Coated



Figure 4.16: All the Strands After Six Months

Notice from all the figures that the obviously worst specimen is the conventional strand which was expected. It had the worst corrosion rating over time (Figure 4.13), worst average six month rating (Figure 4.14), highest average weight loss (Figure 4.15), and worst appearance (Figure 4.16). Also as expected, the epoxy coated strand performed the best. Since the epoxy coated strand was used as the base strand, the next best strand type will be analyzed which is the stainless clad strand. Not including the epoxy coated strand values, the stainless clad strand had the best corrosion rating over time (Figure 4.13), the best six month average (Figure 4.14), a slightly higher weight loss than the copper clad strand (Figure 4.15), and the best appearance along with the stainless steel strand (Figure 4.16).

4.3 Results of Grouted Strand Test

The grouted strand test was conducted for a period of approximately four months. The specimens were made and put into the test setup for about one month before the data logger was connected to take the readings. This allowed the specimens a brief period to create the potential at corrosion known as E_{corr} . Once the data logger was connected, readings were taken for a period of three months. The plots of potential over time were made with the positive values of potential on the plots actually being negative to better show the behavior. After examining the plots of potential versus time for the specimens, it was clear that there was some source of error because all of the specimens were creating more positive potentials over time meaning they were becoming more noble. This is opposite of what should be happening because as the specimens corrode more, they should create more negative potentials or become more active. The simple explanation for the behavior is that the solution the specimens were immersed in evaporated over time and became less corrosive. This would help explain the trend of gain in positive potential over time that all the specimens exhibit. Due to this trend over time, all the specimens will be examined after only one week of data collection where the lines tend to be straight. This value will be considered the corrosion potential, E_{corr} , of the specimen. The black vertical line on all of the plots represents the one week point.

Some of the specimens have rough lines over time that show an up and down motion but still follow a decent trend line while a few of the specimens have very scattered data. The

specimens with the high scatter most likely had an error somewhere in the test setup; therefore they will be ignored. When choosing the representative specimen of each strand type, the most outlying specimen will be discarded, and then the specimen with the least scatter between the remaining two will be chosen. Each of the strand types is discussed below, and a final plot showing the representative specimens of each type will be plotted to show the relative corrosion properties among the strands.

4.3.1 Conventional (CN)

The conventional strands had fairly decent results in that the first week potentials were within one hundred mV_{SCE} of each other, and they all followed similar trends over time. The first and third specimens (CN1 and CN3) had variable scatter over time with CN1 having a severe increase in potential over time at approximately 600 hours and holding that potential until 1200 hours before rejoining the original trend. Due to the scatter in CN1 and CN3, the second specimen CN2 was chosen as the representative specimen with a corrosion potential, $E_{corr} = -875 mV_{SCE}$. Figure 4.17 shows the plot of potential versus time for the specimens.

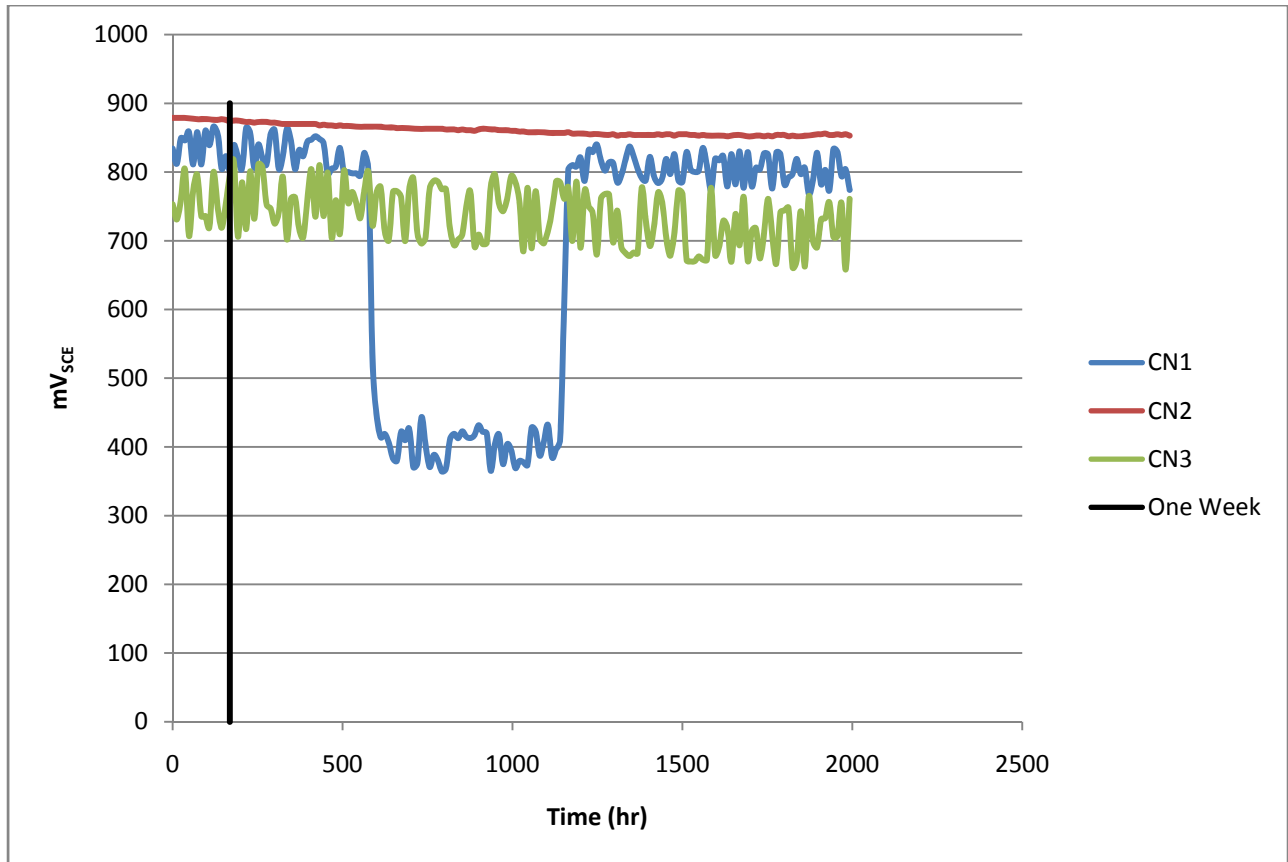


Figure 4.17: Potential vs Time for Conventional Strand

4.3.2 Copper Clad (CC)

Two of the specimens (CC2 and CC3) performed without scatter while CC1 had a considerable amount and was rejected right away. The first week data for both CC2 and CC3 are constant with the corrosion potentials being $E_{\text{corr}2} = -475 \text{ mV}_{\text{SCE}}$ and $E_{\text{corr}3} = -265 \text{ mV}_{\text{SCE}}$. Since both specimens exhibit constant potential versus time in the first week, the average of the two corrosion potentials will be used as the representative value of $E_{\text{corr,AVG}} = -370 \text{ mV}_{\text{SCE}}$. An average line of potential versus time between the two specimens will be used to compare against the other strand types. The potential versus time for the copper clad strands can be seen in Figure 4.18.

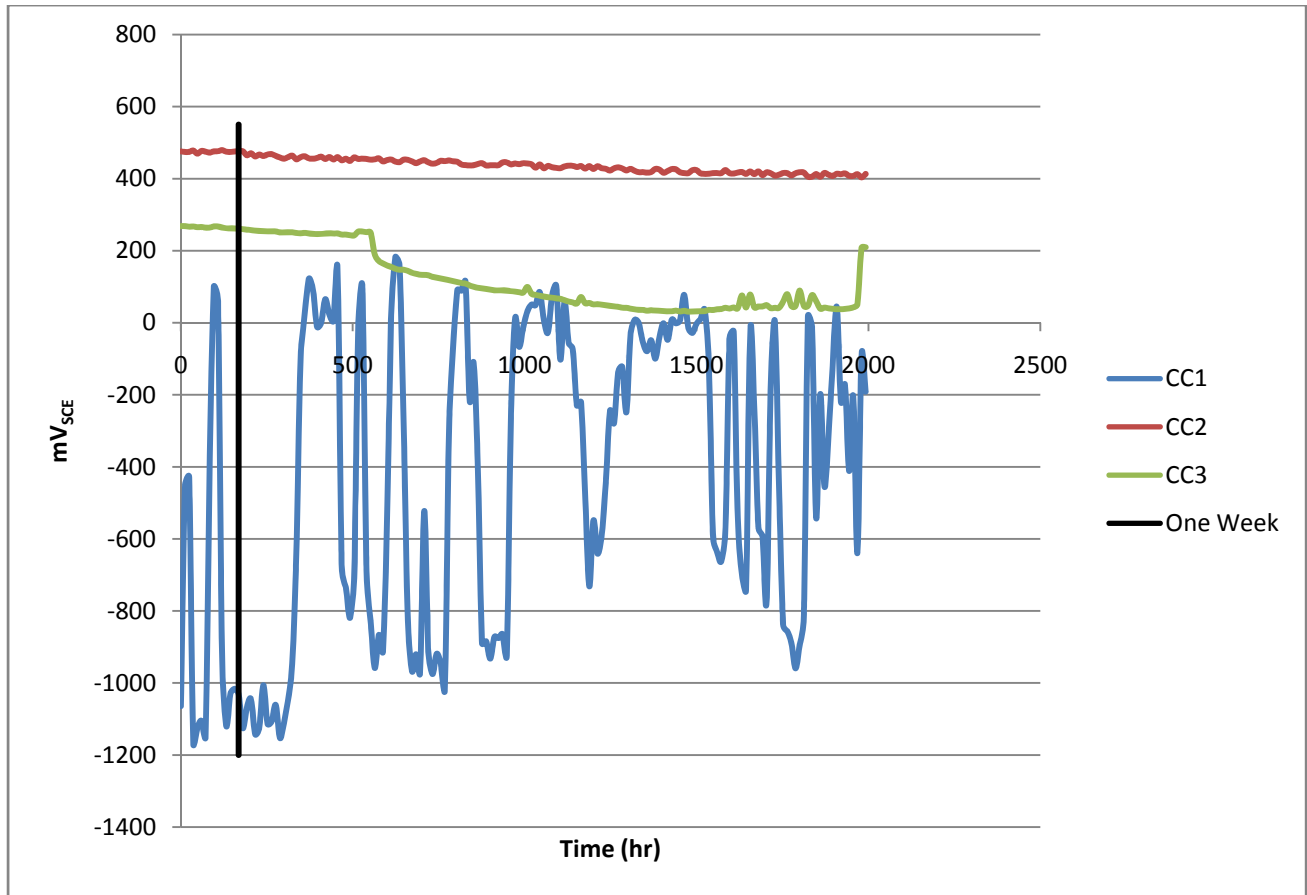


Figure 4.18: Potential vs Time for Copper Clad Strand

4.3.3 Hot Dip Galvanized (GV)

All of the specimens followed almost identical lines in the first week and even up until approximately 600 hours where the third specimen (GV3) has a spike in potential until 1200 hours when the line rejoined the original. Since this same spike is exhibited in the first conventional strand specimen (CN1 in Figure 4.16), the behavior of both is most likely explained by an error in the multiplexer. Since all of the specimens are alike in the first week, the first specimen (GV1) was chosen as the representative specimen by default. The corrosion potential of the specimens is $E_{\text{corr}} = -1025 \text{ mV}_{\text{SCE}}$. Figure 4.19 shows the potential versus time for the specimens.

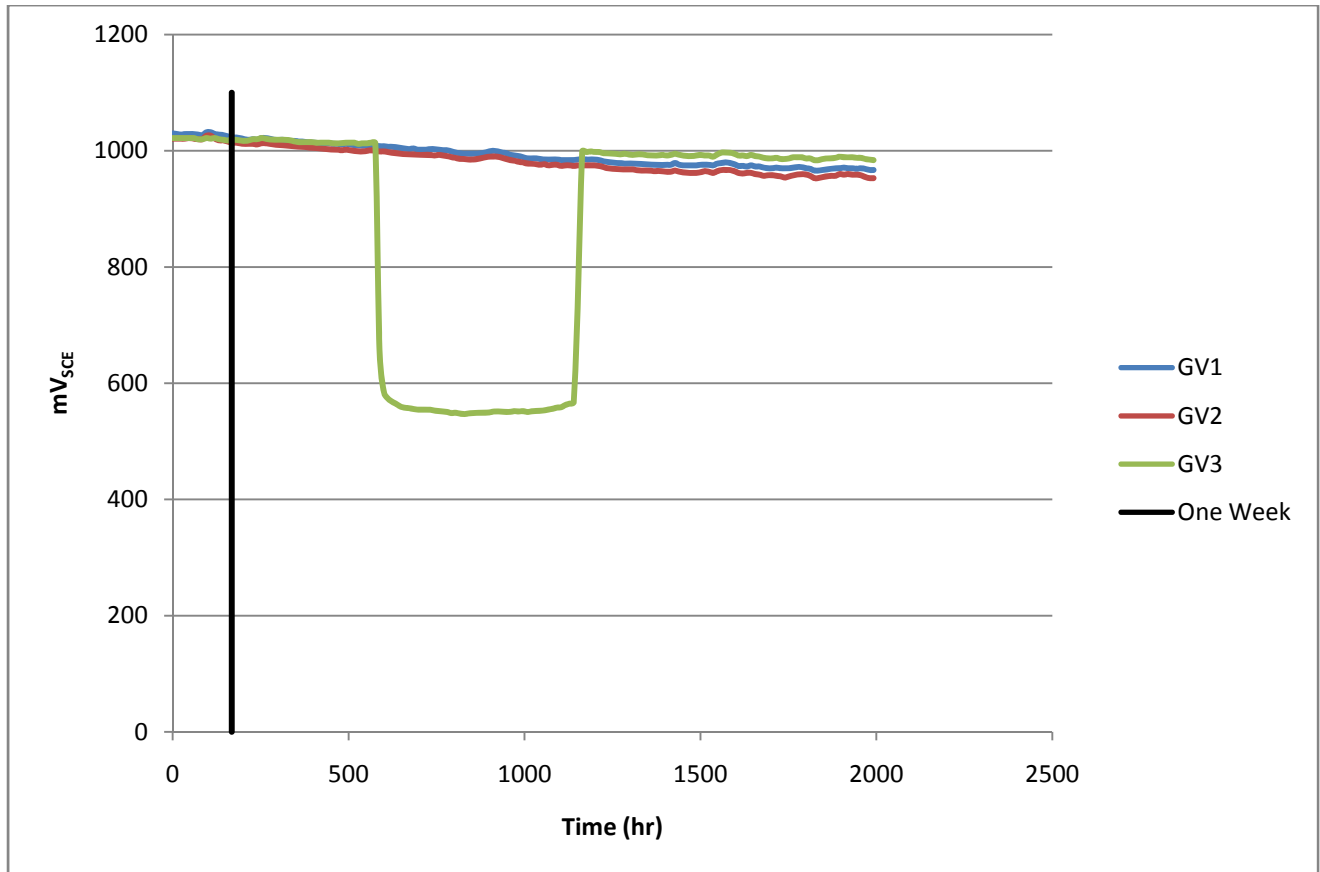


Figure 4.19: Potential vs Time for Hot Dip Galvanized Strand

4.3.4 Stainless Clad (SC)

All the specimens showed some sort of scatter with the third specimen (SC3) having the least over time and the most constant plot in the first week. Therefore, SC3 was chosen as the representative specimen with a corrosion potential, $E_{\text{corr}} = -360 \text{ mV}_{\text{SCE}}$. The plot of potential versus time can be seen in Figure 4.20.

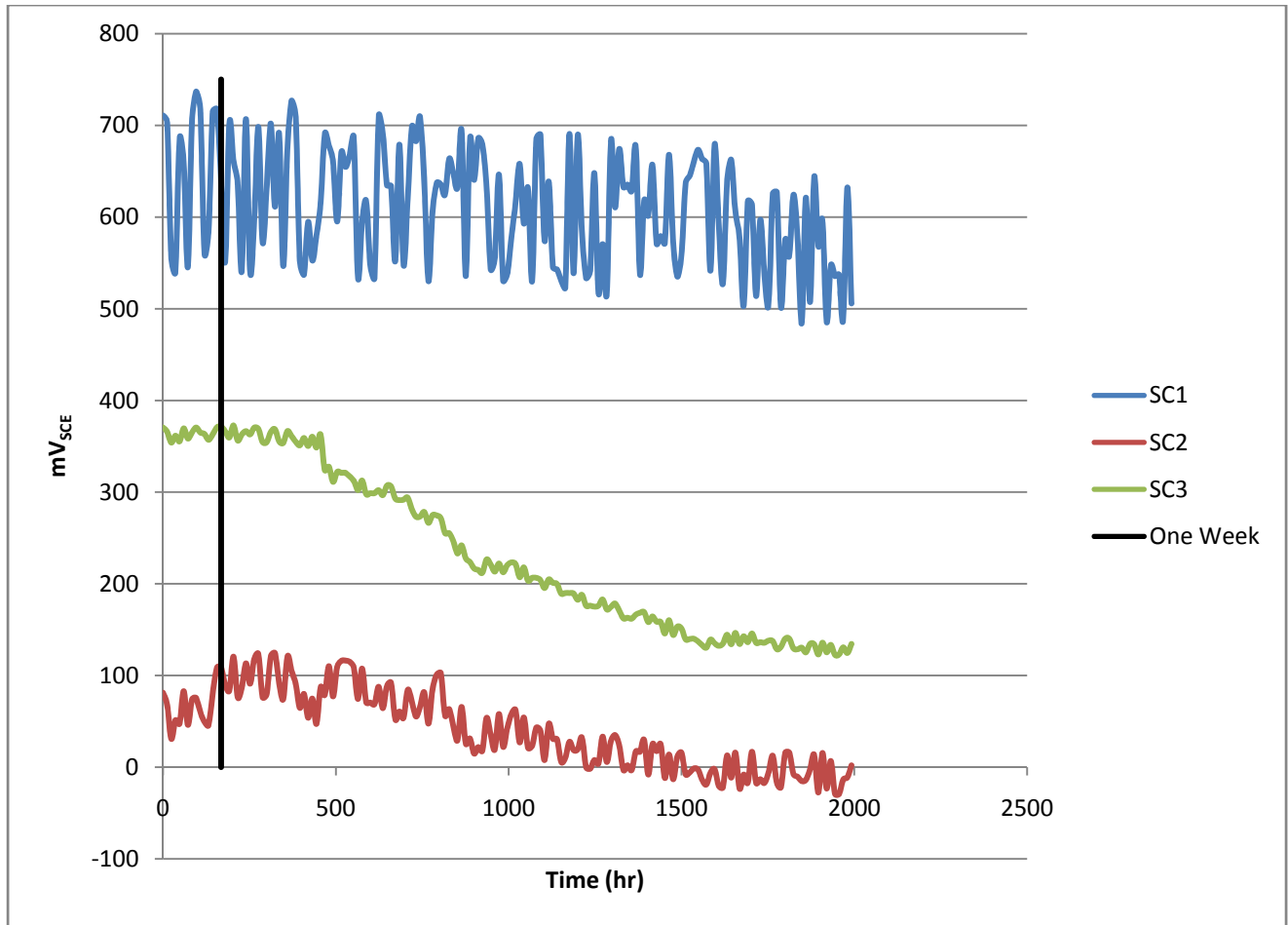


Figure 4.20: Potential vs Time for Stainless Clad Strand

4.3.5 Stainless Steel (SS)

All of the specimens showed smooth lines over time but the third specimen (SS3) was the obvious outlier, so it was removed first. The other two specimens exhibited very similar behavior in the first week but fell off considerably after that over time. Since the second specimen (SS2) showed the least variability over time, it was chosen as the representative specimen. The corrosion potential of SS2 and SS1 are very close; therefore, SS2 will represent the specimen's corrosion potential well. The corrosion potential is $E_{\text{corr}} = -475 \text{ mV}_{\text{SCE}}$. Figure 4.21 shows the potential versus time for the specimens.

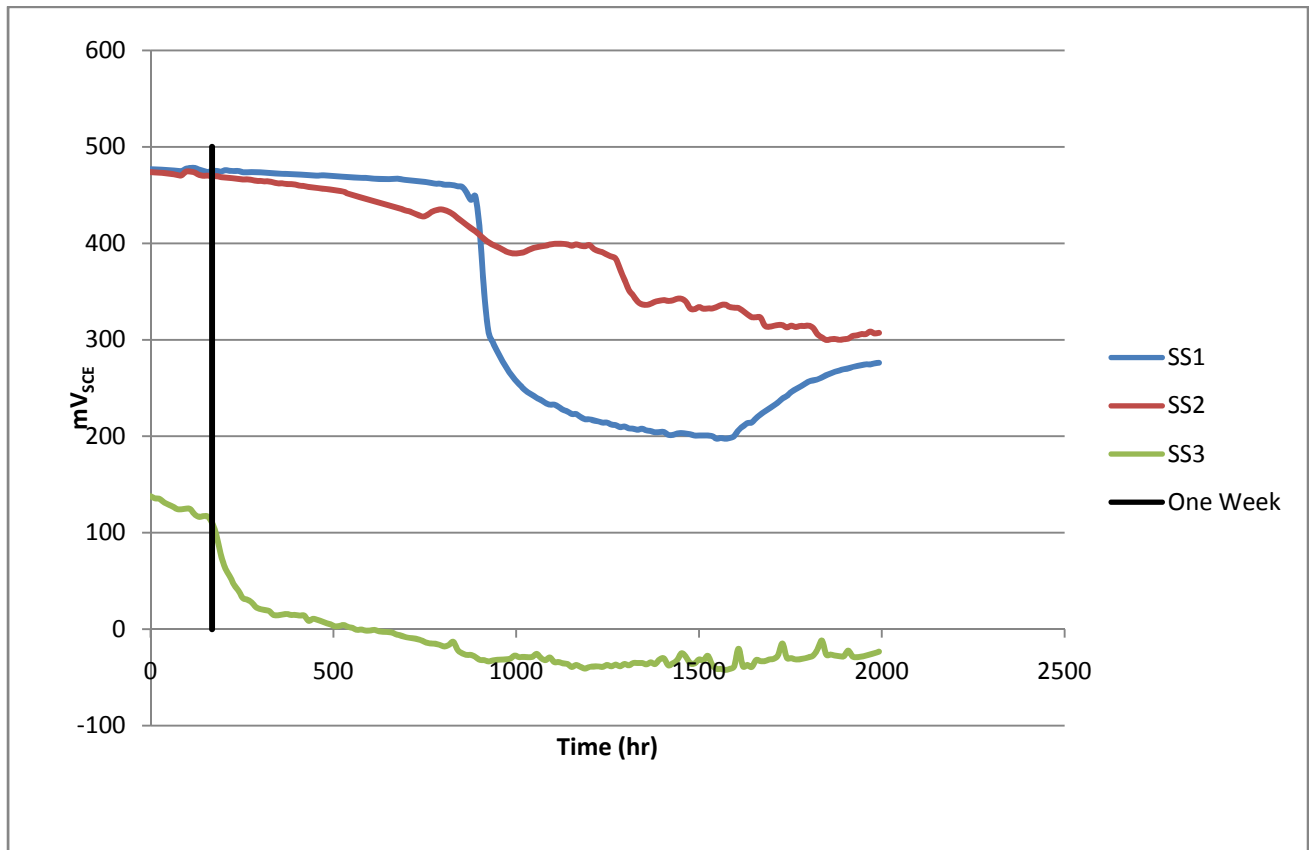


Figure 4.21: Potential vs Time for Stainless Steel Strand

4.3.6 Summary of Grouted Strand Test

Despite the specimens having some scatter and variability over time, the first week represented the corrosion potential well for the specimens. A representative specimen was chosen from each strand type to be plotted and compared relative to each other. Note that an average of the second and third copper clad specimens (CC2 and CC3) was used as the representation. Figure 4.22 shows the potential versus time of the representative strands.

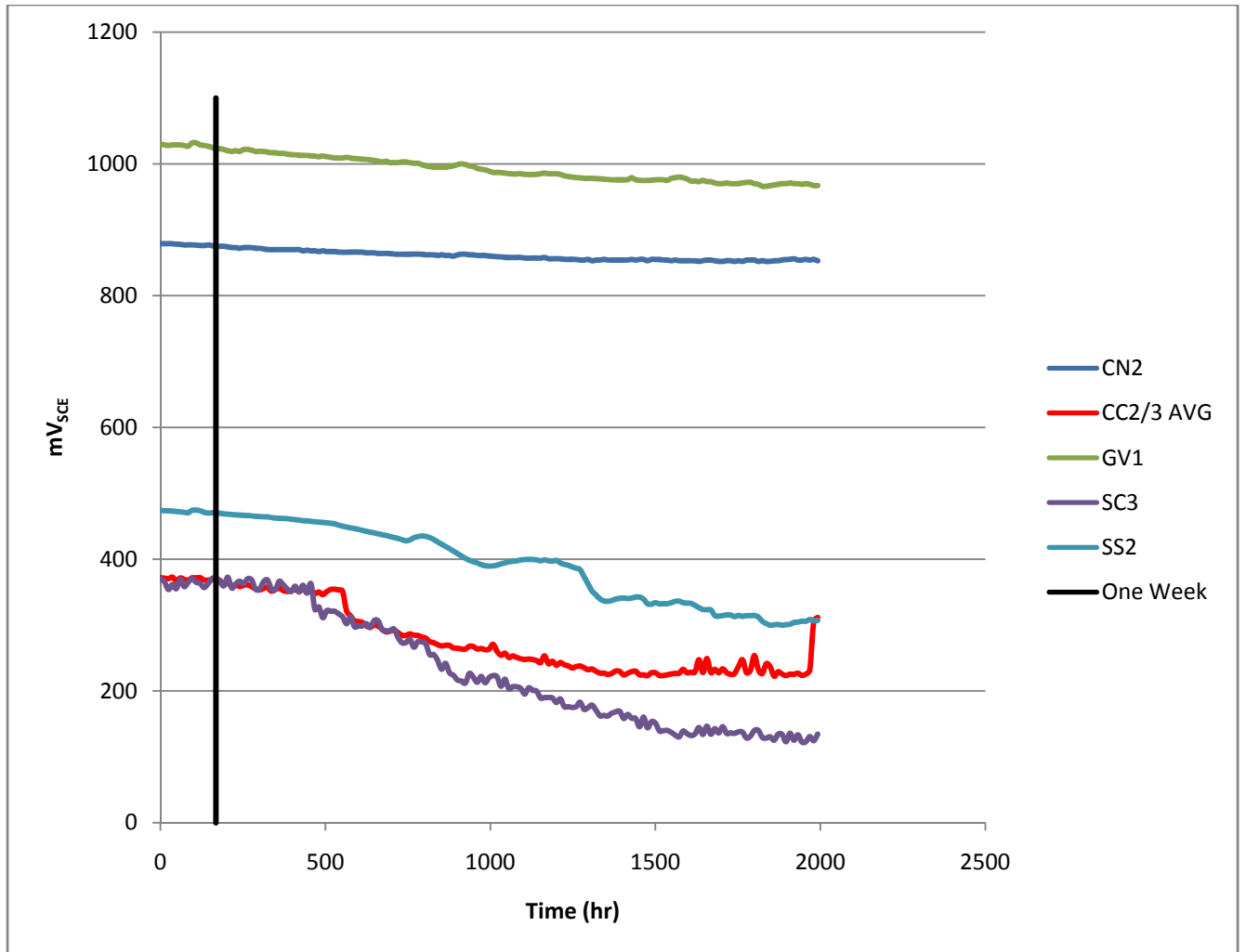


Figure 4.22: Potential vs Time for the Representative Specimens

Note from Figure 4.22 that all the representative specimens have constant potential versus time plots in the first week which represent the corrosion potential. These corrosion potentials can be found in Table 4.9.

Table 4.9: Corrosion Potentials of Representative Specimens

	CN	CC	GV	SC	SS
E_{corr} (mV _{SCE})	-875	-370	-1025	-360	-475

The corrosion potential is a measure of the corrosion tendency of the material with a smaller corrosion potential representing more noble behavior. Therefore, from Figure 4.22 and Table 4.9, it can be seen that the best strand type is the stainless clad strand and the worst is the hot dip galvanized. These results are valid because they follow the emf table exactly in that the hot dip galvanized strand containing zinc is the most active, the conventional strand containing iron is slightly more noble than zinc, and finally, the copper clad and stainless alloys being the most noble. A portion of the emf table can be found in Table 5.1. From the results of the grouted strand test, the specimen that performed the best is the stainless clad strand.

Chapter 5

Accelerated Active Corrosion Testing

5.1 Overview

Project 0-4562 currently being conducted at Ferguson Laboratory is exploring the durability of post-tensioning systems with the usage of different types of duct and tendon material. There is a need to predict the corrosive nature of the tendons prior to the final autopsy in order to have a better understanding of the results. This is achieved by using accelerated corrosion methods to test the specimens. The conditions found in the field are mimicked in the lab to produce similar results. Such conditions include casting the strands in grout encased by a plastic PVC pipe which acts as the tendon duct. A series of accelerated tests are then performed on the specimens including linear polarization resistance testing and potentiodynamic testing. The system used for each test is the same and will be described in detail.

5.2 Description of System

The main electrochemical theories behind the test setup are that of half-cell reactions and mixed potential theory. The test setup utilizes the use of electrodes and an application of potential to measure the corrosive properties. The setup is much like that of a battery, where one element is allowed to corrode, undergoing an electrochemical process. The system consists of another electrode that is more stable, and between the two, the potential created from the corroding element can be measured through the knowledge of half-cell reactions.


5.2.1 Half-Cell Reactions

Half-cell reactions are made up of two types of reactions - cathodic and anodic. The total reaction, which is made up of the two half-cell reactions, is known as the complete or total electrochemical cell. What makes the half-cell reactions appealing for corrosion monitoring is that it is possible to measure a current flow between them. The first step is to set up the

electrodes in the system where the half-cell reactions will occur. The primary electrode in the test setup is the strand encased in grout, also known as the working electrode. In order to measure flow between the electrodes, the half-cell reactions must occur on this working electrode. To achieve this, the second electrode must be naturally more noble. This means that the chosen metal must have a higher electromotive force (emf) potential. This electrode is known as the counter electrode and was chosen to be platinum (Pt) because of its high ranking on the Standard Electromotive Force Potentials Series¹². This series includes the standard potential of many metals relative to the reference potential of hydrogen found in Table 5.1 below. A portion of the emf series is found in Table 5.1.

Table 5.1: Standard Electromotive Force Potentials¹²

	Reaction	Standard Potential, e0 (volts vs. SHE)
	$\text{Au}^{3+} + 3\text{e}^- = \text{Au}$	+1.498
	$\text{Cl}_2 + 2\text{e}^- = 2\text{Cl}^-$	+1.358
	$\text{Pt}^{2+} + 3\text{e}^- = \text{Pt}$	+1.118
	$\text{Fe}^{3+} + \text{e}^- = \text{Fe}^{2+}$	+0.771
	$\text{Cu}^{2+} + 2\text{e}^- = \text{Cu}$	+0.342
	$2\text{H}^+ + 2\text{e}^- = \text{H}_2$	0.000
	$\text{Pb}^{2+} + 2\text{e}^- = \text{Pb}$	-0.126
	$\text{Sn}^{2+} + 2\text{e}^- = \text{Sn}$	-0.138
	$\text{Ni}^{2+} + 2\text{e}^- = \text{Ni}$	-0.250
	$\text{Fe}^{2+} + 2\text{e}^- = \text{Fe}$	-0.447
	$\text{Zn}^{2+} + 2\text{e}^- = \text{Zn}$	-0.762



 More Noble

The half-cell potential (corrosion potential) of the working electrode (strand) can be measured by introducing another electrode into the system. This is known as a reference electrode, and the half-cell potential (corrosion potential) will be measured relative to the known electromotive force potential of the reference electrode. See Figure 5.1 for the system used in testing. The reference electrode chosen is a Saturated Calomel Electrode (SCE) which is a common reference for these tests and is also used in field applications such as Project 4562. Other references are available and can be found in Table 5.2.

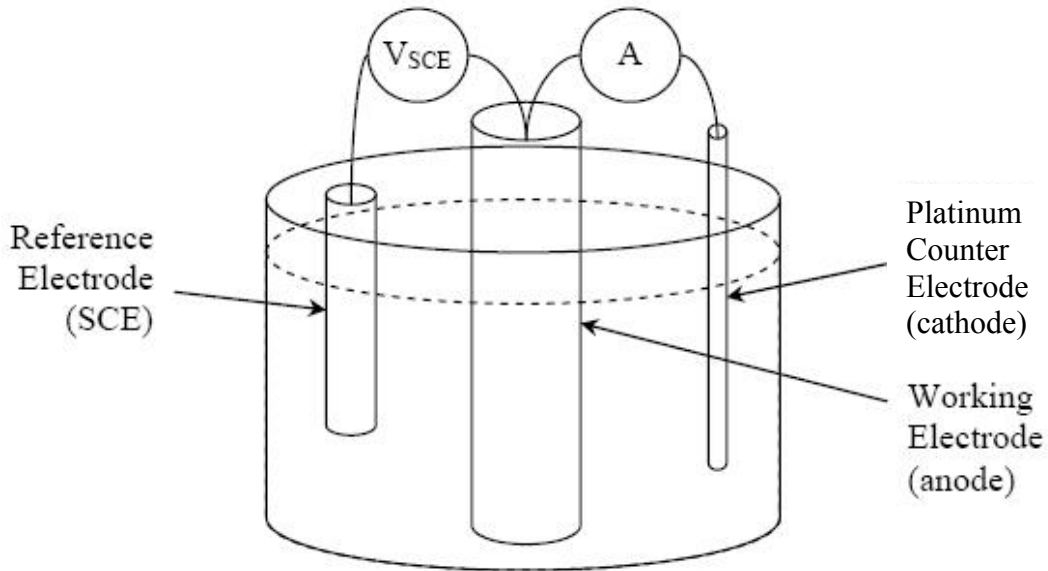


Figure 5.1: Basic Test Setup¹⁴

Table 5.2: Common Secondary Reference Electrodes¹²

Name	Half-Cell Reaction	Potential V vs SHE
Mercury-Mercurous Sulfate	$\text{HgSO}_4 + 2\text{e}^- = \text{Hg} + \text{SO}_4^{2-}$	+0.615
Copper-Copper Sulfate	$\text{CuSO}_4 + 2\text{e}^- = \text{Cu} + \text{SO}_4^{2-}$	+0.318
Saturated Calomel	$\text{Hg}_2\text{Cl}_2 + 2\text{e}^- = 2\text{Hg} + 2\text{Cl}^-$	+0.241
Silver-Silver Chloride	$\text{AgCl} + \text{e}^- = \text{Ag} + \text{Cl}^-$	+0.222
Standard Hydrogen	$2\text{H}^+ + 2\text{e}^- = \text{H}_2$	+0.000

5.2.2 Mixed Potential Theory

The theory behind the results of the tests is based on mixed potential theory. The relation of potential and current in a corroding system is not linear but in fact related exponentially¹². This is described by the Butler-Volmer equation shown in Equation 5.1¹².

$$i = i_0 \left(e^{2.3 \frac{\eta}{\beta_a}} - e^{-2.3 \frac{\eta}{\beta_c}} \right) \quad \text{Equation 5.1}^{12}$$

where

i = current density (I/A where 'I' is the current and 'A' is the exposed area to the electrolyte)

i_0 = exchange current density (Current flow per unit area between reactants and products at equilibrium)

η = overpotential ($\eta = E - E_0$, 'E' is the applied potential and E_0 is the equilibrium potential)

β_a & β_c = Tafel Constants

The Tafel constants in this equation are found from the plot between the applied potential and the log of the current density. The Tafel constants are calculated as the slopes of the respective legs on the plot. Figure 5.2 shows the plot with the Tafel constants present.

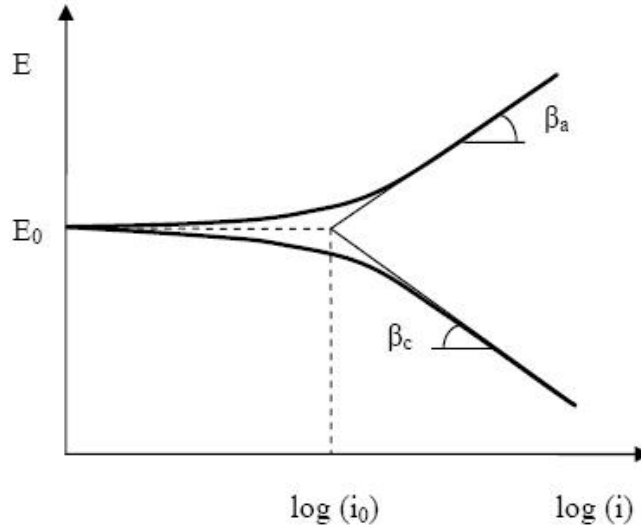


Figure 5.2: Plot of Applied Potential vs log of Current Density¹⁴

When the half-cell reactions, anodic and cathodic, of the working electrode (strand) are combined, the E_0 and i_0 become E_{corr} and i_{corr} , respectively, and there is a mixed result based on the mixed potential theory¹². The values of E_{corr} and i_{corr} represent the corrosion potential and current density respectively for the combined cell. The plot of the mixed potential is highly ideal and does not occur in the field due to the presence of passivity. A plot of the mixed potential is found in Figure 5.3.

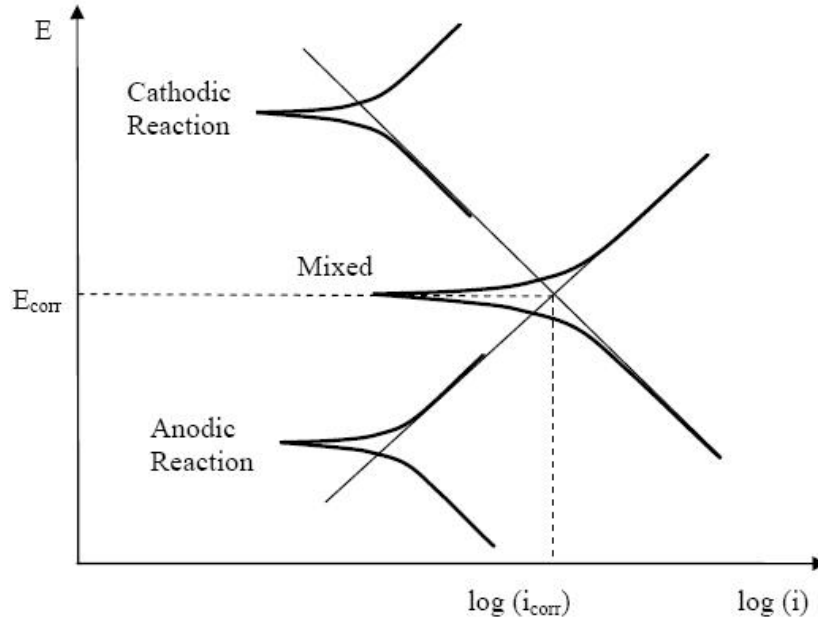


Figure 5.3: Mixed Potential Plot¹⁴

5.3 Linear Polarization Resistance Accelerated Corrosion Testing

The linear polarization resistance (LPR) test is the first of the accelerated corrosion tests performed on the specimens. The actual test stems from polarization resistance theory in which the first part of the curve is linear. The test is similar to that of the potentiodynamic test described in the next section, except the applied potential range is less, usually around +/- 20 mV. This range does not cause damage because the specimen is not polarized. This allows the specimen to be retested if desired. The polarization resistance R_p is the slope of the initial linear portion of the overvoltage versus current plot¹². This plot is found in Figure 5.4.

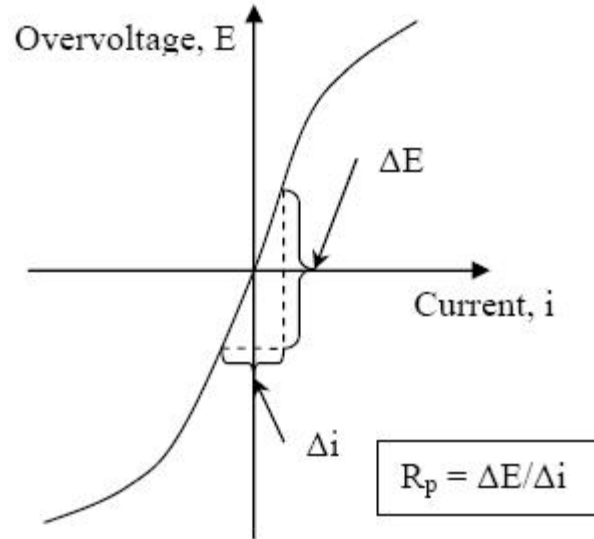


Figure 5.4: Plot of Linear Polarization Resistance¹⁴

R_p is defined as the change in overvoltage divided by the change in current of this initial portion, independent of how linear it actually is. This means that the values are chosen at the end of the proposed linear region even if the actual curve is not particularly linear. Also, the polarization resistance is inversely proportional to the corrosion rate which is dependant upon i_{corr} . This relationship can be seen in Equation 5.2.

$$R_p = \frac{\beta_a \beta_c}{2.3 i_{corr} (\beta_a + \beta_c)} \quad \text{Equation 5.2}$$

Note that R_p is also a function of the Tafel constants which typically range between 112 and 224 mV¹⁴. Due to the different materials of the specimens being tested, the Tafel constants had to be calculated from the potentiodynamic plots of Mac Lean's¹⁴ work. From work done by Pacheco¹⁵, the time to corrosion is related to the polarization resistance by $t_{corr} = 1.25R_p$, where t_{corr} is in hours, and R_p is in $k\Omega cm^2$. This relationship will be used in the results to find the relative time to corrosion among the different strand types.

5.4 Potentiodynamic Accelerated Corrosion Testing

The theory behind potentiodynamic testing is that the potentials are applied in steps, and these steps depend on the specimen and what range of the curve is needed. At each specified step, the current is measured from the system. With these recordings, a plot of applied voltage versus current can be completed and is found in Figure 5.5.

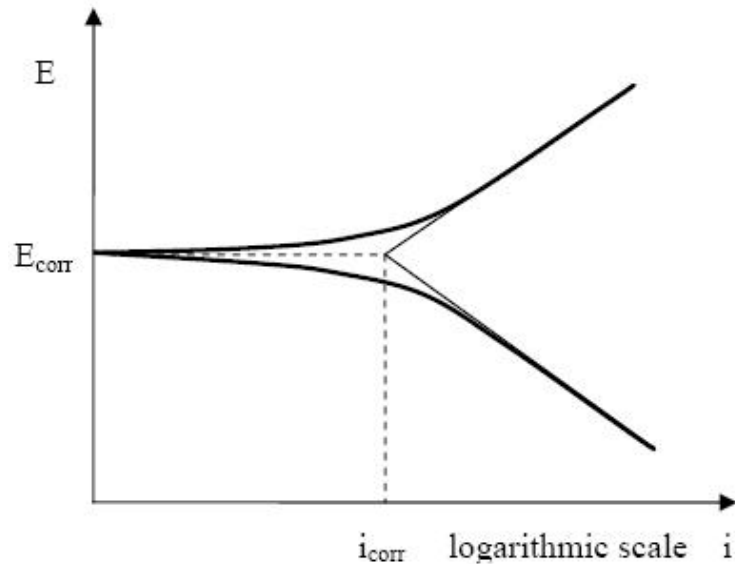


Figure 5.5: Plot of Applied Voltage vs log of Current from Potentiodynamic Test¹⁴

Many values can be obtained from this plot. The point on the plot where the legs begin is the point at which corrosion occurs. The values obtained are potential at corrosion, E_{corr} , and time to corrosion, i_{corr} . From the slopes of the legs, the Tafel constants, β_a and β_c , are calculated¹². The plot must be in semi-log to obtain the Tafel constants. The results from the test are from all the different ranges of passivity which allow a complete description of the behavior and makes this test very appealing. Figure 5.6 shows a potentiodynamic plot of each of the strand types.

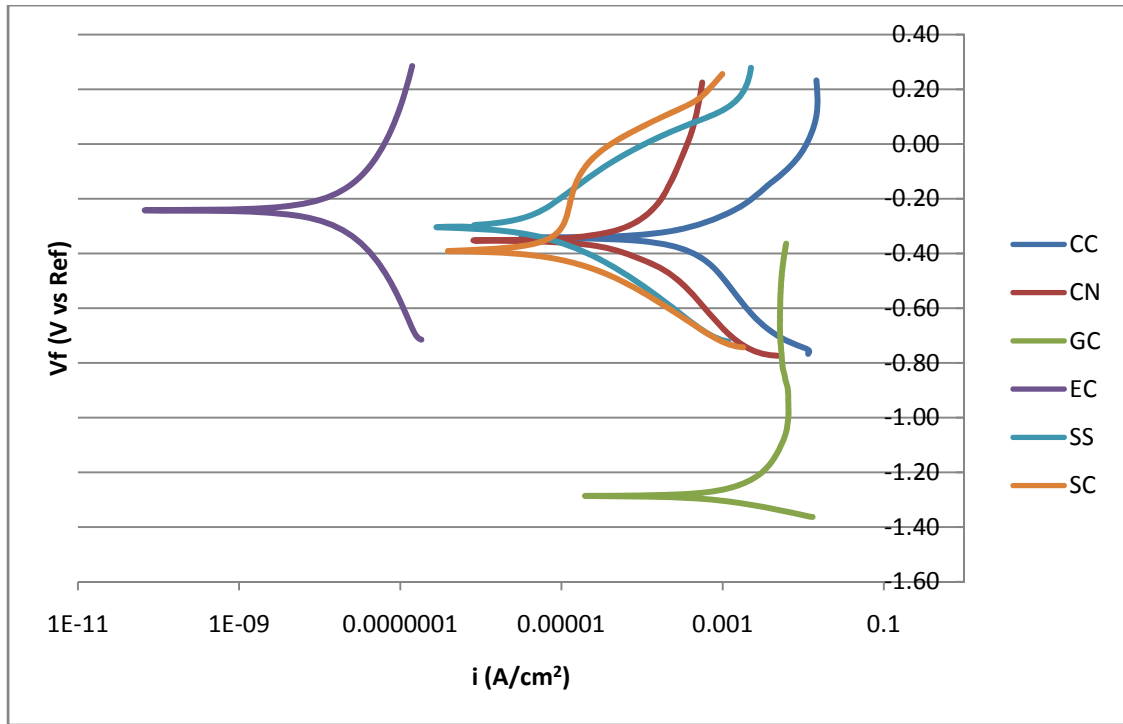


Figure 5.6: Potentiodynamic Plots of all Strand Types

5.5 Testing Setup and Procedure

The setup includes specimens of the different types of strands to be tested using the accelerated corrosion tests mentioned above. The specimens consist of the strands grouted in pipes to represent the field conditions of tendons grouted in ducts. The procedure is very similar to Mac Lean's¹⁴ testing sequence except these specimens will be pre-cracked to allow the electrolyte to reach the strands easier. The device used for pre-cracking the specimens is found in Figure 5.7. The device is fabricated from steel plates and applies a uniform moment across the exposed grout region. The two supports for the exposed grout region (white plate and blades) are lowered down gradually using the all-threaded bolt. The system is deformation controlled which allows for a uniform force and moment across the section. As a result, the variability in cracking is small among all the sections.

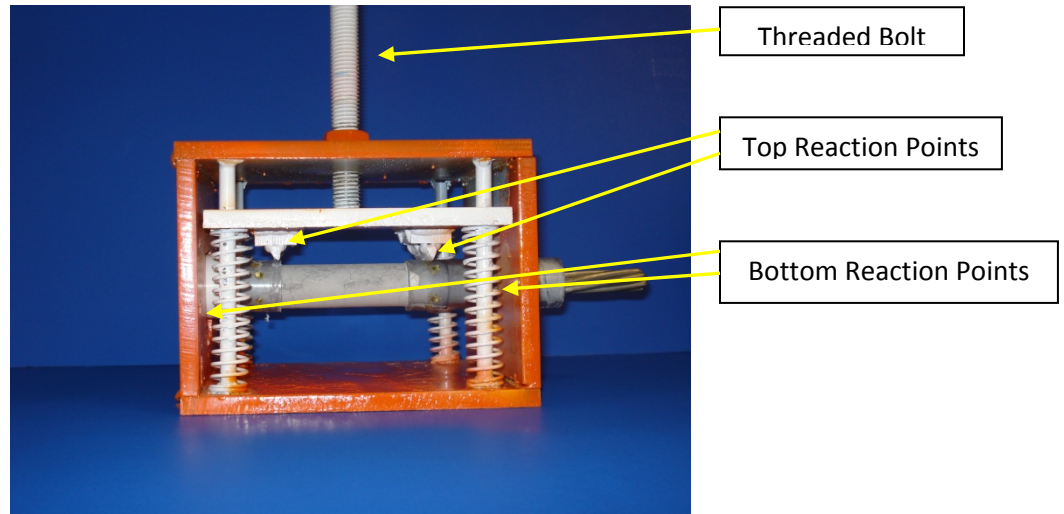


Figure 5.7: Pre-Cracking Device

The pre-cracking exhibits the behavior of actual conditions when the grout used to seal the anchorages of the tendons cracks under certain conditions. Three strands of each type specified in Section 1.5.1 will be tested using these methods making a total of eighteen specimens.

The grout used in the specimens is the same as in Section 3.3.2.1 which is SikaGrout 300PT. The electrolyte used is a 5% chloride solution by weight, stored in a 1000 mL beaker. The specimens are cast and allowed to cure in a fog room for twenty-eight days. After curing, the pipe is removed over the exposed region of grout (See Figure 5.13 below). The specimen is then pre-cracked using the device in Figure 5.7. The exposed region for the 0.5 in. strand is 3.5 in., and for the 0.6 in. strand, the exposed region is 3.2 in. as can be seen in Figure 5.10 in Section 5.6 below. Once cracked, the specimens are ready to be tested. They are placed in the beaker of chloride solution and attached to the equipment. The equipment used was provided and installed by Gamry Electronics and consists of the Series G 750 Potentiostat/Galvanostat/ZRA. The Potentiostat was installed directly inside a computer and can be seen in Figure 5.8.



Figure 5.8: Potentiostat Built into Computer

Along with the specimen known as the working electrode, two more electrodes are added to the setup. One of them is the counter electrode consisting of a platinum clad wire. This material was chosen due to its high nobility in the electromotive potential series allowing the corrosion, or half-cell reactions to occur, on the working electrode. The final electrode used is known as the reference electrode consisting of a saturated calomel electrode. The electromotive force potential of the reference electrode is used as a standard base point to measure the potential of the working electrode. Figure 5.9 shows the final configuration before testing begins.

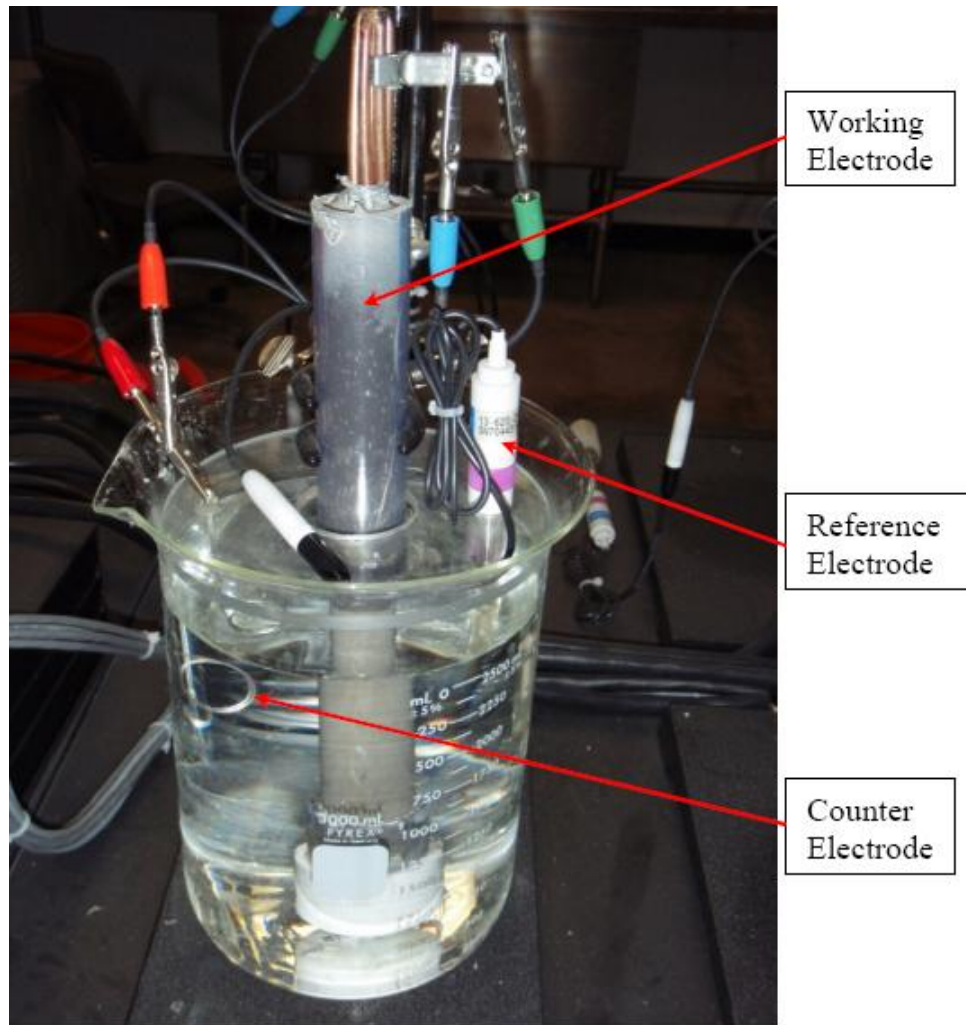


Figure 5.9: Test Setup with Different Electrodes¹⁴

Once all the electrodes are in place and connected to the equipment, the linear polarization resistance test is run first. Since the potential range scanned on the specimen is ± 20 mV, the test only takes about one to two minutes to run. Because the range is so low, the specimen does not polarize permanently and is not damaged which allows the potentiodynamic test to be run. This test scans the range of passivity of the specimen which will show the time to corrosion and give the Tafel constants. The range scanned is ± 500 mV. Throughout the test, a stepping potential is applied which depends on the specimen. At each step, a current is recorded to produce an applied voltage versus current plot showing time to corrosion and allowing the calculation of the Tafel constants. Since the test scans more ranges on the specimen, the time to

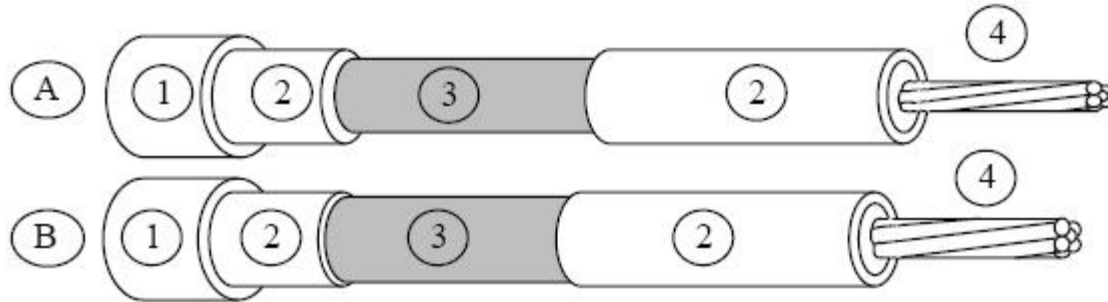
perform the test is approximately forty-five minutes. The testing variables are specified in Table 5.3.

Table 5.3: Testing Variables

	Linear Polarization Resistance	Potentiodynamic
Initial E (mV) vs E_{oc}	-20	-500
Final E (mV) vs E_{oc}	20	500
Scan Rate (mV/s)	0.5	0.5
Sample Period (s)	0.2	5

5.6 Specimen Design and Construction

The specimens chosen for testing consist of the different types of strands specified in Section 1.5.1 cast in grout inside a PVC pipe. Half of the specimens have a diameter of 0.5 in. while the remaining have a diameter of 0.6 in. The grout cover in the exposed region of the specimen needed to be the same so as not to skew the results. The thickness of the grout cover affects the time the electrolyte will reach the specimen and is known as ohmic electrolyte resistance¹⁴. The manufacturer only provided a one inch diameter pipe; therefore, machining would be necessary. The difference in grout cover caused the length of the exposed grout region to be different for each type of specimen. Figure 5.10 shows these configurations.



A: specimen for 0.5 in strands

1. 25.4 mm (1 in) PVC end cap
2. Clear PVC tubing: 50.8 mm (2 in) in end cap & 101.6 mm (4 in)
3. Exposed Grout: 25.4 mm (1 in) dia., length 90 mm (3.5 in)
4. 12.7 mm (0.5 in) prestressing strand: length 305 mm (12 in)

B: specimen for 0.6 in strands

1. 25.4 mm (1 in) PVC end cap
2. Clear PVC tubing: 50.8 mm (2 in) in end cap & 101.6 mm (4 in)
3. Exposed Grout: 28 mm (1.1 in) dia., length 81.3 mm (3.2 in)
4. 15.2 mm (0.6 in) prestressing strand: length 305 mm (12 in)

Figure 5.10: Design of Different Types of Specimens¹⁴

The PVC pipe for the 0.6 in. specimens had to be bored to make the final inside diameter 1.1 in. This was done using a lathe in the same manner as in Section 3.3.2.1. Once again, not only was the PVC section over the exposed grout region bored, but also the outer sections were bored one inch to allow a gradual change of diameter around the exposed region. This can be seen in Figure 5.11.

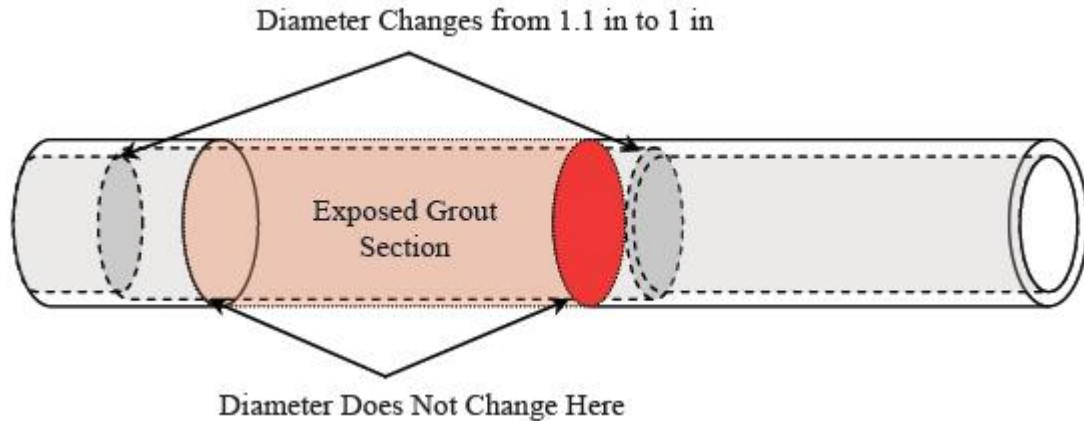


Figure 5.11: Boring Diagram for 0.6 in. Specimens¹⁴

After boring, the exposed grout section was grooved as in Section 3.3.2.1 using the Lagun Republic Mill. There was just enough material left in the groove to keep the section connected. This allowed for easy removal after the specimens cured. To keep the strands centered in the pipe, a grid of 1/16" acrylic rods was placed in each of the outer sections. The holes were drilled using the Lagun Republic Mill. Figure 5.12 shows an outline of the grid. After all the sections were machined, construction of the pipe began. First, the acrylic rods were placed and held using a fast drying epoxy. The brand name is Loctite Quickset Epoxy as used in Section 3.3.2.1. Next, the outer sections were attached using a clear silicone (See Figure 3.15). When the sections were firmly set, the end cap was placed using plumbing cement.

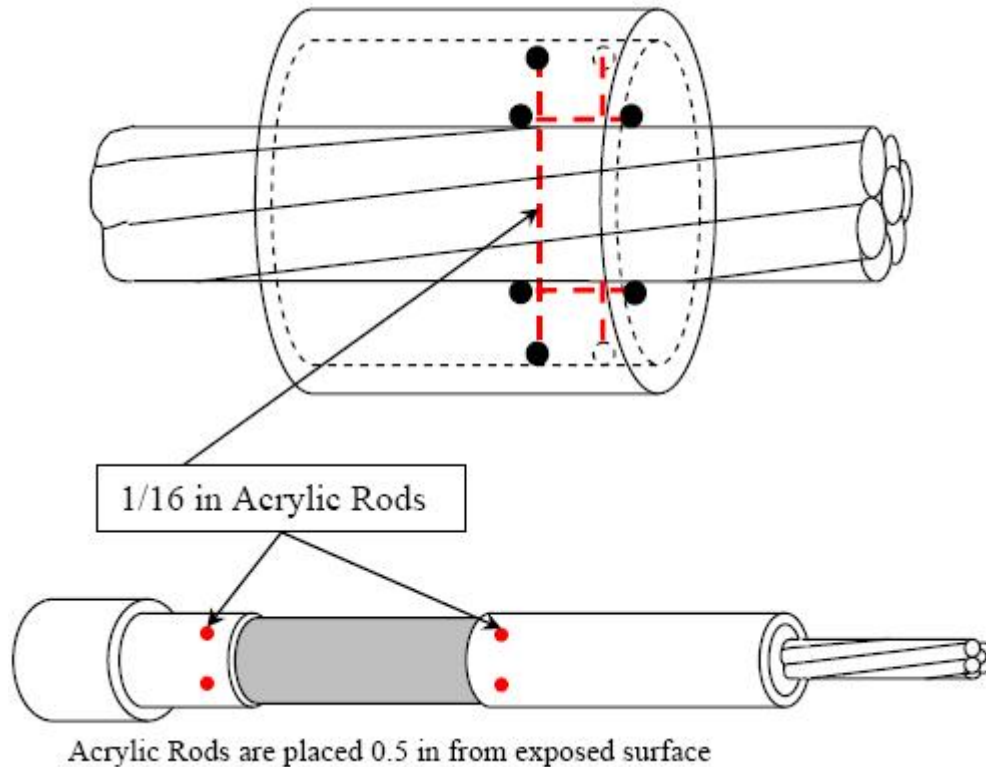


Figure 5.12: Grid Pattern and Location of Acrylic Rods¹⁴

Three strands of each type were chosen for testing. They were cut to a length of twelve in. using the chop saw, and the ends were ground down using the table grinder, both in Figure 3.1. The strands were then cleaned of debris and placed in the pipes through the acrylic grids. The grout used for the specimens was the same as in Section 3.3.2.1 - SikaGrout 300 PT which is a pre-mixed, non-bleed, high-flow grout. The water to cement ratio was chosen as 0.3 to allow for easy flow into the pipes. The grout was mixed using a variable speed mixer with a high-shear blade (See Figure 3.16). A funnel was used to channel the grout into the pipes. The specimens were poured in phases such that six would be tested per day for three days. They were allowed to cure for twenty-eight days in a fog room. Once curing was complete, the pipe over the exposed grout region was removed. Figure 5.13 shows the section after removal of the pipe over the exposed region. The specimens were then placed in the cracking device to be pre-cracked. Then they were put into the electrolyte solution and attached to the testing equipment.



Figure 5.13: Specimen After Removal of Pipe Over Exposed Region

Chapter 6

Results of Accelerated Active Corrosion Testing

6.1 Overview

Two accelerated active corrosion tests were performed to evaluate the corrosion resistance properties of the strand types. The tests include the linear polarization resistance test and the potentiodynamic test outlined in Chapter 5. Sean Mac Lean¹⁴ used these same tests, and his results will be used as a comparison. The new addition to the current tests is that the specimens will be pre-cracked to model actual field conditions which allow the electrolyte to reach the strands quicker. The linear polarization resistance test is the first and main test performed on the specimens. The results produce a relative time to corrosion among the different strand types. The potentiodynamic test is then performed on the specimens and is used to show the different active and passive ranges among the different strand types. The test also produces the Tafel constants of the specimens which are needed in the analysis of the linear polarization resistance plots.

The results of the tests are outlined in the following sections and include plots of the potentiodynamic and linear polarization resistance of the three tests per strand. The linear polarization resistance data were plotted where the current density is equal to zero because the slope of this region is defined as the polarization resistance, R_p , used to evaluate time to corrosion. Values of 5 mV above and below E_{corr} were used to determine the polarization resistance because the plot was assumed to be linear in this region. E_{corr} values from both the linear polarization resistance and potentiodynamic tests were gathered but did not always coincide. Therefore, the values of E_{corr} from the linear polarization resistance test will be used as it was the main test performed. The results of the pre-cracked test series will be compared to those of Mac Lean's. Mac Lean's¹⁴ work included ten tests of each strand type which will be used to compare variability in the different testing series.

The exposed area used for analysis was assumed to be the exposed grout region although it is feasible for the electrolyte to enter into the area between the PVC and grout. If the electrolyte were to enter into the PVC, the time for this to occur and the amount the electrolyte travelled would be unknown. Since the specimens are similar in design and the tests are used for relative comparisons among the strands, it was assumed these actions were the same throughout all the specimens, therefore making the calculations simpler.

The potentiodynamic plots of all the strands show the specimens through a range of potentials. The corrosion potential of the specimen is defined as E_{corr} and can be seen in Figure 6.1.

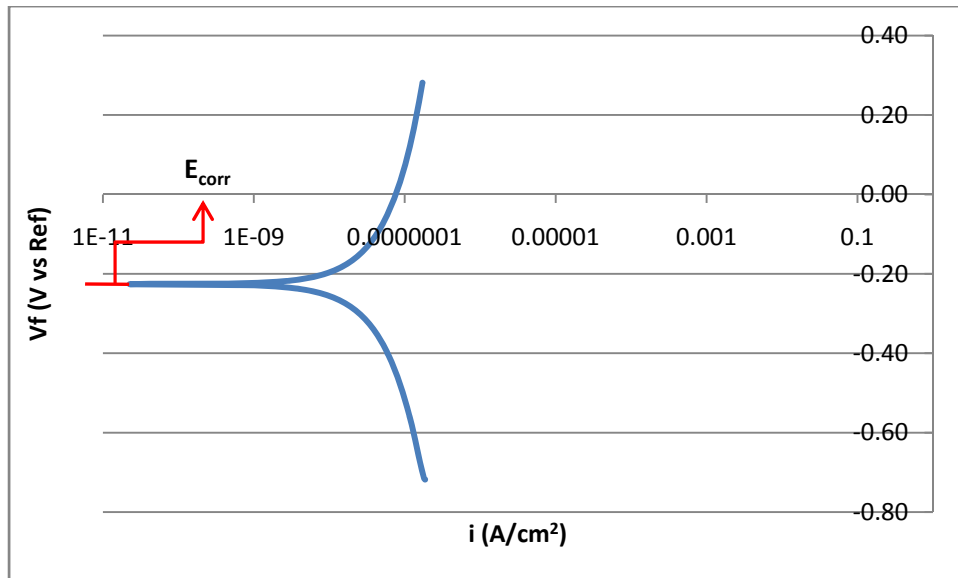


Figure 6.1: Corrosion Potential of Potentiodynamic Plot

6.2 Conventional

The conventional strand is the industry standard for prestressing strands and was used in the accelerated corrosion tests as a standard base to compare the other strands. The results from the tests will be compared relatively against the conventional strand to determine corrosion properties. The conventional strand when encased in grout forms a passive protective layer which keeps the material in the passive state for most potential ranges.

6.2.1 Potentiodynamic Tests

The plots of the three tests of conventional strand are shown in Figure 6.2. The variability in the plots was small with one test having a slightly lower corrosion potential. Mac Lean's¹⁴ tests resulted in a much tighter cluster of plots and less variability. The E_{corr} potentials for Mac Lean's¹⁴ conventional strands were all near $-0.850 \text{ V}_{\text{SCE}}$ which was considerably higher than these results.

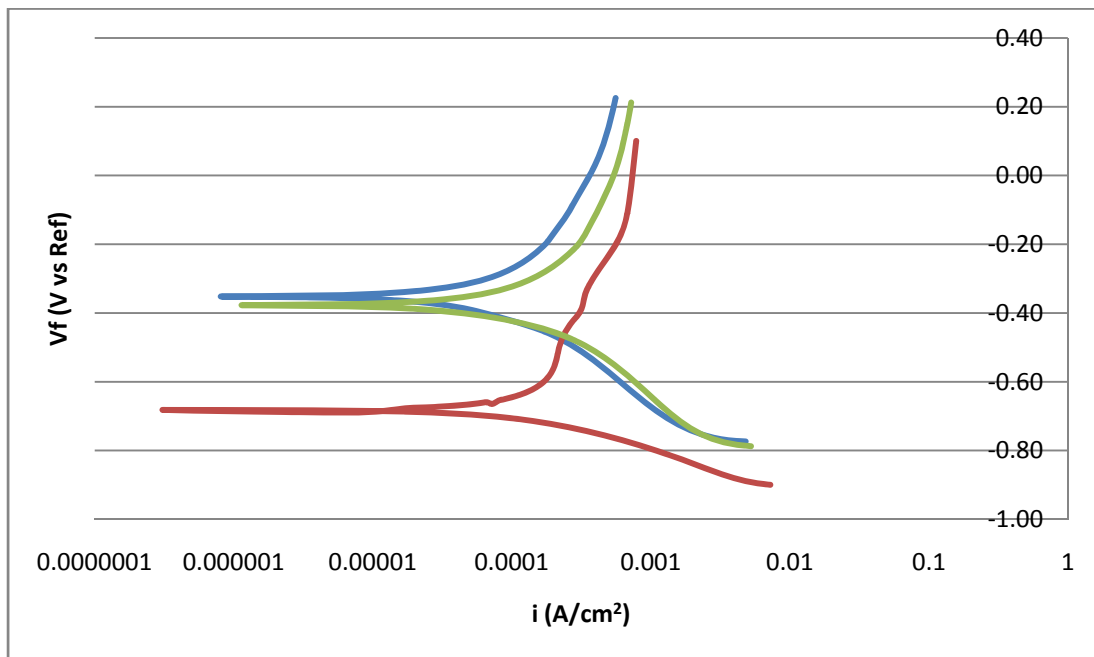


Figure 6.2: Potentiodynamic Plot of Conventional Strand Tests

6.2.2 Linear Polarization Resistance Tests

The results of the linear polarization resistance tests for the conventional strand are shown in Figure 6.3. There was some variability in the results which reflects in the polarization resistance values found in Table 6.1. The results of Mac Lean's¹⁴ tests showed low variability with the values at a current density of zero ranging from $-0.56 V_{SCE}$ to $-0.65 V_{SCE}$ which is a much higher potential range than the pre-cracked specimens.

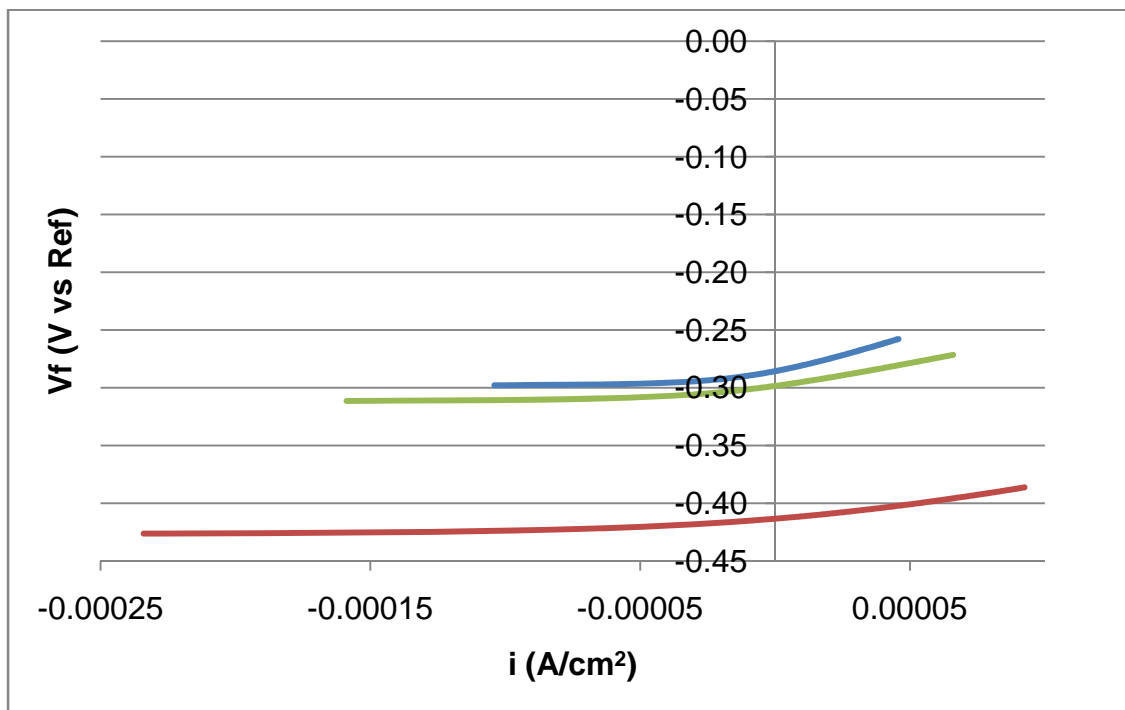


Figure 6.3: Linear Polarization Resistance Plot of Conventional Strand Tests

Due to the relatively low variability in the tests, the average of all three tests will represent the polarization resistance value well. The average polarization resistance is $R_p_{AVG} = 22.48 k\Omega cm^2$ and the average corrosion potential is $E_{CORR_{AVG}} = -0.333 V_{SCE}$. The values of the polarization resistance and corrosion potential for each test are found in Table 6.1. The average polarization resistance of the pre-cracked specimen was higher than Mac Lean's¹⁴ specimens ($10.82 k\Omega cm^2$) which mean that the pre-cracked specimens will have a longer time to corrosion.

This implies that the pre-cracked specimens provide better protection for resistance which is opposite of what we expected. Also, the average corrosion potential for the pre-cracked specimens was lower than that of the normal specimens ($-0.601 V_{SCE}$)¹⁴.

Table 6.1: Linear Polarization Resistance Results for Conventional Strand

	Test 1	Test 2	Test 3
Polarization Resistance, R_p ($k\Omega cm^2$)	31.46	13.46	22.52
Corrosion Potential, E_{corr} (mV vs Ref)	-286	-413	-299

6.3 Copper Clad

Copper is generally known for its corrosion resistance as it forms a green oxide layer which helps protect the material from further oxidation.

6.3.1 Potentiodynamic Tests

The plots of the tests are shown in Figure 6.3. Unlike the conventional strand, there is some variability with only one specimen having a lower corrosion potential. Mac Lean's¹⁴ work produced E_{corr} values with some variability ranging from $-0.20 V_{SCE}$ to $-0.55 V_{SCE}$ which is the region in which the pre-cracked specimens fell. For the two pre-cracked specimens with corrosion potentials near $-0.350 V_{SCE}$, the potentiodynamic plots are defined well while the other specimen has regions that are not as well defined.

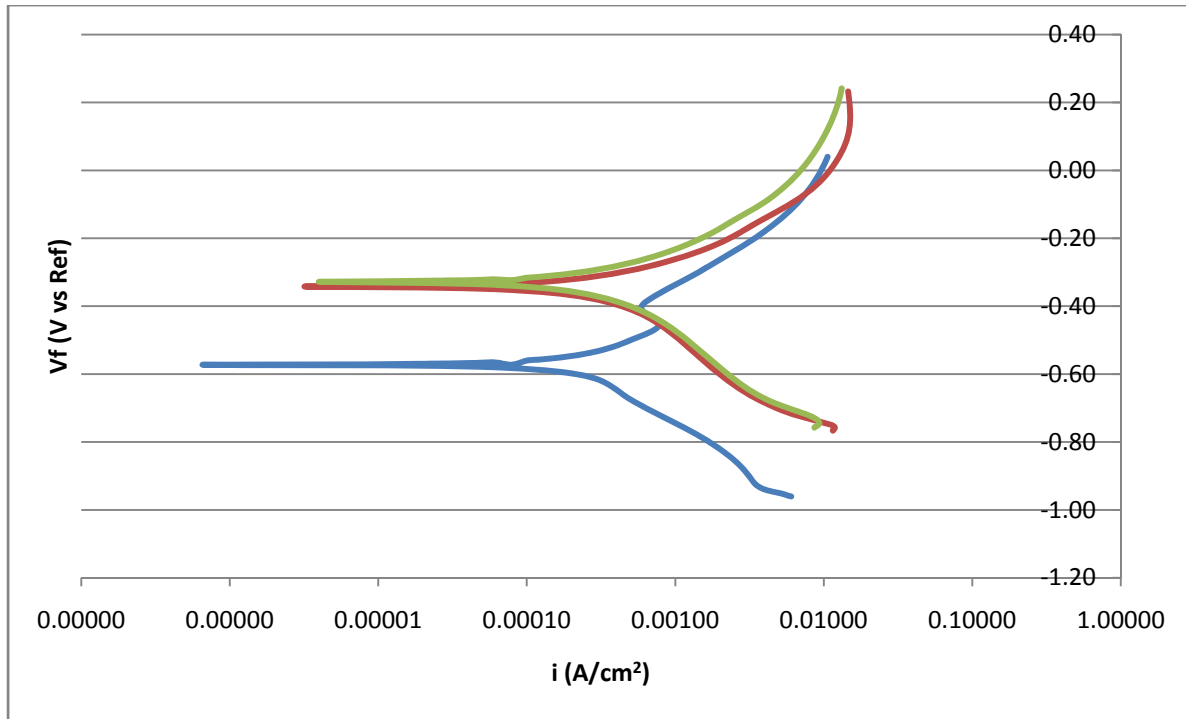


Figure 6.4: Potentiodynamic Plot of Copper Clad Strand Tests

6.3.2 Linear Polarization Resistance Tests

The tests are plotted in Figure 6.5 and from the plot it is seen that the values are very skewed, with one test not having a range of potentials or current. One test does not even exist near the vertical axis where current density is equal to zero. Due to these outliers, the results of these tests should be viewed with caution. Table 6.2 shows the results from the linear polarization resistance test. Notice that one value does not even exist due to a bad test while the others are fairly close to each other. An average of these two values was taken to come up with the average polarization resistance, $R_p \text{ AVG} = 3.68 \text{ k}\Omega\text{cm}^2$ and the corrosion potential, $E_{\text{corr AVG}} = -0.343 \text{ V}_{\text{SCE}}$. The low polarization resistance value is lower than the conventional strand polarization resistance which means that it has a smaller time to corrosion. These results do not agree at all with those of Mac Lean's¹⁴ work. He found that the copper clad strand was better in corrosion resistance than that of conventional strand. The average polarization resistance value of the pre-cracked specimens is smaller than that of the normal specimen ($11.68 \text{ k}\Omega\text{cm}^2$)¹⁴ while the average corrosion potential is higher than the normal specimens ($-0.298 \text{ V}_{\text{SCE}}$)¹⁴.

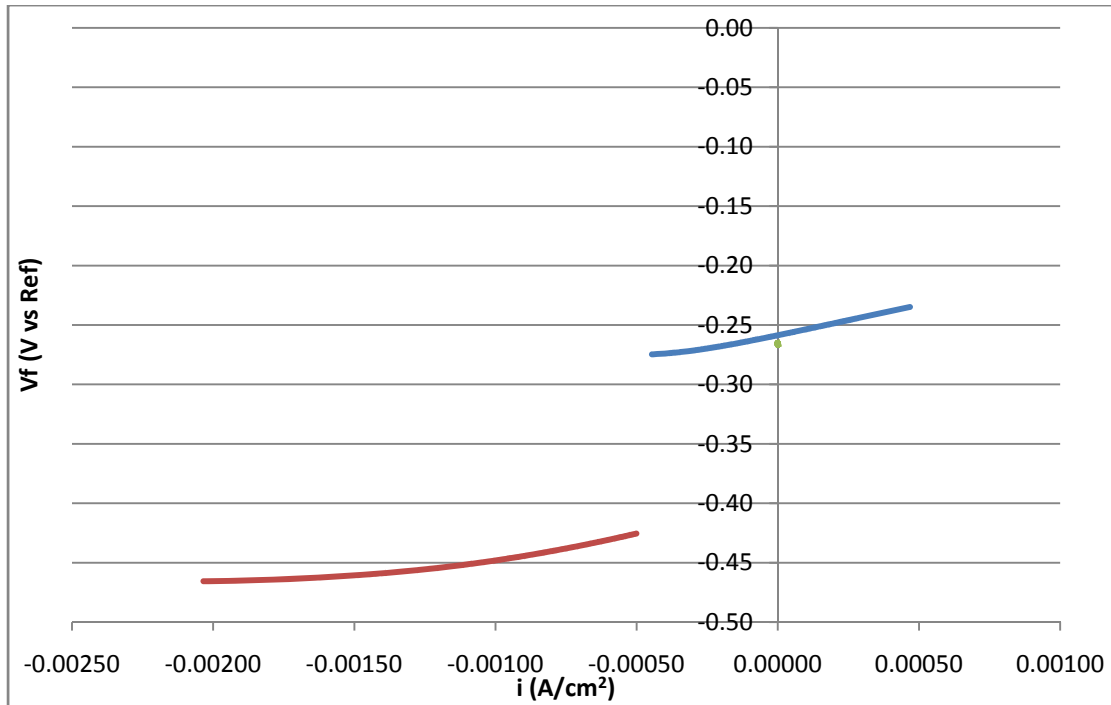


Figure 6.5: Linear Polarization Resistance Plot of Copper Clad Strand Tests

Table 6.2: Linear Polarization Resistance Results for Copper Clad Strand

	Test 1	Test 2	Test 3
Polarization Resistance, R_p ($k\Omega\text{cm}^2$)	3.831	N/A	3.528
Corrosion Potential, E_{corr} (mV vs Ref)	-426	N/A	-259

6.4 Flow-Filled Epoxy Coated

The tests run by Mac Lean had strands that were purposely damaged in order to get some sort of comparable results to the other strand types. The results of Mac Lean’s work showed that

the epoxy coated strands were much more resistant than any of the other strand types¹⁴. Due to this outcome, the specimens in this testing sequence were not predamaged as they were in Mac Lean's in order to see what kind of results would be found when the strands were fully coated with epoxy.

6.4.1 Potentiodynamic Tests

The plots of the results are in Figure 6.6 and can be seen to be very similar with well-defined regions. In addition, there is not much scatter among the specimens. This can be easily explained by the fact that the surfaces were exactly the same, shielding the strand from any of the electrolyte.

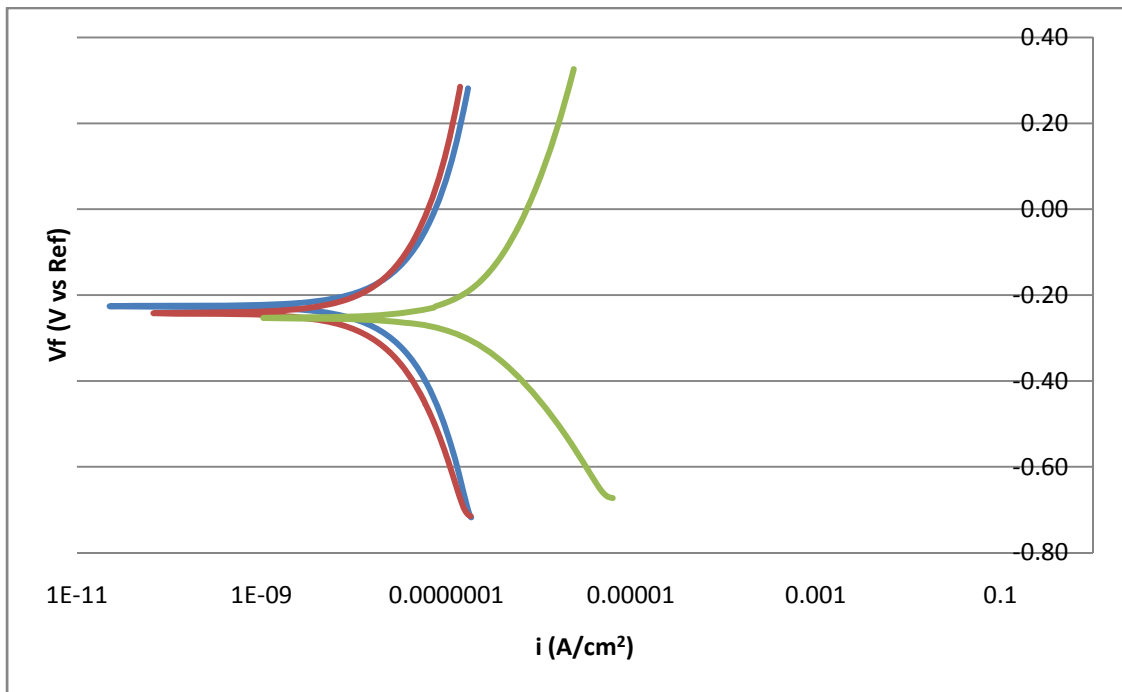


Figure 6.6: Potentiodynamic Plot of Flow Filled Epoxy Coated Strand Tests

6.4.2 Linear Polarization Resistance Tests

The consistency of the potentiodynamic tests did not reflect that of the linear polarization resistance tests. Two of the tests were almost identical while the third was very different, having a wide range of current density. Since the tests were run to find out the results of a perfectly coated strand, they will be ignored when comparing against the other strand types. See Figure 6.7 for the results of the linear polarization resistance test.

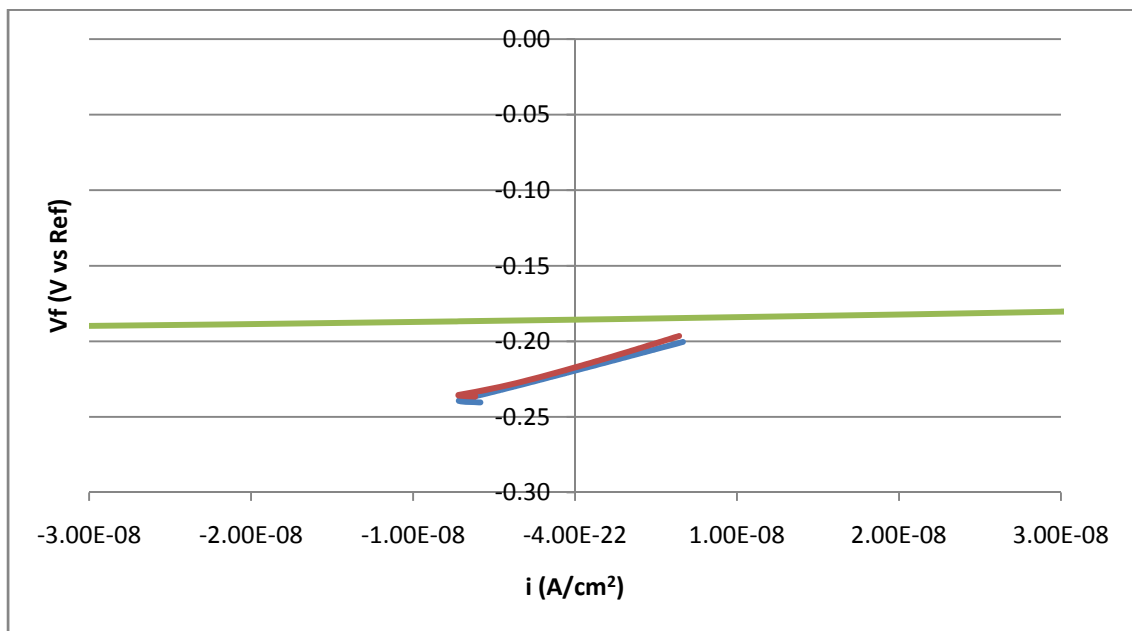


Figure 6.7: Linear Polarization Resistance Plot of Flow-Filled Epoxy Coated Strand Tests

Table 6.3 shows the results of the linear polarization resistance tests, and it is clear from the extremely large values of polarization resistance that the flow-filled epoxy coated strands are highly corrosion resistant which was expected.

Table 6.3: Linear Polarization Resistance Results for Flow-Filled Epoxy Coated Strand

	Test 1	Test 2	Test 3
Polarization Resistance, R_p ($k\Omega cm^2$)	203200	218200	11090
Corrosion Potential, E_{corr} (mV vs Ref)	-219	-217	-186

6.5 Hot Dip Galvanized

The hot dip galvanized strands undergo a process where the steel is coated with molten zinc to form a protective layer over the steel. Zinc is more active than iron in the emf series; therefore, it acts as a sacrificial anode for the steel. During the galvanizing process, the zinc is not applied evenly causing the layers to be thicker in some areas. This difference in thickness is the cause of any variability in the results.

6.5.1 Potentiodynamic Tests

The results of the tests are shown in Figure 6.8. As can be seen, the specimens stayed in the active range over the majority of the ranges of potential. This helps explain the sacrificial behavior of the zinc coating. The results show some variability with one specimen having a slightly lower corrosion potential than the other two. Mac Lean's¹⁴ values of E_{corr} ranged from $-0.30 V_{SCE}$ to $-1.30 V_{SCE}$ which shows considerably more variability than the pre-cracked specimens which fall within this range.

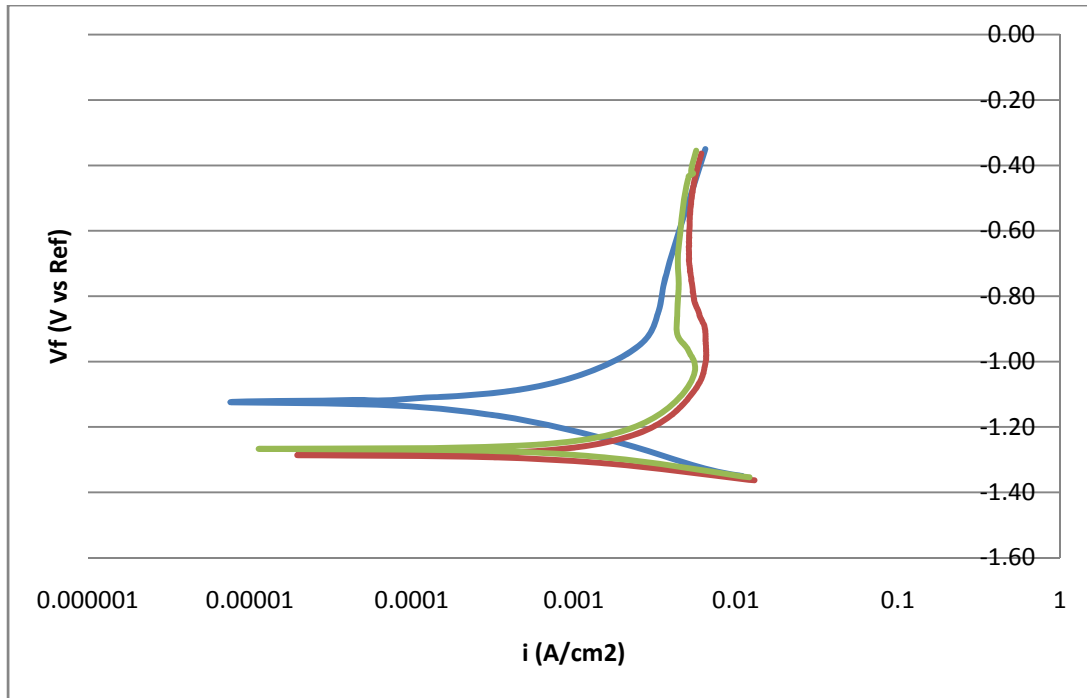


Figure 6.8: Potentiodynamic Plot of Hot Dip Galvanized Strand Tests

6.5.2 Linear Polarization Resistance Tests

The results reflect those of the potentiodynamic test which do not show much variability. All the results are within a close range of potentials. The results can be seen in Figure 6.9. These results do not reflect those of Mac Lean's¹⁴ which showed a high variability among the tests. These values which are the potential when current density is equal to zero ranged from $-0.30 V_{SCE}$ to $-1.05 V_{SCE}$. Table 6.4 shows the results of the linear polarization resistance tests for the pre-cracked specimens. All the results were very similar and are used to obtain the average values. The average polarization resistance is $R_{p\text{ AVG}} = 2.69 \text{ k}\Omega\text{cm}^2$ and the average corrosion potential is $E_{\text{corr AVG}} = -0.805 V_{SCE}$. The average polarization resistance is much lower than that of the conventional strand which means that the hot dip galvanized strand has a smaller time to corrosion which does not match the results of Mac Lean's¹⁴. The average polarization resistance of the pre-cracked specimens is lower than the normal specimens $(20.06 \text{ k}\Omega\text{cm}^2)^{14}$ while the average corrosion potential was higher than the normal specimens $(-0.687 V_{SCE})^{14}$.

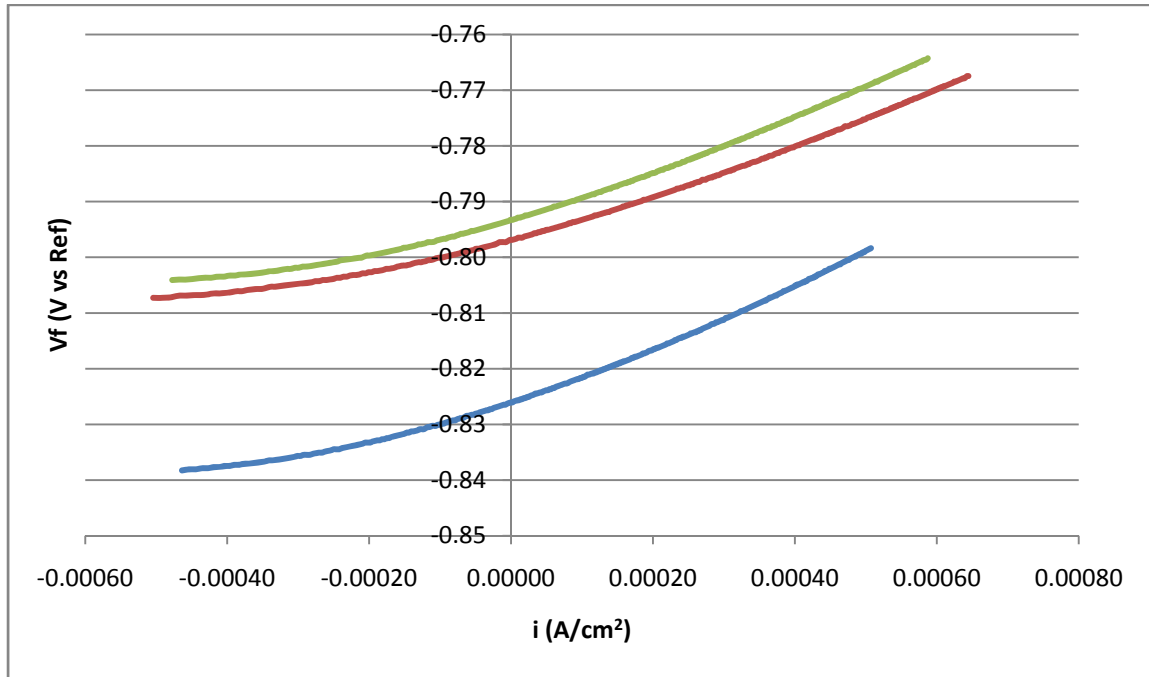


Figure 6.9: Linear Polarization Resistance Plot of Hot Dip Galvanized Strand Tests

Table 6.4: Linear Polarization Resistance Results for Hot Dip Galvanized Strand

	Test 1	Test 2	Test 3
Polarization Resistance, R_p ($k\Omega cm^2$)	2.985	2.418	2.66
Corrosion Potential, E_{corr} (mV vs Ref)	-826	-797	-793

6.6 Stainless Clad

The stainless clad strands undergo a similar process as the copper clad strands except the material used is more expensive and more corrosion resistant. The stainless clad is also very similar to the solid stainless steel strands except different types of stainless steel is used. The results should be similar between the stainless clad strands and solid stainless steel strand. The variability will result from the different types of stainless steel used as some are more resistant than others depending on the amount of chromium and other alloys present. Also, if there are any defects in the stainless clad strands, this could cause the steel within to corrode.

6.6.1 Potentiodynamic Tests

The results of the tests are similar with all having close corrosion potential values and well defined plots. The results are shown in Figure 6.10. Mac Lean's¹⁴ values of E_{corr} ranged from $-0.45 V_{\text{SCE}}$ to $-0.55 V_{\text{SCE}}$. The pre-cracked specimens showed similar variability but not within this range.

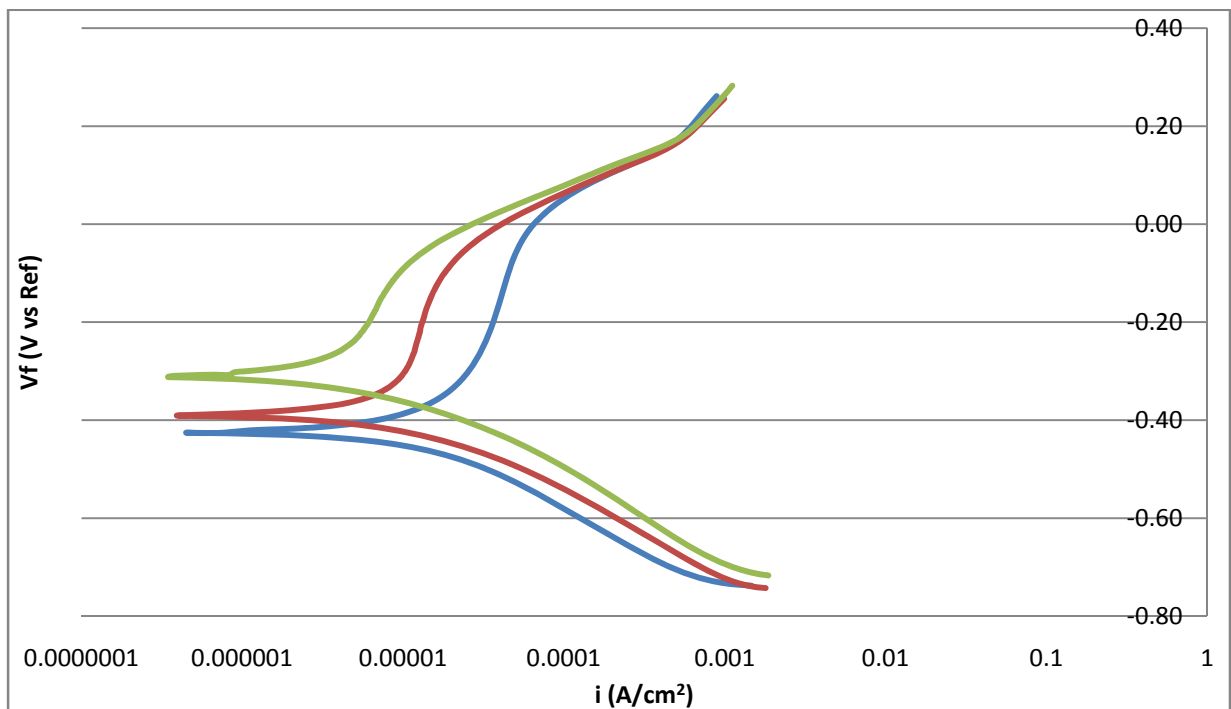


Figure 6.10: Potentiodynamic Plot of Stainless Clad Strand Tests

6.6.2 Linear Polarization Resistance Tests

The results of the tests confirm the consistency of the potentiodynamic tests with all the specimens having similar slopes near the corrosion potential. This allows for all the specimens to be used when finding the average polarization resistance. The average polarization resistance is $R_{p\text{AVG}} = 93.37 \text{ k}\Omega\text{cm}^2$ and the average corrosion potential is $E_{\text{corrAVG}} = -0.258 \text{ V}_{\text{SCE}}$. Both of these results are comparable to Mac Lean's¹⁴ work which shows that the time to corrosion is longer than the conventional strand. The values of potential at zero current density for Mac Lean range from $-0.17 \text{ V}_{\text{SCE}}$ to $-0.23 \text{ V}_{\text{SCE}}$. The pre-cracked specimens showed had similar scatter but not within this range. The average polarization resistance of the pre-cracked specimens is lower than that of the normal specimens ($92.72 \text{ k}\Omega\text{cm}^2$)¹⁴ while the average corrosion potential is higher than the normal specimens ($-0.201 \text{ V}_{\text{SCE}}$)¹⁴. While these values were slightly different, they compared closely with Mac Lean's values. The results of the linear polarization resistance tests can be found in Table 6.5.

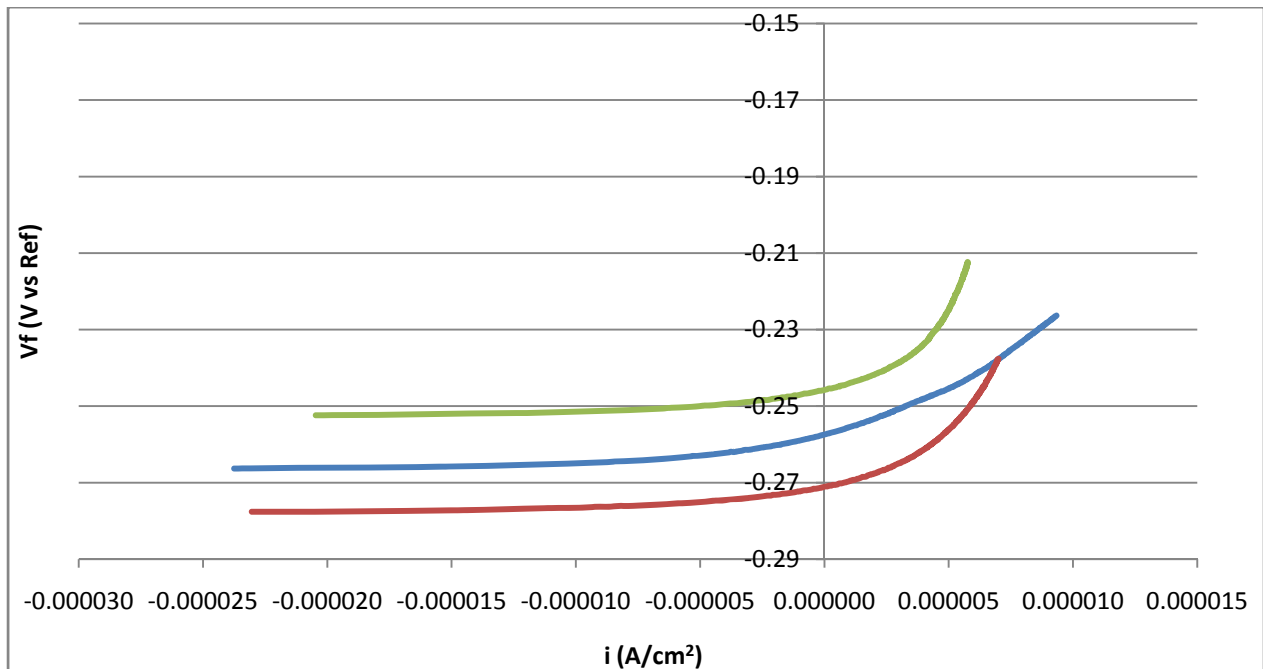


Figure 6.11: Linear Polarization Resistance Plot of Stainless Clad Strand Tests

Table 6.5: Linear Polarization Resistance Results for Stainless Clad Strand

	Test 1	Test 2	Test 3
Polarization Resistance, R_p ($k\Omega cm^2$)	108.7	74.56	85.5
Corrosion Potential, E_{corr} (mV vs Ref)	-257	-271	-246

6.7 Stainless Steel

Stainless steel is known for its corrosion resistance properties and is widely used in marine environments. There are various types of stainless steels with different grades of corrosion resistance which depend on the composition of the material. The results are expected to be similar to those of the stainless clad specimens.

6.7.1 Potentiodynamic Tests

The results of the stainless steel strands are very similar to those of the stainless clad which was expected. Mac Lean's¹⁴ values of E_{corr} ranged from $-0.30 V_{SCE}$ to $-0.60 V_{SCE}$ which agree well with the values of the pre-cracked specimens in Figure 6.12.

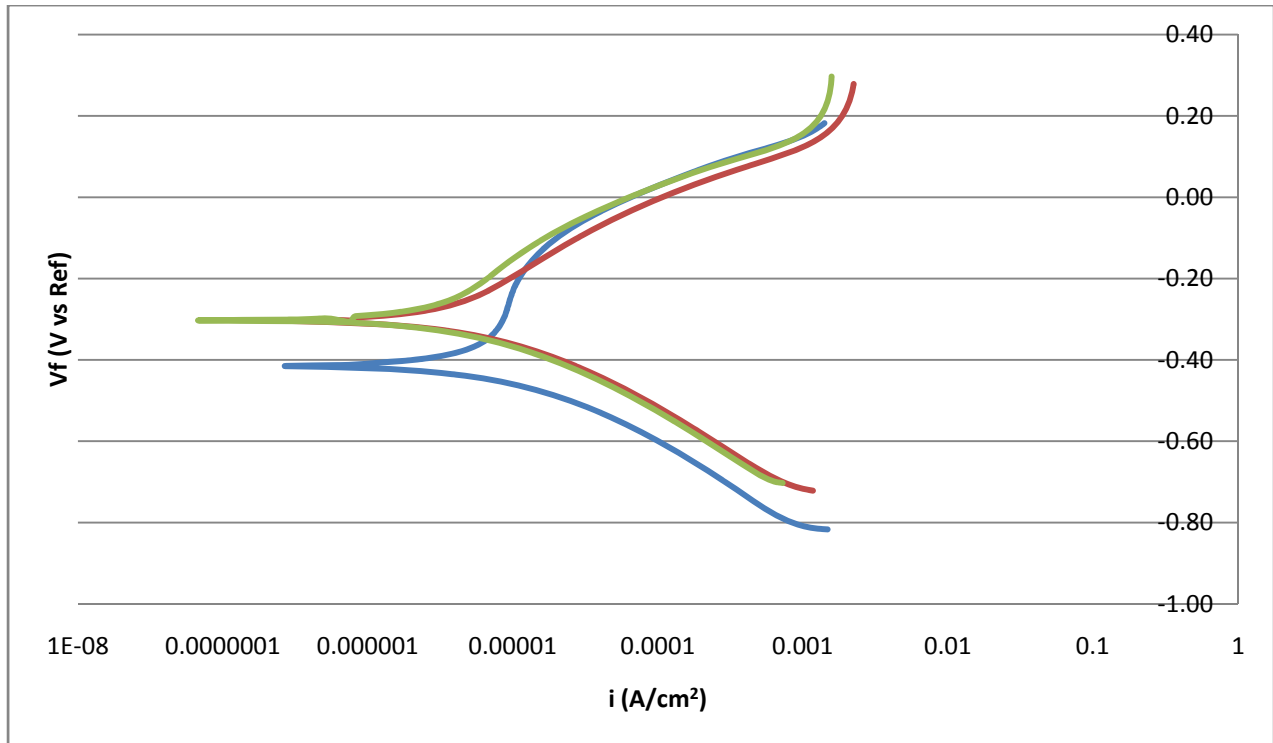


Figure 6.12: Potentiodynamic Plot of Stainless Steel Strand Tests

6.7.2 Linear Polarization Resistance Tests

The results reflect that of the potentiodynamic test showing very similar results with small scatter. The slopes near the corrosion potential are all very close which also reflect well with the stainless clad specimens. The results of the tests can be seen in Figure 6.13. All of the result values were used when finding averages. The average polarization resistance is $R_{p\text{ AVG}} = 89.59 \text{ k}\Omega\text{cm}^2$ and the average corrosion potential is $E_{\text{corr AVG}} = -0.274 \text{ mV}_{\text{SCE}}$. These results are very comparable to Mac Lean's¹⁴ results which also reflect well with the stainless clad specimens. The potential values at zero current density of Mac Lean's¹⁴ tests ranged from $-0.19 \text{ V}_{\text{SCE}}$ to $-0.35 \text{ V}_{\text{SCE}}$. The values of the pre-cracked specimens fall within this range which agree well with the potentiodynamic tests. The average polarization resistance of the pre-cracked specimen is lower than the normal specimens ($100.05 \text{ k}\Omega\text{cm}^2$)¹⁴ while the average corrosion potential is higher than the normal specimens ($-0.243 \text{ V}_{\text{SCE}}$)¹⁴. The results of the linear polarization resistance tests can be found in Table 6.6.

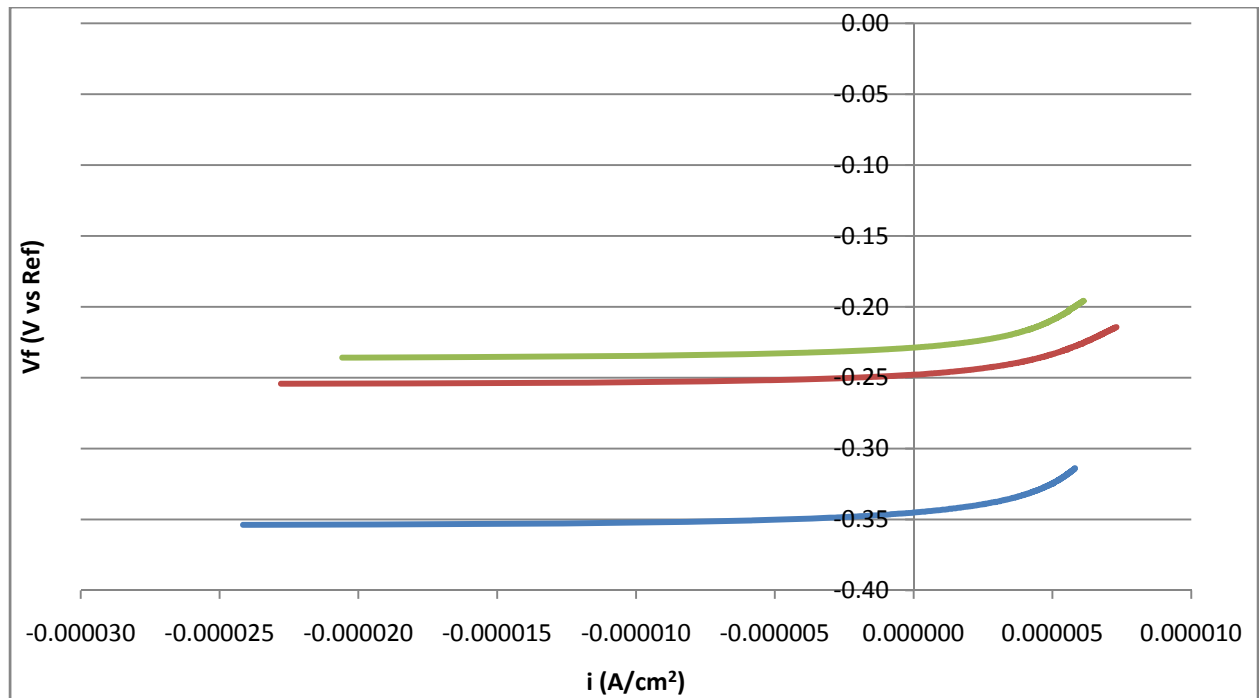


Figure 6.13: Linear Polarization Resistance Plot of Stainless Steel Strand Tests

Table 6.6: Linear Polarization Resistance Results for Stainless Steel Strand

	Test 1	Test 2	Test 3
Polarization Resistance, R_p ($k\Omega cm^2$)	114.9	77.22	87.98
Corrosion Potential, E_{corr} (mV vs Ref)	-345	-248	-229

6.8 Summary

As in Mac Lean's¹⁴ results, the conventional strand was used as a base value to compare the rest of the strand types. The values obtained from the pre-cracked specimens had mixed results when compared to the normal specimens tested by Mac Lean¹⁴. The linear polarization resistance results of the pre-cracked specimens can be seen in Table 6.7. The results of the epoxy coated specimens are included to show the high resistance values when compared to uncoated strands but should not be used to compare with Mac Lean's¹⁴ results.

Table 6.7: Summary of Pre-Cracked Linear Polarization Results for All Tests

	CN	CC	GV	SC	SS	EC
Polarization Resistance, Rp (kΩcm ²)	22.48	3.68	2.69	93.37	89.59	144163
Rp vs CN	1	0.16	0.12	4.15	3.99	6413
Corrosion Potential, Ecorr (mV vs Ref)	-333	-343	-805	-258	-274	-207

As was explained in Mac Lean's work, Dr. Pacheco and Dr. Schokker found a relation between the polarization resistance and time to corrosion which did not prove to be useful for the results of these testings^{14,15}. Although the direct correlation of their work was not used, the fundamental concept of comparing time to corrosion based on the polarization resistance was used for the results. The actual time to corrosion cannot be specified for the specimens, but a comparative look among the strands based on the polarization resistance has a good indication of relative properties. The average polarization resistance values of all the specimens were normalized with the average polarization resistance of the conventional strand and can be seen in Table 6.7. The correlation used for analyzing the comparative time to corrosion for the specimens is as the polarization resistance increases, the time to corrosion increases. By looking at the results, it is clear that the copper clad and hot dip galvanized strands performed worse than

the conventional strand, while the stainless clad and the stainless steel strands performed better. Figure 6.14 shows a bar chart summarizing these values.

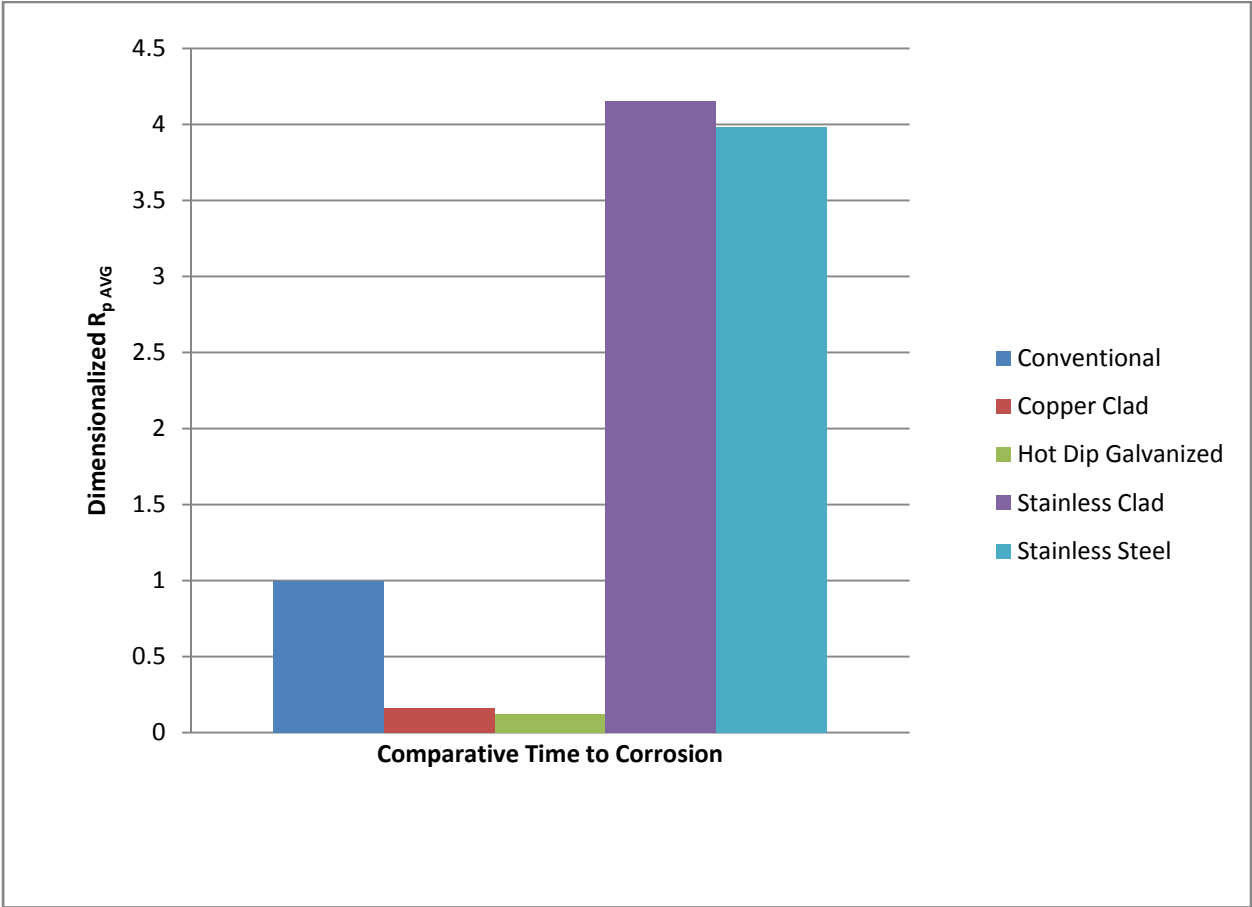


Figure 6.14: Comparison of Times to Corrosion for Pre-Cracked Specimens

From the chart, the results become clear that there are two clusters of results. The copper clad and the hot dip galvanized strands performed very similar having a time to corrosion that is about 15% that of conventional strand while stainless clad and stainless steel strands performed similar having a time to corrosion that is four times greater than that of conventional strand. The stainless clad and stainless steel strands performed as expected having the best corrosion resistant properties. The copper clad and hot dip galvanized strands did not perform as expected

having much worse corrosion properties. The results of Mac Lean’s work can be seen in Figure 6.15¹⁴ showing the relative time to corrosion of normal specimens which are not pre-cracked.

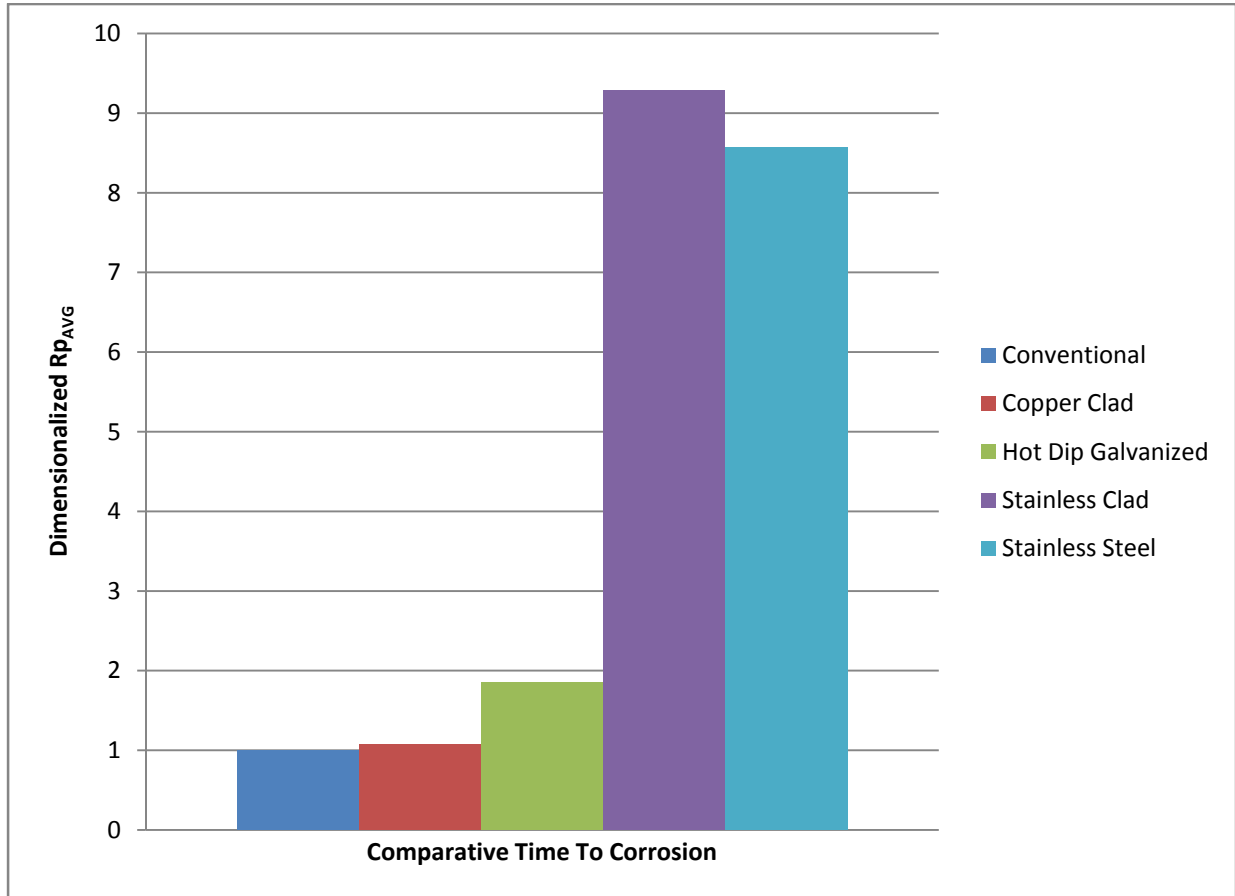


Figure 6.15: Comparison of Times to Corrosion for Normal Specimens¹⁴

From Figure 6.15, the two clusters of data can be clearly seen. The first cluster is the copper clad and hot dip galvanized specimens, and the second is the stainless clad and stainless steel specimens. The results of the copper clad and hot dip galvanized normal specimens are obviously not the same as the pre-cracked specimens because in the pre-cracked test results they have smaller times to corrosion while in the normal test results they have slightly longer times to corrosion. The stainless clad and stainless steel pre-cracked specimens agreed very well with the normal specimens having similar times to corrosion but are about half the value.

The specimens used during this testing sequence are exactly the same as those used in Mac Lean's¹⁴ testing but with pre-cracked exposed areas. The purpose of testing the specimens with pre-cracked exposed areas was to represent the specimens in the field conditions and to compare the results with Mac Lean's¹⁴. The results had mixed trends among the different strand types. The comparative results can be found in Table 6.8. The normal values are those of Mac Lean's¹⁴ work, and the pre-cracked values represent this testing sequence.

Table 6.8: Comparative Results of Linear Polarization Resistance Tests

		CN	CC	GV	SC	SS
Polarization Resistance, Rp (kΩcm ²)	Normal	10.82	11.68	20.06	100.50	92.72
	Pre-Cracked	22.48	3.68	2.69	93.37	89.59
Rp vs CN	Normal	1	1.08	1.85	9.29	8.57
	Pre-Cracked	1	0.16	0.12	4.15	3.99
Corrosion Potential, Ecorr (mV vs Ref)	Normal	-601	-298	-687	-201	-243
	Pre-Cracked	-333	-343	-805	-258	-274

The general trend is that if a specimen had a higher polarization resistance, it also had a lower corrosion potential. All the specimens followed this trend which helps to validate the results. When looking at the normalized values of the polarization resistance, it is clear that the copper clad and hot dip galvanized strand results did not follow that of Mac Lean's¹⁴ work. Not only did the results show a worse time to corrosion, but they are also considerably lower. Also, the hot dip galvanized strand was worse than the copper clad strand for the pre-cracked specimen which did not agree with Mac Lean's¹⁴ results. The poor results could be explained by the skewed results represented by the copper clad, but this was not apparent in the hot dip galvanized results which were all very close. Therefore, the results can be viewed as valid.

When comparing the normalized results of the stainless clad and stainless strands, it is seen that the trend of the pre-cracked specimens agreed with those of Mac Lean's. While the

pre-cracked specimens have normalized values less than half of the respective values of Mac Lean's¹⁴ tests, they still follow the overall trend. The stainless clad strand also outperformed the stainless strand by a small amount which agrees well with Mac Lean's¹⁴. Percent differences of the pre-cracked specimens versus the normal specimens are outlined in Table 6.9. A positive percent difference represents a pre-cracked specimen with a higher value than the normal specimen.

Table 6.9: Percent Differences Between Normal and Pre-Cracked Specimens

	CN	CC	GV	SC	SS
Polarization Resistance, Rp (kΩcm ²)	107.8	-68.5	-86.6	-7.1	-3.4
Rp vs CN	0.0	-84.8	-93.6	-55.3	-53.5
Corrosion Potential, Ecorr (mV vs Ref)	-44.6	14.9	17.2	28.4	12.8

Overall, the trend of the pre-cracked specimens produces smaller polarization resistance values which correspond to smaller times to corrosion. This can be seen in Table 6.9 with the negative values. An interesting observation is that the polarization resistance of the base conventional strand is higher for the pre-cracked specimens which does not follow the trend. Other than this outlier, it seems that by pre-cracking the specimens, the time to corrosion is much faster than if the grout is fully intact which was the expected result.

Chapter 7

Indications of Tests

7.1 Major Trends

The results of each test follow major trends among the strand types. For each test conducted, the trends of the strand types will be evaluated. After all of the results are examined, it should be clear as to which strand type performs the best in terms of corrosion resistance.

7.1.1 Large Scale Exposure Beams Half-Cell Data

The large scale exposure beams undergo a wet and dry cycle of exposure to a chloride solution. Every month, half-cell readings are taken of the specimens to try and predict the corrosion activity in the beam. A ranking of the most and least likely corroded beams is tabulated and can be found in Tables 7.1 and 7.2 respectively.

Table 7.1: Least Corroded Specimens

	Beam #	Duct Type	Tendon Type
1)	5.3	P2	SS
2)	5.2	P2	SC
3)	7.1	FE	CN
4)	4.2	P1	SS
5)	2.4	P1	CC
6)	3.3	P2	CC
7)	3.2	P2	GV
8)	3.4	P1	GV
9)	3.1	P2	CN

Table 7.2: Most Corroded Specimens

	Beam #	Duct Type	Tendon Type
1)	7.3	FE	GV
2)	T.1	GV	CN
3)	2.2	GV	GV
4)	1.4	GV	CN
5)	1.2	GV	CC
6)	1.1	GV	CN

From these two tables, the trend that is followed is that the most likely corroded duct is the hot dip galvanized and least likely corroded duct is the two-way ribbed plastic. When considering strands, the most likely corroded is split between conventional and hot dip galvanized strands. The least likely corroded is split between the stainless steel and stainless clad strands. The copper clad strand has a result that puts it somewhere in between these two clusters.

7.1.2 Exposed Strand Test

The exposed strand test involved the bare strands undergoing a wet and dry cycle where the strands were exposed to a chloride solution. The test was conducted for six months where a weight loss was calculated for each strand. Also, a monthly corrosion rating was associated with each strand. From these results, the strands were normalized and compared to the epoxy coated strand which served as the base strand. A comparison of the average six month rating and average weight loss was used to show the trends of this test. These are shown in Figures 7.1 and 7.2 respectively.

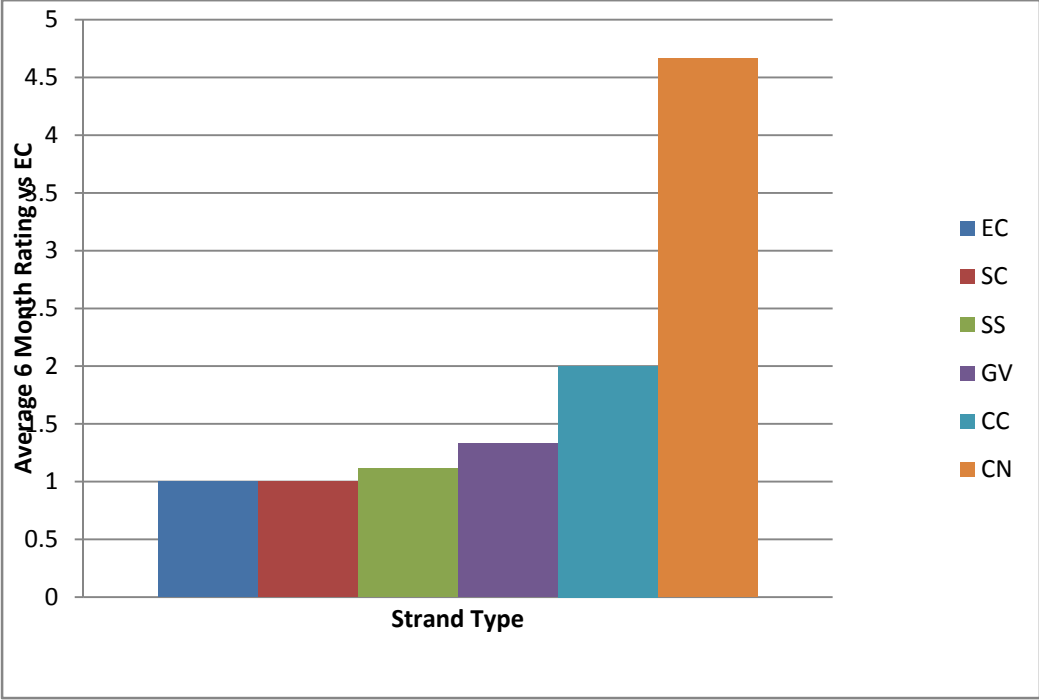


Figure 7.1: Average Six Month Rating vs Epoxy Coated Strand

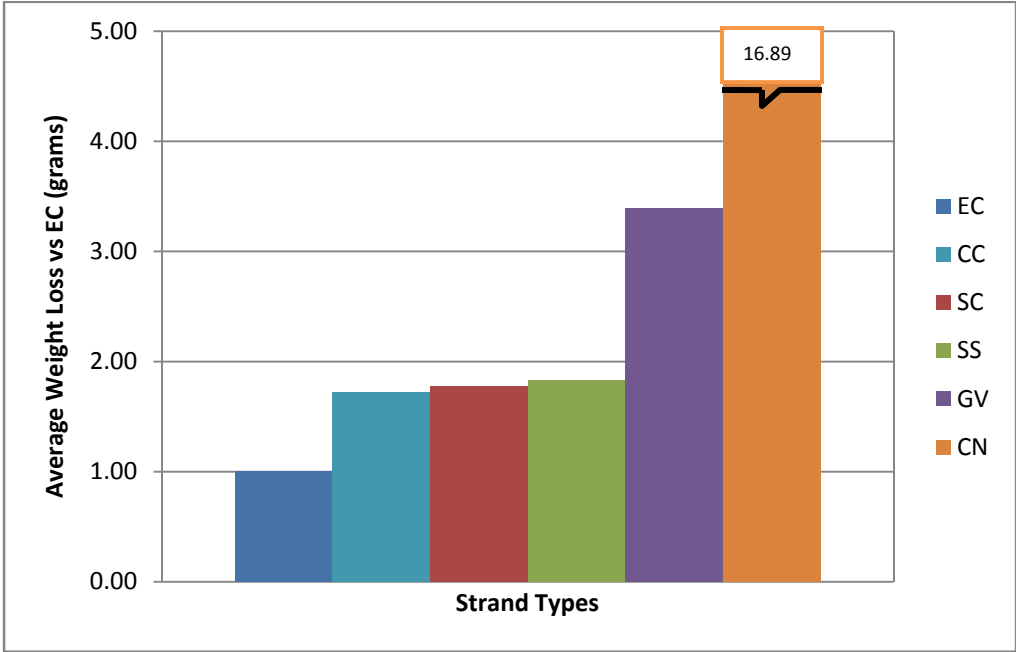


Figure 7.2: Average Weight Loss vs Epoxy Coated

From the plots, it is obvious that the best strand type is the epoxy coated strand, and the worst is the conventional strand. This was expected because the epoxy coated strand did not allow any solution to reach the bare metal while the conventional strand is completely exposed. After analyzing the plots further, the next best strands are the stainless clad and stainless steel exhibiting similar properties. The copper clad and hot dip galvanized exhibited some variability among the different systems with the copper clad strands having a smaller weight loss than the stainless clad and stainless steel strands, but a larger corrosion rating at six months which was one strand type better than the conventional. The hot dip galvanized strands performed one strand type better than the conventional strand in the average six month rating but showed more weight loss. From these observations, the epoxy coated strand performed best followed by the stainless clad and stainless steel right after. The copper clad strands performed better than the hot dip galvanized overall due to the second best weight loss and slightly worse six month corrosion rating than hot dip galvanized. And finally, the conventional strand is the worst strand in both cases.

7.1.3 Grouted Strand Test

The grouted strand test involved the strands being encased in grout inside a PVC tube with both bare ends epoxyed to help prevent corrosion. The specimens are immersed in a chloride solution and monitored for potential over time as they electrochemically produce a potential. The potential corrosion is described as the potential versus time for the first week where the plots are constant. The corrosion potential is then used as a comparison to verify which strands have the best corrosion resistance. A lower value of corrosion potential corresponds to better resistance properties. Figure 7.3 shows the potential versus time of the representative specimens of each strand type while Table 7.3 has the corresponding corrosion potentials of these representative specimens.

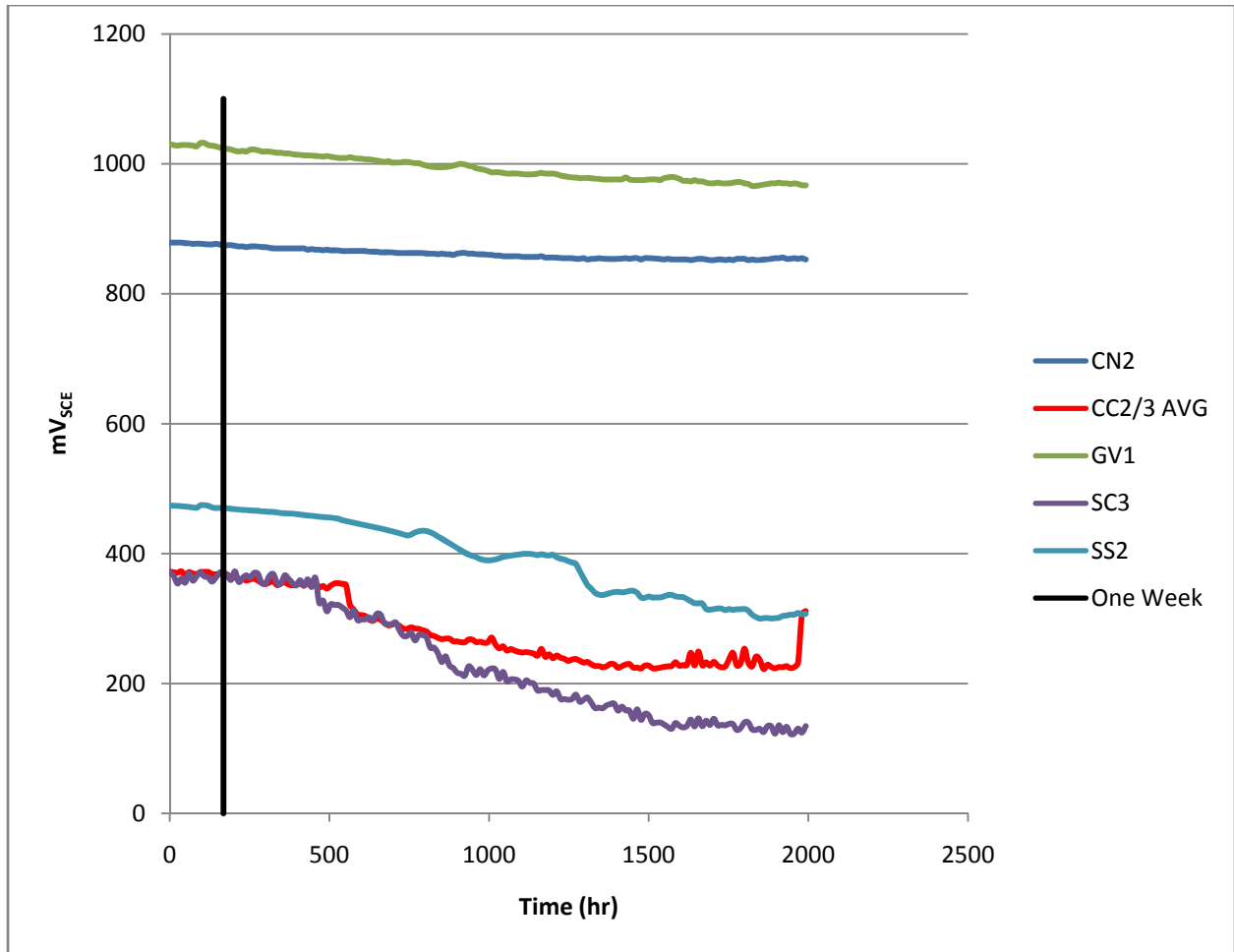


Figure 7.3: Potential vs Time for the Representative Specimens

Table 7.3: Corrosion Potential of Representative Specimens

	CN	CC	GV	SC	SS
E_{corr} (mV _{SCE})	-875	-370	-1025	-360	-475

From Figure 7.3 and Table 7.3, it is clear that the best specimen is the stainless clad strand, and the worst specimen is the hot dip galvanized strand. The copper clad strand exhibits similar behavior to the stainless clad strand, and the stainless steel strand follows closely behind

these. The conventional strand is next showing the fourth best behavior before the hot dip galvanized strand.

7.1.4 Accelerated Active Corrosion Test

The accelerated active corrosion test specimens are very similar to the grouted test specimens except the bare strands are left out of the specimen to be able to attach to the equipment used in analyzing them. The tests conducted on the specimens are the potentiodynamic test used to gather the Tafel constants and the linear polarization resistance test used to gather the polarization resistance of each specimen. The polarization resistance is then used to look at the relative time to corrosion against the base conventional strand. Two methods were used during the testing. They are (1) the normal exposed area done by Mac Lean¹⁴ known as the normal specimens and (2) the current method of pre-cracking the exposed area to allow the chloride solution to penetrate the grout faster. The relative times to corrosion of the normal and pre-cracked sections will be analyzed to determine the trend associated with the testing sequence. Table 7.4 shows a side-by-side comparison of the results between the normal and pre-cracked specimens. The normal specimens are seen in Figure 7.4 and the pre-cracked in Figure 7.5.

Table 7.4: Comparative Results of Linear Polarization Resistance Tests

		CN	CC	GV	SC	SS	EC
Polarization Resistance, Rp (kΩcm ²)	Normal	10.82	11.68	20.06	100.50	92.72	1000
	Pre-Cracked	22.48	3.68	2.69	93.37	89.59	144163
Rp vs CN	Normal	1	1.08	1.85	9.29	8.57	92.42
	Pre-Cracked	1	0.16	0.12	4.15	3.99	6413
Corrosion Potential, Ecorr (mV vs Ref)	Normal	-601	-298	-687	-201	-243	-409
	Pre-Cracked	-333	-343	-805	-258	-274	-207

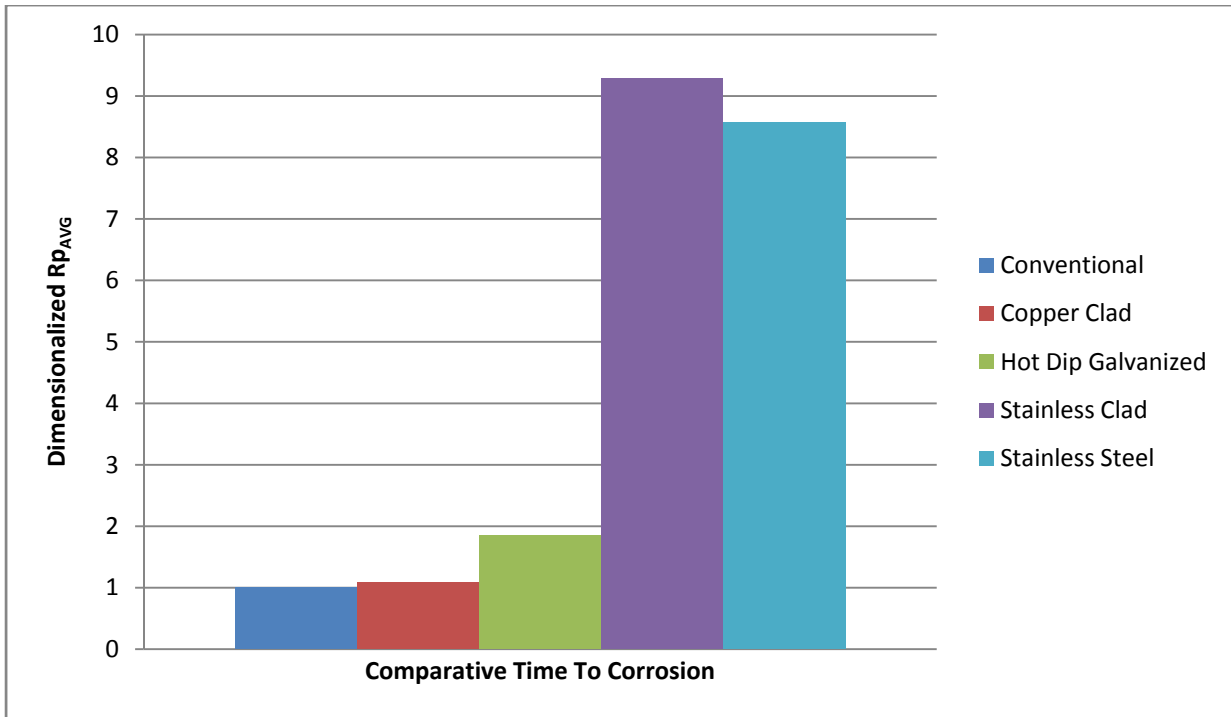


Figure 7.4: Comparison of Times to Corrosion for Normal Specimens¹⁴

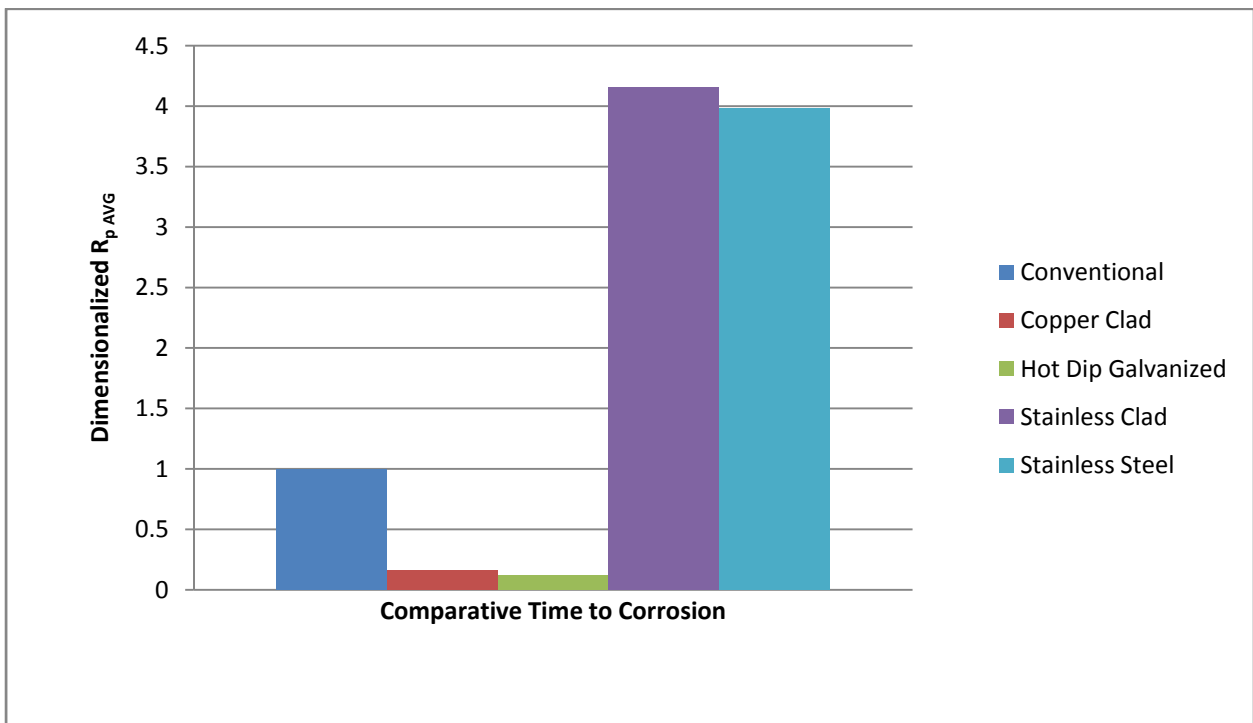


Figure 7.5: Comparison of Times to Corrosion for Pre-Cracked Specimens

Note that the epoxy coated strand results were removed from the figures because they were obviously the best strand type by far from Table 7.4. Beyond that, the best strand types are the stainless clad and stainless steel strand having relative times to corrosion of approximately nine times better for the normal specimens and about four times better for the pre-cracked specimens when compared to the conventional strand. The next cluster of strands is the copper clad and hot dip galvanized strands. For the normal specimens, they exhibited slightly longer times to corrosion while for the pre-cracked specimens, they exhibited much shorter times to corrosion. It must also be noted that the conventional strands showed an overall increase due to pre-cracking while all the other strand types showed an overall decrease. From these results, the trend seems to be that the best strand type is the epoxy coated, followed by the stainless clad and stainless steel strands, with the stainless clad strands performing slightly better in each test sequence. Beyond these trends, it is difficult to assign any value to the copper clad, hot dip galvanized, and conventional strands. From the normal test specimens, the copper clad and hot dip galvanized strands did only slightly better than the conventional strands while reversely, they did much worse in the pre-cracked specimens. Therefore, the conventional strands could be considered to have performed better than both the copper clad and hot dip galvanized strands overall. Finally, since the results of the copper clad and hot dip galvanized strands were very similar in both test sequences, they could be considered to have similar properties.

7.2 Strand Type Recommendations

The trends of all the tests will be used as a comparison to help determine the best strands to be used in post-tensioned applications of prestressed bridges. The trends gathered from the supplementary tests only consider the corrosion properties of the strands and do not show any indication of the mechanical properties. Mac Lean¹⁴ performed mechanical properties on the strand types, and these values will be used to assess the final rankings. Table 7.5 shows the results of the mechanical testing.

Table 7.5: Ultimate Strengths¹⁴

Type	Nominal Diameter (in)	Area (in ²)	Breaking Strength (kips)	Met Gr. 250 Requirement	Met Gr. 270 Requirement
Conventional	0.6	0.217	61.5	Yes	Yes
Epoxy Coated	0.5	0.153	43.7	Yes	Yes
Hot Dip Galvanized	0.5	0.153	40.9	Yes	No
Copper Clad (Nominal Area)	0.5	0.144	25.9	No	No
Copper Clad (Steel Area)	0.438	0.108	25.9	No	No
Stainless Clad (Nominal Area)	0.6	0.217	57.5	Yes	No
Stainless Clad (Steel Area)	0.5	0.153	57.5	Yes	Yes
Stainless Steel	0.6	0.217	48.9	No	No

From Table 7.5, it is clear that the conventional and epoxy coated strands meet both requirements for ultimate strengths while the copper clad and the stainless steel strands do not meet either of the requirements. The hot dip galvanized strands meet the Grade 250 requirement but not the Grade 270 requirement. This leaves the stainless clad strand that meets both requirements when the stainless cladding is not considered but does not meet the Grade 270 requirement when the cladding is considered. Since the stainless clad is a structural metal, it will be considered in the final area making the stainless clad strands only meet the Grade 250 requirement.

A ranking system of the strands was done for each test sequence based on corrosion resistance properties. Table 7.6 outlines these rankings with 1 having the best corrosion resistance properties and 6 having the worst. Note that epoxy coated strands were not used in the large scale exposure beams and will not be included in the ranking. Also note that the epoxy coated strands were excluded from the grouted strand test because of the knowledge that they would outperform the other types.

Table 7.6: Strand Rankings Based on Corrosion Resistance

Test	Best 1	2	3	4	5	Worst 6
Half-Cells	SS	SC	CC	GV	CN	N/A
Exposed Strand	EC	SC	SS	CC	GV	CN
Grouted Strand	SC	CC	SS	CN	GV	N/A
Accelerated (Normal)	EC	SC	SS	GV	CC	CN
Accelerated (Pre-Cracked)	EC	SC	SS	CN	CC	GV
Overall	EC	SC	SS	CC	GV	CN

From Table 7.6, the overall rankings describe the final order of strand types in terms of corrosion resistance. As was expected, epoxy coated strands performed the best and conventional strands the worst. The next cluster that was present in all the trends is the stainless clad and stainless steel strand with stainless clad being better than stainless steel. The final cluster of copper clad and hot dip galvanized was also paired together throughout the trends with copper clad performing better.

When combining the rankings based on corrosion resistance with the values of ultimate strength, the overall rankings are not the same, as some of the strands are not able to meet any of the mechanical properties. This refers to the stainless steel and copper clad strands which perform well in corrosion resistance but not in mechanical strength. If Grade 270 requirements are needed, then the only two strands available to use is the conventional and epoxy coated strand. In this case, the epoxy coated strand is the obvious choice. If Grade 250 requirements are needed, then the stainless clad and hot dip galvanized strand can be considered where again, the epoxy coated strand is the first choice followed by stainless clad, then hot dip galvanized, and finally conventional strand. Therefore, based on all the tests including the mechanical tests, it is clear that the epoxy coated strand outperforms the others and is the best choice in the post tensioned application.

Chapter 8

Conclusions

8.1 Conclusions

The tests conducted and reported on are all supplementary to the large-scale beam specimens to help get an insight into the behavior of the strands before the final autopsy. Chapter 7 elaborates on the major trends of the tests and puts them in a ranking of how they performed. Below are some final conclusions on the tests which will help predict the strand behavior of the large-scale beams.

- The epoxy coated strand dominated the others in corrosion resistance along with meeting all industry requirements for mechanical properties.
- The conventional strand was the worst of all types in resisting corrosion but met all industry requirements for mechanical properties.
- The stainless clad and stainless steel strands behaved similar to one another throughout all the corrosion tests performing very well and only slightly behind the epoxy coated strand.
- The stainless steel strand did not meet any of the requirements for mechanical properties making it insufficient. Further research must be done to improve these aspects.
- The stainless clad strand met the Grade 250 but not the Grade 270 requirements for mechanical properties making it a valid choice in a field application.
- The copper clad and hot dip galvanized strand followed similar trends throughout the corrosion tests, but overall, the copper clad strand performed better. Both strand types performed worse than the stainless clad and stainless steel strands.
- The copper clad strand did not meet any of the requirements for mechanical properties making it insufficient. Further research must be done to improve these aspects.
- The hot dip galvanized strand met the Grade 250 but not the Grade 270 requirements for mechanical properties.

8.2 Recommendations

Project 0-4562 is a continuation of Project 0-1405 which was conducted to explore the corrosion activity of post-tensioned applications. The large-scale exposure beams began exposure March 2006 and were originally planned to be autopsied March 2010 after four years. From the conclusions of Turco²¹, it was apparent that in order to obtain better results, the exposure time would need to be extended beyond four years. An autopsy schedule is proposed which selects half of the beams to be opened at four years and the other half at six years. The beams were chosen so there would be a good representation at each autopsy. The autopsy layout can be found in Table 8.1. Note that the specimens with the circled 'A' are to be autopsied at four years.

Table 8.1: Autopsy Layout of the Large-Scale Beam Specimens

Duct	Prestressed - Strand Type						Non-Prestressed Conventional Rebar
	Conventional	Hot Dip Galvanized	Copper Clad	Stainless Clad	Stainless	Flowfilled	
Galvanized	G - 1.4	Ⓐ - NG - 2.2	Ⓐ - NG - 1.2	NG - 1.3	NG - 4.1		
	NG - 1.1						
	Ⓐ - G - T.2						
	Ⓐ - NG - T.1						
One-Way Ribbed Plastic	NG - 2.3	Ⓐ - NG - 3.4	Ⓐ - NG - 2.4		Ⓐ - NG - 4.2		
Two-Way Ribbed Plastic	G - 5.1	Ⓐ - NG - 3.2	NG - 3.3	NG - 5.2	NG - 5.3		
	Ⓐ - NG - 3.1						
Fully Encapsulated	Ⓐ - NG - 7.1	NG - 7.3				NG - 7.4	
	NG - 7.2						
None							black - 4.4
							epoxy - 4.3

G = Galvanized Bearing Plate, NG = Non-Galvanized Bearing Plate

Shaded = Corrosion Visually Observed as of February 2009

NOTE: For each specimen with plastic ducts, one duct will be coupled and the other will be continuous

Bibliography

1. Ahern, M.E. (2005). *Design and Fabrication of a Compact Specimen for Evaluation of Corrosion Resistance of New Post-Tensioning Systems*. MSc. Thesis, The University of Texas at Austin.
2. ASTM A 416/A 416M (2006). Standard Specifications for Steel Strand, Uncoated Seven-Wire for Prestressed Concrete. *American Society for Testing and Materials*, West Conshohocken, PA.
3. ASTM C 876 (1999). Standard Test Method for Half-Cell Potentials of Uncoated Reinforcing Steel in Concrete. *American Society for Testing and Materials*, West Conshohocken, PA.
4. ASTM G 1 (2003). Standard Practice for Preparing, Cleaning, and Evaluating Corrosion Test Specimens. *American Society for Testing and Materials*, West Conshohocken, PA.
5. ASTM G 102 (2004). Standard Practice for Calculation of Corrosion Rates and Related Information from Electrochemical Measurements. *American Society for Testing and Materials*, West Conshohocken, PA.
6. ASTM G 15 (2007). Standard Terminology Relating to Corrosion and Corrosion Testing. *American Society for Testing and Materials*, West Conshohocken, PA.
7. ASTM G 3 (2004). Standard Practice for Conventions Applicable to Electrochemical Measurements in Corrosion Testing. *American Society for Testing and Materials*, West Conshohocken, PA.
8. ASTM G 5 (2004). Standard Reference Test Method for Making Potentiostatic and Potentiodynamic Anodic Polarization Measurements. *American Society for Testing and Materials*, West Conshohocken, PA.
9. ASTM G 59 (2003). Standard Test Method for Conducting Potentiodynamic Polarization Resistance Measurements. *American Society for Testing and Materials*, West Conshohocken, PA.
10. Collins, M.P., and Mitchell, D. (1997). *Prestressed Concrete Structures*. Response Publications.

11. Hamilton, H.R. (1995). *Investigation of Corrosion Protection Systems for Bridge Stay Cables*. PhD Dissertation, The University of Texas at Austin.
12. Jones, D.A. (1996). *Principals and Prevention of Corrosion*. Prentice Hall (Second Edition).
13. Kouril, M., Novak, P., and Bojko, M. (2006). Limitations of the Linear Polarization Method to Determine Stainless Steel Corrosion Rate in Concrete Environment. *Cement and Concrete Composites*, 28, 228-235.
14. Mac Lean, S. (2008). *Comparison of the Corrosion Resistance of New and Innovative Prestressing Strand Types used in the Post Tensioning of Bridges*. MSc. Thesis, The University of Texas at Austin.
15. Pacheco, A.R. (2003). *Evaluating The Corrosion Protection of Post-Tensioning Grouts: Standardization of an Accelerated Corrosion Test*. PhD Dissertation, The Pennsylvania State University.
16. Pacheco, A.R., Schokker, A.J., and Hamilton, H.R. (2006). *Development of a Standard Accelerated Corrosion Test for Acceptance of Post-Tensioning Grouts in Florida*. University of Florida.
17. Salas, R.M., Schokker, A.J., West, J.S., Breen, J.E., and Kreger, M.E. (2004). *Project Summary Report 0-1405-S, Durability Design of Post-Tensioned Bridge Substructure Elements*. Center for Transportation Research, The University of Texas at Austin.
18. Salcedo-Rueda, E., Schokker, A.J., Breen, J.E., and Kreger, M.E. (2003). *Project Summary Report, Bond and Corrosion Studies of Emulsifiable Oils Used for Corrosion Protection in Post-Tensioned Tendons*.
19. Schokker, A.J. (1999). *Improving Corrosion Resistance of Post Tensioned Substructures Emphasizing High Performance Grouts*. PhD Dissertation, The University of Texas at Austin.
20. Schokker, A.J., (2007). *Modifications to the PTI Specification for Grouting of Post-Tensioned Structures*. PTI Ballot Proposal.

21. Turco, G.P. (2007). *Durability Evaluation of Post-Tensioned Concrete Beam Specimens After Long-Term Aggressive Exposure Testing*. MSc. Thesis, The University of Texas at Austin.
22. Turco, G.P., Salas, R.M., Schokker, A.J., West, J.S., Breen, J.E., and Kreger, M.E. (2007). *Project Technical Report 0-4562-2, Durability Evaluation of Post-Tensioned Concrete Beam Specimens After Long-Term Aggressive Exposure Testing*. Center for Transportation Research, The University of Texas at Austin.
23. West, J.S. (1999). *Durability Design of Post Tensioned Bridge Substructures*. PhD Dissertation, The University of Texas at Austin.

VITA

Ryan David Kalina was born April 8, 1985 to Roland and Theresa Kalina in Shiner, Texas. He is the middle child – older sister, Nikki, and younger sister, Rachel. He graduated from Schulenburg High School in May 2003. Ryan attended the University of Texas at Austin where he graduated with the degree Bachelor of Science in Civil Engineering in December 2007. He then pursued a Master of Science in Structural Engineering also at the University of Texas at Austin. While pursuing his Master’s degree, Ryan worked under Dr. John Breen on the corrosion resistance of different prestressing strand types. Ryan graduated in May 2009 and accepted a position with Nelson Architectural Engineers in Houston.

Permanent Address: 25 Creekwood Drive
Schulenburg, TX 78956

This thesis was typed by the author.